



Control of the structure and the properties of polydopamine in suspensions, in films and in gels for biomedical applications

Salima El Yakhli El Yakhli - El Hadouchi

► To cite this version:

Salima El Yakhli El Yakhli - El Hadouchi. Control of the structure and the properties of polydopamine in suspensions, in films and in gels for biomedical applications. Material chemistry. Université de Strasbourg, 2020. English. NNT : 2020STRAE013 . tel-03191284

HAL Id: tel-03191284

<https://theses.hal.science/tel-03191284>

Submitted on 7 Apr 2021

HAL is a multi-disciplinary open access archive for the deposit and dissemination of scientific research documents, whether they are published or not. The documents may come from teaching and research institutions in France or abroad, or from public or private research centers.

L'archive ouverte pluridisciplinaire **HAL**, est destinée au dépôt et à la diffusion de documents scientifiques de niveau recherche, publiés ou non, émanant des établissements d'enseignement et de recherche français ou étrangers, des laboratoires publics ou privés.

ÉCOLE DOCTORALE Physique et Chimie-Physique
UMRS 1121 Biomatériaux et bioingénierie

THÈSE présentée par :
Salima EL YAKHLIFI – EL HADOUCHI

soutenue le : **17 septembre 2020**

pour obtenir le grade de : **Docteur de l'université de Strasbourg**

Discipline/ Spécialité : Chimie des matériaux

**Control of the structure and the properties
of polydopamine in suspension, in films
and in gels for biomedical applications**

THÈSE dirigée par :

M. BALL Vincent

Professeur, Université de Strasbourg

RAPPORTEURS :

Mme. WEIL Tanja

Professeur, Max Planck Institute (Allemagne)

M. PIELES Uwe

Professeur, FHNW Muttenez (Suisse)

AUTRES MEMBRES DU JURY :

Mme. PAEZ Julieta-Irene

Maître de conférences, INM Leibniz (Allemagne)

M. PONCHE Arnaud

Maître de conférences, IS2M Mulhouse

M. SCHLATTER Guy

Professeur, ICPEES Strasbourg

A dissertation submitted to
the Doctoral School of Physics (ED182)
of the Université de Strasbourg
to obtain the degree of
Doctor of Philosophy



CONTENTS

REMERCIEMENTS	8
ACKNOWLEDGEMENTS	10
MAIN ABBREVIATIONS	12
INTRODUCTION GENERALE (FRENCH VERSION)	13
GENERAL INTRODUCTION	15
CHAPTER 1:	19
STATE OF THE ART	19
INTRODUCTION	19
1. GENERAL FEATURES OF POLYDOPAMINE (PDA)	20
1.1. PDA, A BIOMIMETIC ADHESIVE	20
1.2. PDA, AN EUMELANIN ANALOGUE	22
2. PDA A PROMISING COATING METHOD	24
2.1. SURFACE COATING TECHNIQUES VERSUS PDA DEPOSITION	24
2.2. PDA COATING METHOD	25
3. HOW TO AVOID PRECIPITATION IN SOLUTION AND TO PRODUCE STABLE NANOMATERIALS	27
4. APPLICATIONS OF POLYDOPAMINE BASED NANOMATERIALS	31
CONCLUSIONS	34
REFERENCES	35
LIST OF THE FIGURES – CHAPTER 1	41
LIST OF THE TABLES – CHAPTER 1	41
CHAPTER 2 :	44
MATERIALS AND METHODS	44
INTRODUCTION	44
1. MATERIALS	45
1.1. MATERIALS FOR NANOPARTICLES SYNTHESIS	45
1.2. MATERIALS FOR FILMS FORMATION	45
1.3. MATERIALS FOR GELS FORMATION	46
2. PREPARATION OF THE SAMPLES	46
2.1. FORMATION OF THE PDA@ALP NANOPARTICLES	46
2.2. FORMATION OF THE (PAH)@PDA FILMS	47
2.3. FORMATION OF THE PDA FILMS	48
2.4. FORMATION OF THE GELATIN@PDA GELS	50
3. SAMPLES CHARACTERIZATION	51
3.1. CHARACTERIZATION OF THE PDA@ALP NANOPARTICLES	51
3.1.1. Ultraviolet-Visible (UV-Vis) spectroscopy	51
3.1.2. Enzymatic activity of the PDA@ALP nanoparticles	52
3.1.3. Transmission electron microscopy (TEM)	53
3.1.4. Atomic force microscopy (AFM)	54
3.1.5. Dynamic light scattering (DLS) – Zeta Potential	54
3.2. CHARACTERIZATION OF THE DOPA/OXIDANT FILMS	54
3.2.1. Atomic force microscopy (AFM)	54

3.2.2. Static contact angle measurements	54
3.2.3. X-Ray photoelectron spectroscopy (XPS)	55
3.2.4. Cyclic voltammetry (CV)	55
3.2.5. Antioxidant analysis of the PDA@oxidant films	55
3.2.6. Matrix-assisted laser desorption mass spectrometry with time of flight analysis	56
3.3. CHARACTERIZATION OF THE GEL@PDA GELS	57
3.3.1. Rheology	57
3.3.2. Scanning electron microscopy (SEM)	57
CONCLUSION	59
REFERENCES	60
LIST OF THE FIGURES – CHAPTER 2	61
LIST OF THE TABLES – CHAPTER 2	61

CHAPTER 3:

FORMATION OF ENZYMATICALLY ACTIVE SIZE-CONTROLLED POLYDOPAMINE NANOPARTICLES	64
INTRODUCTION	64
1. RECENT ADVANCES IN THE CONTROL OF PDA NANOPARTICLES AT INSERM 1121	65
1.1. CONTROL OF THE SIZE OF PDA NANOPARTICLES	65
1.1.1. Influence of the addition of Human Serum Albumin during dopamine oxidation	65
1.1.2. Influence of the KE sequence in PDA formation	66
1.2. OXIDATION CONTROL OF THE PDA FORMATION	67
1.3. OUR STRATEGY	68
2. FORMATION OF SIZE-CONTROLLED PDA NANOPARTICLES	69
2.1. OXIDATION OF DOPAMINE WITH SODIUM PERIODATE	69
2.1.1. Color change during oxidation	69
2.1.2. Reproducibility	69
2.2. INFLUENCE OF THE ADDITION OF ALP IN DOPAMINE SOLUTION	70
2.2.1. Kinetics of PDA@ALP formation analyzed by UV Vis spectroscopy	70
2.2.2. Influence of the dopamine/protein ratio on the PDA nanoparticles' size	71
2.2.3. Structure of the PDA@ALP nanoparticles	72
3. ENZYMATIC ACTIVITY OF THE PDA@ALP NANOPARTICLES	74
3.1. ANALYSIS OF THE ENZYMATIC ACTIVITY WITH PNP METHOD	74
3.2. KINETICS REACTION	76
4. APPLICATION OF THE PDA@ALP NANOPARTICLES	78
4.1. FORMATION OF MULTILAYERS FILMS	78
CONCLUSION	81
REFERENCES	82
LIST OF THE FIGURES – CHAPTER 3	83
LIST OF THE TABLES – CHAPTER 3	83

CHAPTER 4:

INFLUENCE OF DIFFERENT OXIDANTS ON THE PHYSICO-CHEMICAL CHARACTERISTICS OF POLYDOPAMINE COATINGS	86
INTRODUCTION	86
1. MORPHOLOGY OF THE DOPA/OXIDANT FILMS	87

1.1. FILMS ROUGHNESS	87
1.2. FILMS THICKNESS	88
2. CHEMICAL COMPOSITION OF THE DOPA/OXIDANT-XH FILMS	91
2.1. UV VIS ANALYSIS	91
2.2. XPS ANALYSIS	93
3. ELECTROCHEMICAL BEHAVIOR OF THE DOPA/OXIDANT-XH FILMS	98
4. PROPERTIES OF THE DOPA/OXIDANT-XH FILMS	99
4.1. ANTIOXIDANT PROPERTIES	99
4.1.1. Basic features of antioxidants	99
4.1.2. Antioxidant activity of the PDA/oxidant-xh films	100
CONCLUSIONS	103
REFERENCES	104
LIST OF THE FIGURES – CHAPTER 4:	105
LIST OF THE TABLES – CHAPTER 4:	105
SUPPORTING INFORMATION	106
AFM SURFACE TOPOGRAPHIES	106
XPS SPECTRA	109
CYCLIC VOLTAMMETRY	110
 CHAPTER 5 :	 113
 GELATIN@POLYDOPAMINE-BASED HYDROGELS	 113
INTRODUCTION	113
1. BASIC FEATURES OF GELATIN AND PDA GEL	114
1.1. GELATIN HYDROGELS	114
1.2. GELATIN@POLYDOPAMINE-BASED HYDROGELS	114
1.3. OUR STRATEGY	116
2. FORMATION OF GELATIN@PDA HYDROGELS	117
2.1. INFLUENCE OF THE DOPAMINE CONCENTRATION	117
2.1.1. Influence on the elasticity	117
2.1.2. Influence on the adhesion energy	119
2.1.3. Microstructure analysis of gelatin@PDA hydrogels	120
2.2. INFLUENCE OF THE GELATION TIME AND PEELING SPEED	122
2.2.1. Influence of the gelation time and peeling speed on the maximal force	122
2.2.2. Influence of the gelation time and peeling speed on the adhesion energy	123
2.2.3. Type of rupture	124
CONCLUSION	125
REFERENCES	126
LIST OF THE FIGURES – CHAPTER 5:	128
GENERAL CONCLUSION AND PERSPECTIVES	129
CONCLUSION GENERALE (FRENCH VERSION)	132
 ANNEXES	 135
LIST OF PUBLICATIONS	136
 UN NOUVEAU CHAPITRE DE LA THESE / NCT 2020	 137
INTRODUCTION	139

CADRE GENERAL ET ENJEUX DE MA THESE	140
MON TRAVAIL DE THESE	140
INTERET DE MON TRAVAIL	140
POURQUOI CETTE THESE	141
CONTEXTE PROFESSIONNEL	141
DEROULEMENT ET GESTION DU PROJET DE THESE	142
PRINCIPALES ETAPES DU PROJET	142
ANIMATION ET COORDINATION	143
I. LES REUNIONS DE PROJET	143
II. LES RELATIONS / PARTENAIRES EXTERIEURS	143
MISE EN VALEUR DES COMPETENCES TRANSVERSALES ET TRANSFERABLES	144
CONCLUSION / REMERCIEMENTS	145

Remerciements

Je tiens à remercier mon directeur de thèse, le Prof. Vincent Ball, pour sa bienveillance, sa patience et sa présence tout au long de cette aventure doctorale. J'ai eu l'immense honneur de pouvoir bénéficier de son savoir-faire, de son savoir-être, de ses nombreuses et variées compétences ainsi que de sa créativité durant ces trois dernières années. Une galaxie de merci à toi Vincent qui a toujours été prêt à m'accompagner, à m'aider dès que j'en avais besoin, tes qualités humaines m'ont beaucoup appris et inspirées. Je te suis infiniment reconnaissante pour ton enseignement, pour ton dévouement difficilement égalable, et même pour nos échanges philosophiques, écologiques, politiques.

J'aimerais remercier toutes les personnes avec qui j'ai pu me former et apprendre, et à celles et ceux qui ont généreusement donné de leur temps et de leur énergie pour m'aider à avancer sur mes travaux, en particulier Youri Arntz pour m'avoir partagé son expertise avec l'AFM toujours dans une ambiance conviviale à l'haut-rhinoise, merci à Joseph Hemmerlé aussi pour sa gentillesse exemplaire. Je tiens à remercier Naji Kharouf pour les analyses MEB, ainsi que Eric Matthieu pour sa collaboration et sa rigueur. J'aimerais chaleureusement remercier Florent Meyer qui m'a facilité mes enseignements de TD.

Ces trois années ont été possibles grâce au financement de la faculté de chirurgie dentaire, je remercie donc madame la doyenne Corinne Taddei-Gross, ainsi que Pierre Schaaf directeur de l'unité 1121 pour m'avoir accueilli au sein du laboratoire.

Mes remerciements s'adressent aussi à toute l'équipe de l'unité pour leur sympathie en particulier Emine, Christine, Eya, Sophie, Annabelle, Jean-Yves, Philippe... et toutes celles et tous ceux que je n'ai pas cités et qui font la richesse de cette équipe. Un big merci également à toute l'équipe de pharma où j'ai beaucoup apprécié faire de la diffusion de la lumière, et plus précisément à Florence et May pour vos attachantes personnalités.

Je souhaiterais remercier aussi toutes les personnes avec qui j'ai pu collaborer et travailler durant cette thèse :

Merci à toute la team du Prof. Ovidiu Ersen de l'IPCMS, plus particulièrement à Dris Ihiawakrim qui a pris de son temps pour m'accorder de longues heures d'analyse TEM, ainsi qu'à Nathaly Ortiz Pena pour sa bonne humeur.

Merci au Prof. Marco d'Ischia de l'université de Naples pour ses réflexions intellectuelles, et à sa très compétente et sympathique doctorante Maria-Laura Alfieri (devenue docteur depuis !). Merci à l'équipe de l'ISIS : Artur Ciesielski et Matilde Eredia pour nous avoir permis de faire des mesures XPS et contribuer à l'analyse des données.

Préparer sa thèse à l'université de Strasbourg signifie aussi suivre des formations transversales en plus des formations scientifiques, avec donc la possibilité d'acquérir des compétences transversales qui ont d'une certaine manière contribué à la réussite de cette thèse.

Je tiens donc à chaleureusement remercier toute la team du Jardin des sciences avec qui j'ai pu apprendre à mieux communiquer mes travaux de recherche et à m'initier à la médiation scientifique notamment via Kid's University et ma thèse en 180 secondes. Merci à Amandine

et Vanessa pour leur touchante implication ainsi qu'à tous les doctorant-e-s qui ont partagé cette folle et enrichissante aventure, en particulier à Farah, Charlotte et Warda.

J'aimerais aussi remercier toute l'équipe de la SATT Conectus pour avoir proposé le programme « Mature Your PhD » et pour leur accompagnement sur le projet de colle chirurgicale.

Aussi, je remercie l'équipe responsable du programme de valorisation des compétences « Nouveau chapitre de la thèse » grâce à qui j'ai pu identifier mes compétences acquises durant ce doctorat mais surtout aussi grâce à qui j'ai appris à traduire cette thèse pour le monde industriel. Encore, je remercie l'équipe de l'institut du développement et de l'innovation pédagogique (IDIP) avec qui j'ai pu apprendre à concevoir des enseignements selon différentes approches innovantes.

Avant de finir, je voudrais remercier mon jury de thèse, notamment les professeurs Tanja Weil et Uwe Pieleles qui m'ont fait l'honneur d'accepter d'en être les rapporteurs, mais aussi les autres membres du jury : Arnaud Ponche, Julieta-Irene Paez et Guy Schlatter qui m'honorent de leur participation.

Pour terminer, j'aimerais exprimer toute ma gratitude à mes parents qui m'ont toujours soutenu et ont fait de moi la femme que je suis aujourd'hui, mes remerciements sont aussi pour mes frères et sœurs, mes neveux et nièces qui sont la joie de nos yeux et nos cœurs, et à tous mes proches. Un merci à toi, ma best, qui m'accompagne depuis la maternelle, ce fût un honneur de grandir avec toi. Un merci à toutes celles et ceux que je n'ai pas cités mais qui sont chers à mon cœur.

Enfin, je remercie mon mari, mon plus grand soutien, mon inspiration et ma force, merci d'être la lumière et l'homme formidable que tu es au quotidien, et ma petite nébuleuse chérie née en fin de thèse et qui m'aide chaque jour à être une meilleure personne.

Aknowledgements

I would like to thank my thesis supervisor, Prof. Vincent Ball, for his benevolence, his patience and his presence throughout this doctoral adventure. I have had the immense honor of being able to benefit from his know-how, his interpersonal skills, his many and varied skills as well as his creativity over the past three years. A galaxy of thanks to you Vincent who has always been ready to accompany me, to help me whenever I needed it, your human qualities have taught me a lot and inspired me. I am infinitely grateful to you for your teaching, for your hard-to-match dedication, and even for our philosophical, ecological and political exchanges.

I would like to thank all the people with whom I was able to train and learn, and to those who generously gave of their time and energy to help me move forward on my work, in particular Youri Arntz for having shared his expertise with the AFM always in a friendly Upper Rhine atmosphere, thanks to Joseph Hemmerlé also for his exemplary kindness. I would like to thank Naji Kharouf for the SEM analyzes, as well as Eric Matthieu for his collaboration and his rigor. I would like to warmly thank Florent Meyer who made my TD lessons easier.

These three years were made possible by funding from the Faculty of Dental Surgery, so I would like to thank Dean Corinne Taddei-Gross, as well as Pierre Schaaf Director of Unit 1121 for welcoming me to the laboratory.

My thanks also go to the whole team of the unit for their sympathy in particular Emine, Christine, Eya, Sophie, Annabelle, Jean-Yves, Philippe... and all those who I did not mention and who do the richness of this team. A big thank you also to the whole pharma team where I really enjoyed doing dynamic light scattering, and more specifically to Florence and May for your endearing personalities.

I would also like to thank all the people with whom I was able to collaborate and work during this thesis:

Thanks to the whole team of Prof. Ovidiu Ersen from IPCMS, especially Dris Ihiawakrim who took his time to give me long hours of TEM analysis, and Nathaly Ortiz Pena for her good humor.

Thanks to Prof. Marco d'Ischia from the University of Naples for his intellectual reflections, and to his very capable and sympathetic doctoral student Maria-Laura Alfieri (who has since become a doctor!).

Thanks to ISIS team Artur Ciesielski and Matilde Eredia for allowing us to do XPS measurements and help with data analysis.

Preparing a thesis at the University of Strasbourg also means following transversal training in addition to scientific training, with therefore the possibility of acquiring transversal skills which in a way contribute to the success of this thesis.

I would therefore like to warmly thank the entire team of the Jardin des sciences with whom I was able to learn to better communicate my research work and to initiate myself into scientific mediation, particularly through Kid's University and my thesis in 180 seconds. Thanks to

Amandine and Vanessa for their touching involvement and to all the doctoral students who shared this crazy and enriching adventure, in particular to Farah, Charlotte and Warda.

I would also like to thank the entire SATT Conectus team for offering the "Mature Your PhD" program and for their support on the surgical glue project.

Also, I would like to thank the team responsible for the skills enhancement program "New chapter of the thesis" thanks to which I was able to identify the skills acquired during this doctorate but above all also thanks to whom I learned to translate this thesis for the industrial world. Too, I would like to thank the educational development and innovation institute (IDIP) with whom I was able to learn to design my courses according to different innovative approaches.

Before finishing, I would like to thank my thesis jury, in particular Professors Tanja Weil and Uwe Piele who did me the honor of accepting to be the reviewers, but also to the other members of the jury: Arnaud Ponche, Julieta-Irene Paez and Guy Schlatter who honor me with their participation.

To conclude, I would like to express all my gratitude to my parents who have always supported me and made me the woman I am today, my thanks are also for my brothers and sisters, my nephews and nieces who are the joy to our eyes and hearts, and thanks to all my loved ones. A thank you to you, my best, who has been with me since kindergarten, it was an honor to grow up with you. A thank you to all those whom I did not mention but who are dear to my heart.

Finally, I thank my husband, my greatest support, my inspiration and my strength, thank you for being the light and the wonderful man that you are on a daily basis, and my dear little baby girl who teaches me every day to be a better person.

Main abbreviations

ALP	Alkaline phosphatase
AFM	Atomic force microscope
NPs	Nanoparticles
PAH	Poly(allylamine)
PDA	Polydopamine
PNP	p-nitrophenyl phosphate
TEM	Transmission electronic microscope
SEM	Scanning electronic microscope

Introduction générale (french version)

De nos jours, la modification de surface joue un rôle central dans une variété de domaines d'applications, que ce soit pour en améliorer la biocompatibilité, pour la rendre antimicrobienne, pour contrôler son hydrophobicité, ou pour libérer des molécules spécifiques, pour n'en citer que quelques-unes. Dans tous les cas, nous sommes très souvent contraints de traiter les surfaces afin de leur conférer des propriétés ciblées et transformer le matériau initial en produit de grande valeur. Il existe plusieurs types de modifications de surface qui ont fait leurs preuves. Cependant, ces techniques sont généralement spécifiques au substrat. Les différentes techniques de modification de surface peuvent nécessiter plusieurs étapes de traitement avant d'atteindre l'objectif souhaité. Le contrôle des fonctionnalités de surface est donc très recherché. La nécessité de développer des revêtements plus simples et plus universels s'est donc rapidement imposée dans la recherche en sciences des matériaux.

La polydopamine (PDA), inspirée de la substance adhésive des moules marines (1), est précisément un matériau adhésif qui permet de recouvrir quasiment tous les types de surfaces tout en présentant de nombreux avantages : facile à synthétiser, facile à fonctionnaliser, des propriétés biocompatibles, photothermiques et antioxydantes.

Le pouvoir adhésif remarquable de la PDA a ouvert la voie à des revêtements universels qui nous épargnerait les nombreuses étapes de modification de surface. En effet, il est possible de recouvrir une surface (verre, plastique, Teflon, tissu...) simplement en l'immergeant dans une solution de dopamine et en laissant le revêtement prendre place lors de l'oxydation de la dopamine. Cette remarquable facilité d'usage laisse facilement deviner le large éventail d'applications possibles des films de PDA. Par exemple, en médecine, les revêtements de PDA peuvent être utilisés pour améliorer la bio-intégration (2) ou encore comme nano-vecteur multifonctionnel biocompatible pour la chimiothérapie (3). La couleur noire de la PDA a également des applications prometteuses en cosmétique comme teinture capillaire (4) entre autres. Il semble que la seule limite soit notre imagination.

Cependant, la facilité de synthèse de la PDA comporte encore des inconvénients. Lors de l'oxydation de la dopamine, le matériau obtenu en solution a tendance à précipiter. Il en résulte ainsi un gaspillage important de matière avec un rendement qui pourrait facilement être augmenté avec une amélioration de la méthode de préparation. De plus, lors de la formation des nanoparticules (NPs), de gros agrégats instables se forment, ce qui peut compliquer leur mise en application. Enfin, comme le mécanisme de formation de la PDA n'a pas encore été complètement élucidé, plusieurs efforts de recherche sont nécessaires pour mieux utiliser ce matériau d'intérêt.

Dans ce contexte, cette thèse vise à étudier le contrôle de la structure et des propriétés de la PDA à l'état de suspension, sous forme de nanoparticules, à l'état de films et dans des hydrogels.

Après avoir abordé l'état de l'art des matériaux à base de PDA dans le premier chapitre, le matériel et méthode de la partie expérimentale de cette thèse sera détaillé dans le deuxième chapitre.

Dans le troisième chapitre, nous étudierons comment, inspiré de l'eumélanine de la peau, nous pouvons empêcher la précipitation de la PDA à l'aide d'une protéine, à savoir la phosphatase alcaline (ALP), et l'influence de celle-ci dans le contrôle de la taille des NPs de PDA. Après la caractérisation de ces NPs, nous explorerons ensuite l'activité enzymatique que l'ALP confère à la PDA. Au-delà du souci de valoriser la PDA pour éviter la perte de matériau, l'objectif de cette première partie est de synthétiser des NPs actives, à taille contrôlée qui soient stables d'un point de vue colloïdal en vue de futures applications biomédicales.

Dans le quatrième chapitre, nous nous focaliserons sur l'influence de différents oxydants sur les propriétés physico-chimiques des films de PDA. Nous étudierons l'effet sur la structure chimique, l'électrochimie et l'activité antioxydante. L'intérêt de cette étude est d'identifier les conditions optimales de préparation de la PDA et de mieux comprendre l'influence des méthodes d'oxydation. Cette analyse combinatoire vise à mettre en lumière les techniques de synthèse qui favorisent la préparation de films plus épais, sans dégradation et présentant des propriétés antioxydantes.

Enfin, nous explorerons l'influence de la présence de nanoparticules de PDA incorporées dans des hydrogels de gélatine et étudierons leur effet sur les propriétés telle que l'élasticité et l'énergie d'adhésion grâce aux mesures rhéologiques. Le but de cette dernière partie est d'étudier le rôle que peut jouer la présence de PDA dans des gels, dans l'intention de développer des gels biomédicaux.

References

1. Lee H, Dellatore SM, Miller WM, Messersmith PB. Mussel-inspired surface chemistry for multifunctional coatings. *Science*. 19 oct 2007;318(5849):426-30.
2. Jeong KJ, Wang L, Stefanescu CF, Lawlor MW, Polat J, Dohlman CH, et al. Polydopamine coatings enhance biointegration of a model polymeric implant. *Soft Matter*. 21 sept 2011;7(18):8305-12.
3. Zhong X, Yang K, Dong Z, Yi X, Wang Y, Ge C, et al. Polydopamine as a Biocompatible Multifunctional Nanocarrier for Combined Radioisotope Therapy and Chemotherapy of Cancer. *Adv Funct Mater*. 2015;25(47):7327-36.
4. Gao ZF, Wang XY, Gao JB, Xia F. Rapid preparation of polydopamine coating as a multifunctional hair dye. *RSC Adv*. 25 juin 2019;9(35):20492-6.
5. Bergtold C, Hauser D, Chaumont A, El Yakhli S, Mateescu M, Meyer F, et al. Mimicking the Chemistry of Natural Eumelanin Synthesis: The KE Sequence in Polypeptides and in Proteins Allows for a Specific Control of Nanosized Functional Polydopamine Formation. *Biomacromolecules*. 10 2018;19(9):3693-704.

General introduction

Today, the field of surface modification plays a central role in a variety of fields of applications, whether to improve biocompatibility, to make it antimicrobial, to control its hydrophobicity, or to release specific molecules, to cite just a few. In all cases, we are very often forced to treat surfaces to give them targeted properties and transform the initial material in a highly valuable product. There are several types of surface modifications that have been proven to work. However, generally these techniques are substrate-specific. The different surface modification techniques may require several processing steps before reaching the desired goal. Tailoring of surface functionalities is therefore in great demand. The need to develop easier and more universal coatings rapidly took hold in research in the materials sciences.

Polydopamine (PDA), inspired by the adhesive substance of sea mussels (1), is precisely an adhesive material that allows to coat almost any surface while having many advantages: easy to synthesize, easy to functionalize, biocompatible, photothermal and antioxidant properties.

The remarkable adhesive power of PDA paves the way for universal coatings that would do away with the many stages of surface modification. Indeed, it is possible to deposit PDA on a substrate simply by immersing the latter in a dopamine solution and then letting the coating take place during the oxidation of dopamine. All this lets easily guess the broad range of possible applications of PDA films. For instance, in medicine PDA coatings can be used to enhance biointegration (2) or as a biocompatible multifunctional nanocarrier for combined radioisotope therapy and chemotherapy (3). The black color of PDA has also promising applications in cosmetics as a hair dye (4) among others. It seems that the only limit is our imagination.

However, the ease of synthesizing the PDA films still hides drawbacks. During preparation, the material obtained in solution, simultaneously to the material sticking on surfaces, tends to precipitate. Therefore, this results in a significant waste of material with a yield that could easily be increased provided that its synthesis is improved. In addition, during the formation of nanoparticles (NPs), large aggregates of large unstable NPs are formed which can complicate their application. Finally, as the mechanism of PDA formation has not yet been fully elucidated, several research efforts are needed to better use this material of interest.

In this context, this thesis aims to study the control of the structure and properties of PDA in the state of suspension, in the form of nanoparticles, in the state of films and present in the gel state.

After discussing the state of the art of PDA materials in the first chapter, the materials and methods used in the experimental part of this thesis will be detailed in the second chapter.

In the third chapter we will study how-by inspiration from the eumelanin of the skin- we can prevent the precipitation of PDA with the help of a protein, namely alkaline phosphatase (ALP). After the characterization of the obtained nanoparticles, we will then explore the enzymatic activity that this protein confers to PDA. Beyond the concern to valorize PDA to avoid the loss

of material, the objective of this first experimental part is to synthesize active NPs, with controlled size which are stable from a colloidal point of view for future biomedical applications.

In the fourth chapter, we will focus on the influence of different oxidants on the physicochemical properties of PDA films. We will investigate the effect on the chemical structure, electrochemistry, and antioxidant activity. The interest of this study is to identify the optimal conditions for the preparation of PDA and to better understand the influence of oxidation methods. This combinatorial analysis aims to highlight the synthesis techniques which favor the preparation of thicker films, without degradation and exhibiting antioxidant properties.

Finally, we will explore the influence of PDA nanoparticles incorporated in gelatin-based gels and study their effect on the elasticity and adhesion energy of the hydrogel by rheological measurements. The aim of this last part is to study the role that the presence of PDA can play in gels, with the intention of developing hydrogels for biomedical use.

References

1. Lee H, Dellatore SM, Miller WM, Messersmith PB. Mussel-inspired surface chemistry for multifunctional coatings. *Science*. 19 oct 2007;318(5849):426-30.
2. Jeong KJ, Wang L, Stefanescu CF, Lawlor MW, Polat J, Dohlman CH, et al. Polydopamine coatings enhance biointegration of a model polymeric implant. *Soft Matter*. 21 sept 2011;7(18):8305-12.
3. Zhong X, Yang K, Dong Z, Yi X, Wang Y, Ge C, et al. Polydopamine as a Biocompatible Multifunctional Nanocarrier for Combined Radioisotope Therapy and Chemotherapy of Cancer. *Adv Funct Mater*. 2015;25(47):7327-36.
4. Gao ZF, Wang XY, Gao JB, Xia F. Rapid preparation of polydopamine coating as a multifunctional hair dye. *RSC Adv*. 25 juin 2019;9(35):20492-6.
5. Bergtold C, Hauser D, Chaumont A, El Yakhlifi S, Mateescu M, Meyer F, et al. Mimicking the Chemistry of Natural Eumelanin Synthesis: The KE Sequence in Polypeptides and in Proteins Allows for a Specific Control of Nanosized Functional Polydopamine Formation. *Biomacromolecules*. 10 2018;19(9):3693-704.

Chapter 1

*« Go take your lessons from Nature: this is where
our future lies. » Leonard de Vinci*

Chapter 1:

State of the art

INTRODUCTION	19
1. GENERAL FEATURES OF POLYDOPAMINE	20
1.1. PDA, A BIOMIMETIC ADHESIVE	20
1.2. PDA, AN EUMELANIN ANALOGUE	22
2. PDA : A PROMISING COATING METHOD	24
2.1. SURFACE COATING TECHNIQUES VERSUS PDA DEPOSITION	24
2.2. PDA COATING METHOD	25
3. HOW TO AVOID PRECIPITATION IN SOLUTION AND TO PRODUCE STABLE NANOMATERIALS	27
4. APPLICATIONS OF POLYDOPAMINE BASED NANOMATERIALS	31
CONCLUSIONS.....	34
REFERENCES.....	35
LIST OF THE FIGURES – CHAPTER 1	41
LIST OF THE TABLES – CHAPTER 1	41

Chapter 1:

State of the art

Introduction

Inspired by marine mussels, **Polydopamine (PDA)** became rapidly as one of the most promising candidates for surface modifications. Owing to its affordance, PDA combines simplicity, its extraordinary ability to modify a surface in a single step, and its potential to be used in an overly broad type of fields as medicine, biology, cosmetic, industrial and other domains.

In this chapter, we will begin by describing **the origin and basic features of PDA** and illustrate its affordance with some **examples of applications**. We will compare **PDA coatings** to other commonly employed surface modification methods. Also, we will highlight the problems encountered during its synthesis and introduce an emerging solution to get around it.

1. General features of Polydopamine (PDA)

PDA, a biomimetic adhesive

Many marine animals have developed adhesive strategies to deal with the dynamic ocean environment. Indeed, marine mussels are endowed with a remarkable sticky capacity, hence the French expression "*cling to your rock like a mussel*". Their amazing strength of adhesion was at the origin of considerable interdisciplinary research effort this last decade.

In particular, *Mytilus edulis* attach themselves to a wide variety of substrates by spinning a large number of byssal threads from their pads. Previous studies on their foot proteins (1) have revealed the presence of a large amount of L-lysine, 3,4-dihydroxy-L-phenylalanine, namely DOPA, and 3- and 4-hydroxyproline. Several DOPA-containing proteins have been identified from the adhesive pads of *M. edulis* (Mefp). Waite and co-workers demonstrated that adhesive strength is directly correlated to the DOPA content and that DOPA oxidation beyond 5-10 mol % of total DOPA compromises adhesion (2). It appeared that the composition of high catechol and high primary and secondary amine contents contribute to byssal adhesion.

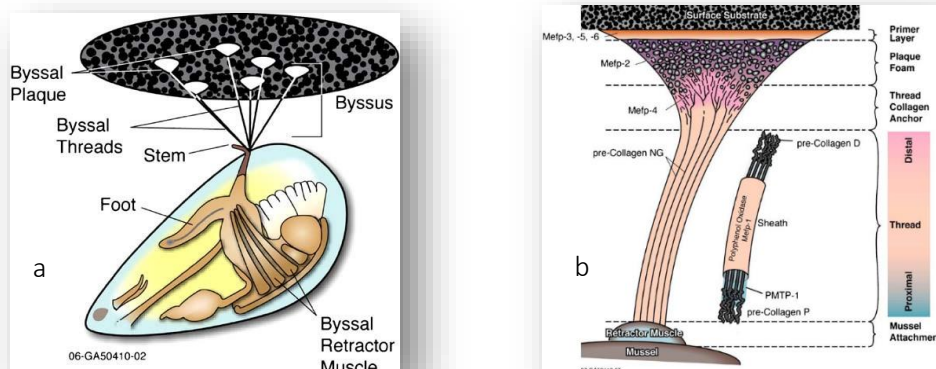


Figure 1: a) Anatomy of *M. edulis* mussel and byssus structures. b) Location of adhesive-related proteins identified in the byssus of *M. edulis*. (3)

Some experiments were done to evaluate the role of catechols in contributing to the adhesion strength (4). They compared three groups: one group with both catechol and amine, another one with catechol removed while maintaining amine, and finally a group without amine but maintaining catechol. The results showed weak adhesion when both compounds are not simultaneously present, suggesting that a combination and the proximity in space of catechol and amine are especially important to initiate strong adhesion.

Making the hypothesis that the coexistence of DOPA and Lysine groups may be crucial for achieving adhesion to a wide spectrum of materials, Lee et al. (5) identified dopamine as a small

molecule that contains both functionalities. They succeeded in developing a simple method to synthesize Polydopamine by oxidation of dopamine, dissolved oxygen (O_2) being the oxidant. The oxidation product, dopamine-quinone, undergoes a nucleophilic intramolecular cyclization reaction leading to the formation of 5,6-dihydroxyindole (DHI) (6). These two compounds seem to be of crucial importance for initiating the synthesis of PDA. A study conducted by D'Ischia and his group (7), reported that replacing the amine group of dopamine with a hydroxyl group, as in hydroxytyrosol, results in the formation of polymeric materials completely devoid of adhesion and film properties, but the addition of amines in a caffeic acid solution allows for the deposition of a film at the solid-liquid interface. Additionally, catechols are anchors that immobilize the polymer coating onto a surface and allow to form intermolecular chemical cross-links improving the stability of the obtained coatings (8).

According to the existing models, either PDA is composed of non-covalent assemblies of dopamine, dopamine-quinone and DHI, or rather of heteropolymers composed of catecholamine, quinone and indole repeat units. The complexity of PDA comes from the fact that different reaction pathways are possible after the initial oxidation step. Once dopamine-quinone formed by auto-oxidation of dopamine, it can follow three competing pathways as described more precisely in Fig. 2 that gives an overview of the current models. In their experiments, D'Ischia et al (9) prepared different sets of PDA samples in dicarboxylic acid (PDCA) and pyrrole-2,3,5-tricarboxylic acid (PTCA). PTCA derives from two linked DHI and PDCA derives from terminal indole units unsubstituted at the 2 position. They finally demonstrated that PDA consists in three building blocks. A first possibility (a) would imply dimerization of dopamine that would lead to non-covalent self-assembly of subunits to form quinhydrone. These units would then undergo further oxidation and intramolecular cyclization, to generate DHI units.

Other routes would lead to form covalent coupling of catecholamine/quinone/indole heteropolymer or eumelanin-like oligo-indoles. Indeed, the second path (b), would consist on DHI-based structures that may grow from cyclization. A third way (c), would lead to mixed species for example by attack of DHI to various monomer and oligomer quinone species. The combination of these chemical pathways leads to a multifunctional complex molecular system composed of diverse groups and structural moieties, including planar indole units, catechol or quinone functions and amino and carboxylic acid groups, making the PDA a very unusual and complex material.

PDA is then either considered as a polymeric material or a self-assembled material made from oligomers of 5,6-dihydroxyindole (10,11) Recently some evidence for the role of cation- π interactions in the formation and structure of PDA has also been provided (12).

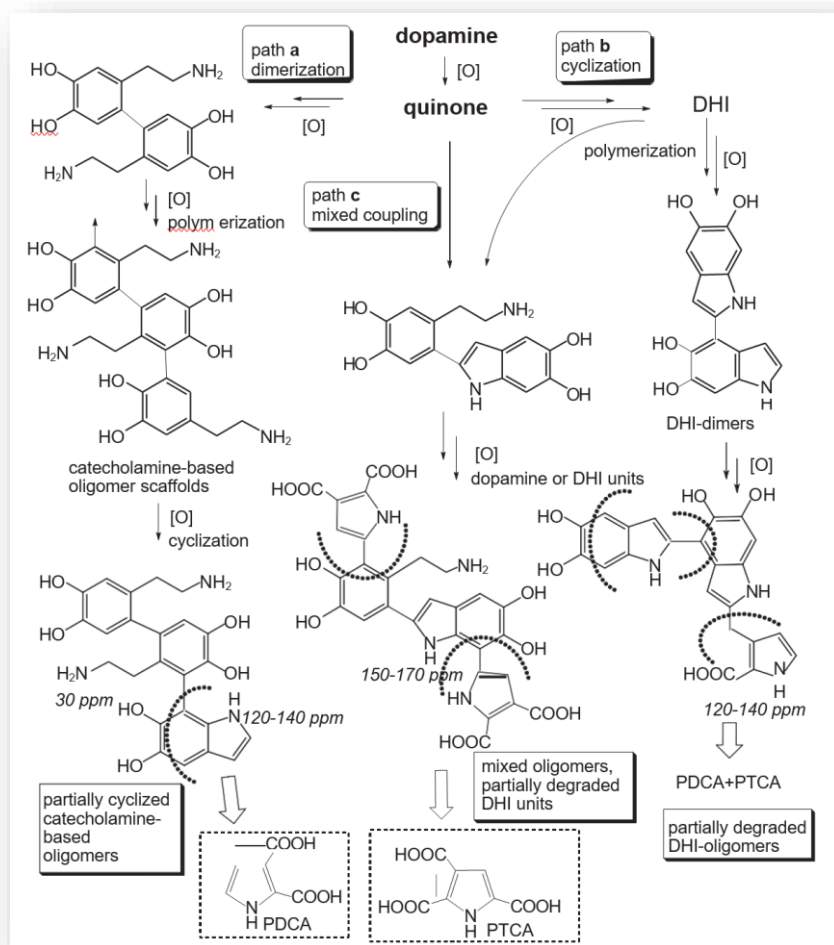


Figure 2: Simplified overall view of main reaction pathways involved in polydopamine formation. A proposed origin of the eumelanin markers, PDCA and PTCA, is highlighted. Reproduced from ref (9) with authorization.

Other models suggest that PDA is an analogue of the skin eumelanin as discussed below in the next section. Up to now, the chemical basis for the mechanism of PDA formation is not totally elucidated, thus some research efforts are still made to better understand its structure.

PDA, an eumelanin analogue

There are two major pigments in the skin: eumelanin (black/brown) and pheomelanin (reddish/brown). Each one is produced in melanocytes and derives from the amino acid L-Tyrosine which is hydroxylated and cyclized through the action of Tyrosinase and other pigmental enzymes (13). The former enzyme catalyzes the conversion of L-Tyrosine to L-DOPA and then L-DOPA to the corresponding quinone (Fig. 3) (14,15).

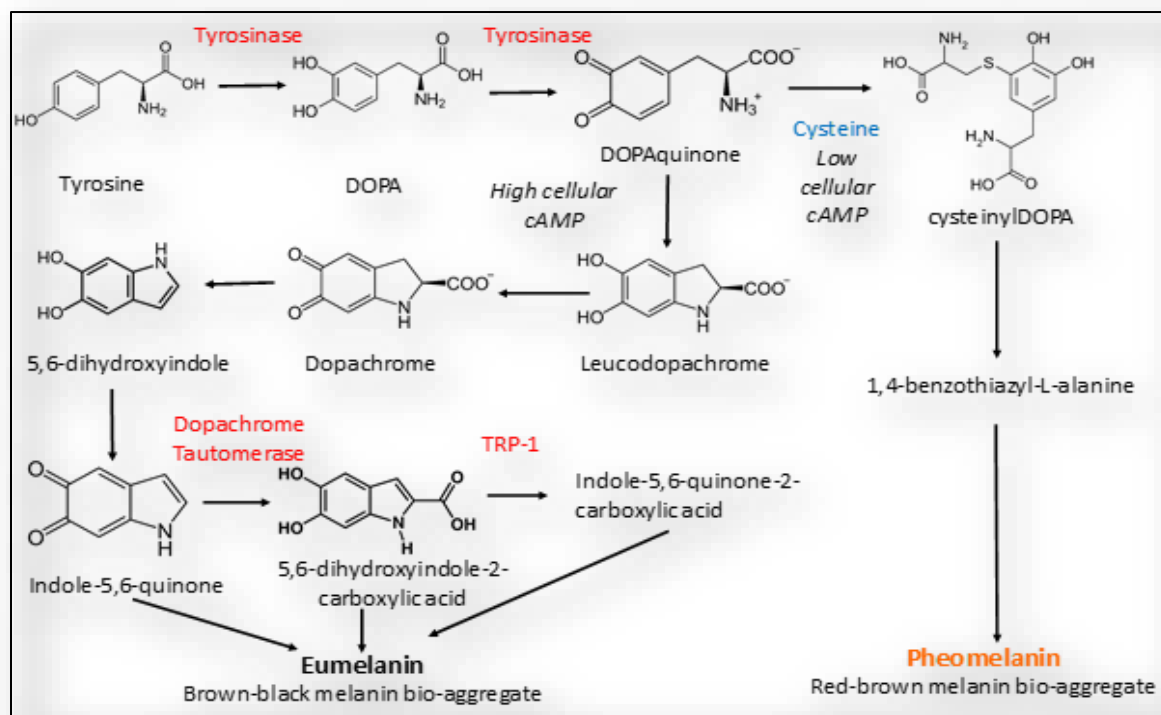


Figure 3: Chemical pathways leading to eumelanin and to pheomelanin and the enzymes (in red characters) implied in the different chemical steps. Modified from ref. [13] with authorization. Nomenclature: DOPA: 3,4-dihydroxyphenylalanine, TRP-1: Tyrosinase related protein.

Owing to a similar oxidation pathway, PDA shares various physicochemical properties with eumelanin. The building blocks of eumelanin are 5,6-dihydroxyindole-2-carboxylic acid (DHICA) and 5,6-dihydroxyindole (DHI) (Fig. 3) (16). Eumelanin and PDA have extremely close absorption spectra covering the entire wavelength range of the UV-vis domain in the electromagnetic spectrum (14,17–19). In addition, their fluorescence quantum yield is extremely low with most of the absorbed light being converted into heat (20). This is well known in the skin which undergoes heating after exposure to sunlight. Concerning PDA, this property is at the basis of applications as a possible photothermal material.

Therefore, PDA is also referred to as a “eumelanin-like” material since DHI (and its oxidized forms) is the key building block of both PDA and eumelanin (14). Actually, the term of polydopamine is misleading since it is probably not a real polymer but more likely a complex self-assembled amorphous material (11). Based on *ab initio* calculations of the structure-property-function relationship of PDA and eumelanin, a large number of oxidized DHI oligomers have been evaluated to compare their molecular structures. The obtained findings highlighted that more planar structures are energetically more favorable and that cyclic molecular structures could reduce the energy of a DHI based tetramer and make it more stable. This afforded a set of molecular models for more specific modeling of eumelanin-like materials (21). The assumption of tetrameric dopamine based structures (22–24) as building blocks of PDA is however heavily debated (25) and additional experimental proofs are required.

Owing to their similar chemical composition, PDA as a “synthetic eumelanin” are the focus of increasing interest as UV-absorbing agents, antioxidants, and free radical scavengers. Those properties are particularly interesting in the colloidal state, provided the oxidation products of catecholamines may be stabilized against aggregation and/or flocculation. In addition, eumelanin in the skin is always of controlled hierarchical size and surrounded by proteins (26). This is not the case of PDA which is an amorphous precipitate when produced in the absence of additives. It is hence a natural idea to add well suited additives to dopamine to control its self-assembly/polymerization process. Thus, some experiments including addition of components and their results will be discussed in chapter 3.

2. PDA: a promising coating method

2.1. Surface coating techniques versus PDA deposition

Surface modification consists on modifying the surface of a material by bringing physical, chemical, or biological properties to target specific functionalities. Surface modification plays a central role in a variety of application domains from electronics to medicine. Indeed, it is an extremely old domain of human technology: for instance more than 5000 years old fragments of potteries are found with a surface coating.

There are lots of chemical modification and surface functionalization techniques which are described in a large number of review articles. The current coating toolkits include irradiative chemisorption, layer-by-layer processes (27) (LbL), self-assembled-monolayers (SAM) (28), chemical vapor deposition (CVD)... However, most of these methods have limitations in that they are substrate specific, some of them require complex multistep processes, others need expensive equipment and others can only be performed in organic solvents. Hence, we need easier, cost effective, environmentally friendly, and universal coating processes.

In this context, PDA rapidly became a material of choice that can coat almost all kinds of substrates via different chemical mechanisms: covalent and non-covalent binding, π - π interactions, hydrogen bonds, catechol-metal coordination and electrostatic interactions. Table 1 below gives a reduced sample of the substrates which can be coated with PDA to illustrate its versatility. Table 2 gives a comparison between LbL and PDA coating methodologies.

It has even been shown that PDA can modify Teflon microchannel walls and thus lead to some applications of the modified chips that are difficult with native Teflon chips (29). The same holds true to make Teflon cell adhesive (30). Another example of the PDA versatility is an interesting study (31) that could demonstrate that in the absence of stirring, a PDA film can be formed at the air/water interface thanks to an hypothetical heterogeneous nucleation process.

A group of researchers (32) explored the use of PDA to develop a rapid and effective PDA-based method for dyeing human hair with a black color.

Materials	References
Cellulose	(33)
Silk	(34)
Hydroxyapatite	(5)
Nylon	(35)
Paper	(36)
Graphene	(37)
Glass	(5)
SiO ₂	(5)
Polystyrene (PS)	(5)
Polyethylene (PE)	(38,39)
Polyethylene terephthalate (PET)	(5)
Polyester	(39)

Table 1: Exhaustive list of materials that can be modified by PDA

LBL	PDA
Many coating cycles	One-step
Need of specific polymers or other components to provide particular functions	No need specific additional polymers PDA films exhibits intrinsic chemical reactivity
Polymers used are of high molecular weight Not suited for 3D porous materials	The building block of PDA, dopamine, has a low molecular weight Suited for 3D porous materials
Control of thickness by varying the number of coating cycles	Kinetic process

Table 2: Comparison of two surface modification methods : LBL versus PDA deposition.

2.2. PDA coating method

The coating method of PDA is quite simple as illustrated in Fig. 4: it involves the immersion of the target material in an aqueous alkaline solution of dopamine during a certain time duration. As we will see in chapter 3 dopamine concentration and experimental time are important parameters in controlling the deposition kinetics and the roughness of the obtained coatings. Then, a deposition of a conformal PDA coating occurs during the process. Finally, the coated material can be used directly or can be modified at wish.

More precisely, the first published method of PDA coating (5) employed 2 mg/mL of dopamine hydrochloride dissolved in 10 mM Tris buffer at pH = 8.5.

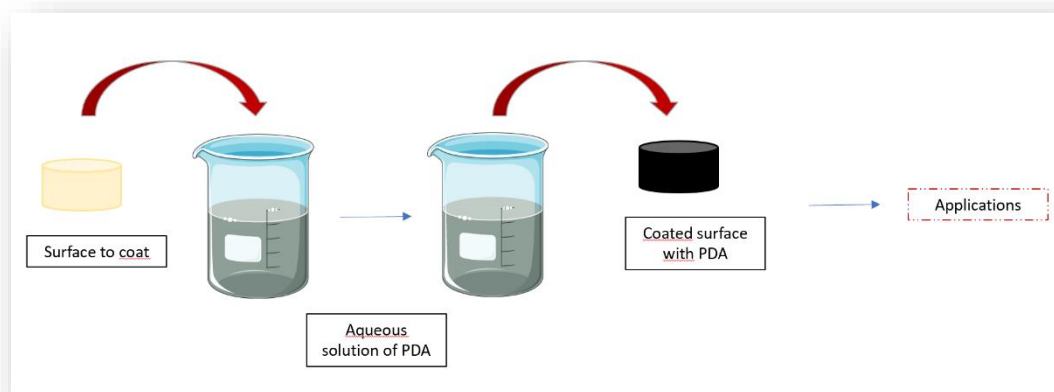


Figure 4: Polydopamine coating method

Due to this easy processing, in a one pot preparation method, PDA proved to be a powerful tool for chemical and biomedical applications (40,41).

Functional molecules containing nucleophilic groups (thiols, amines) can be easily immobilized onto quinones present in the structure of PDA to obtain synthetic derivatives (42,43). Otherwise, PDA was used to immobilize antibodies onto various kinds of surfaces in order to detect influenza viruses (44). Indeed, a mixture of PDA and an immunoglobulin-binding protein that enables an antibody to have an optimal orientation (protein G) was synthesized. The antibody binding efficiency depends on the PDA/protein G ratio that can be optimized.

A study highlighted that PDA film thickness and morphology are influenced by the dopamine concentration (45). A pulsed deposition technique was reported for micro-structuring PDA films using scanning electrochemical microscopy (46), achieving a better control of film thickness. The morphology and properties of the PDA films can also be influenced by adding metallic ions in the dopamine solution. As it has been demonstrated in a comparison study of the oxidative polymerization of dopamine in the presence of Na^+ , Ca^{2+} , Mg^{2+} and Co^{2+} cations has been investigated and the influence of those cations on the PDA films' structure has been evidenced (47).

Unfortunately, the oxidation process leading to PDA coatings from solution processes, oxidation and polymerization/self-assembly, leads also to the formation of a useless precipitate in the solution. Efforts have been devoted to avoid such a precipitation process and to control the self-assembly of the oxidation products of dopamine (and other catecholamines) in solution to get stable nano-colloids. In the next section, we will describe the synthesis methods yielding of PDA nanoparticles in the absence or in the presence of templating agents.

3. How to avoid precipitation in solution and to produce stable nanomaterials

As we have seen in the previous section, O₂ triggered autoxidation of dopamine in alkaline aqueous solutions is a standard method for PDA formation. But unlike as for PDA coatings, the preparation procedures of PDA nanoparticles (PDA@NPs) are still limited and new protocols are widely desirable. Indeed, some properties, as photothermal and free radical scavenging, can be influenced by the PDA@NPs size owing to obvious surface /volume ratios. Synthetic eumelanins yield huge polydisperse aggregates (48). However, if the catecholamine concentration is extremely low, the regime where small and stable nanoparticles are formed in the absence of film deposition on the walls of the reaction beaker can be reached. The colloidal stability of those nanoparticles is due to their pH dependent zeta potential: the PDA films and the obtained particles are negatively charged above the isoelectric point of PDA which is close to 4.9 (49). An interesting way to improve the surface charge on water soluble melanin was to perform their synthesis in the presence of a higher partial pressure in oxygen allowing to increase the number of carboxylic groups on the obtained colloids (50). Grafting of thiol-terminated methoxy-poly(ethylene glycol) on PDA synthesized in the presence of NaOH allowed to produce stable and biocompatible nanoparticles with less than 100 nm diameter (51).

At higher concentration in dissolved catecholamines, which is required to obtain a better yield in nanoparticles, the obtained colloids are too large to be stabilized and precipitation occurs after a few hours of oxidation. Fortunately, it has been shown that the addition of additives in the dopamine solution at typically 1 mg/mL (or 5 mM) like surfactants, polymers, polyelectrolytes or some proteins allow to get PDA of controlled size. Polymers like poly(vinyl alcohol) (52) and surfactant micelles (53) allow for the production of stable suspensions of PDA. Strikingly, in the presence of sodium dodecyl sulphate or cetyltrimethylammonium bromide, the hydrodynamic diameter of the PDA particles formed in the presence of oxygen at pH = 8.5 decreases with an increase in surfactant concentration up to their critical micellar concentration (CMC). For surfactant concentrations higher than the CMC the diameter of the PDA containing particles is similar to that of the surfactant micelles (Fig. 5), suggesting that the PDA formation occurs preferentially in the core of the micelles. This point requires of course additional investigations.

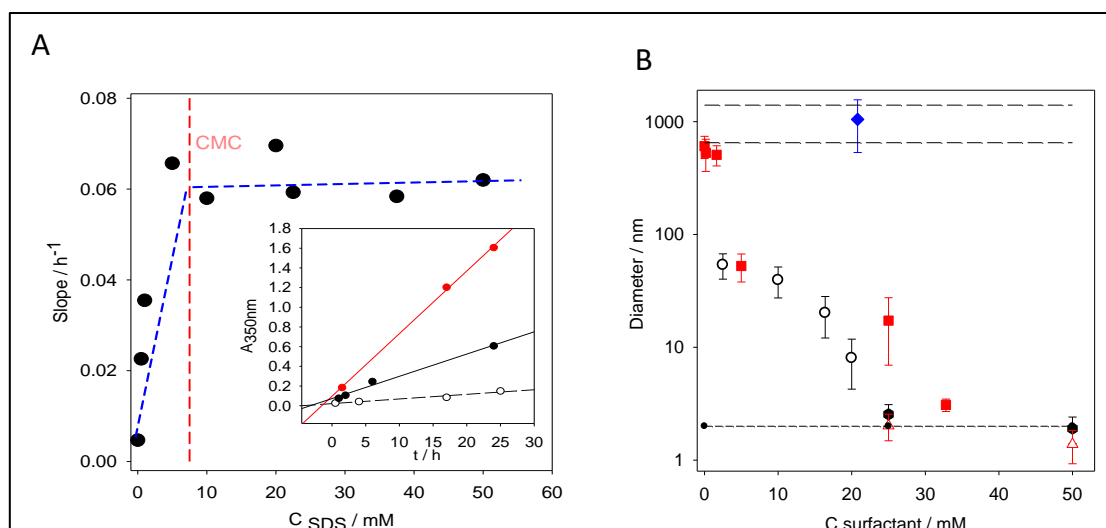


Figure 5: A : Rate of PDA formation as followed by UV-vis spectroscopy at $\lambda = 350$ nm as a function of the concentration in SDS (---●---). Each point is obtained from a curve as those represented in the inset (SDS at 0 (○) 0.5 (●) and 5 mM). The straight lines correspond to linear regressions to the data.

B: Evolution of the size of PDA aggregates as a function of the surfactant concentration in the case of SDS (○), CTAB (■) and Triton X-100 (◆). The upper long dashed lines correspond to the size domain of PDA prepared in the absence of surfactant whereas the lower short dashed line corresponds to the size of the surfactant micelles (measured in the case of SDS (■) and CTAB (△)). Modified from ref. (53) with authorization.

Another method to control PDA formation and to avoid precipitation is the use of boric acid as an adjuvant that is able to stop the deposition of PDA on surfaces and simultaneously to control self-assembly of PDA in solution to get stable colloidal aggregates (54). Boric acid forms strong hydrogen bonds with catechol moieties (Fig. 6B) which has the consequence to strongly increase the oxidation potential of dopamine (Fig 6A). Adding boric acid to dopamine solutions after a given oxidation and self-assembly duration allows to stop the growth of the PDA based nanoparticles to a controlled and reproducible size provided the boric acid/dopamine ratio is higher than about 5 (54).

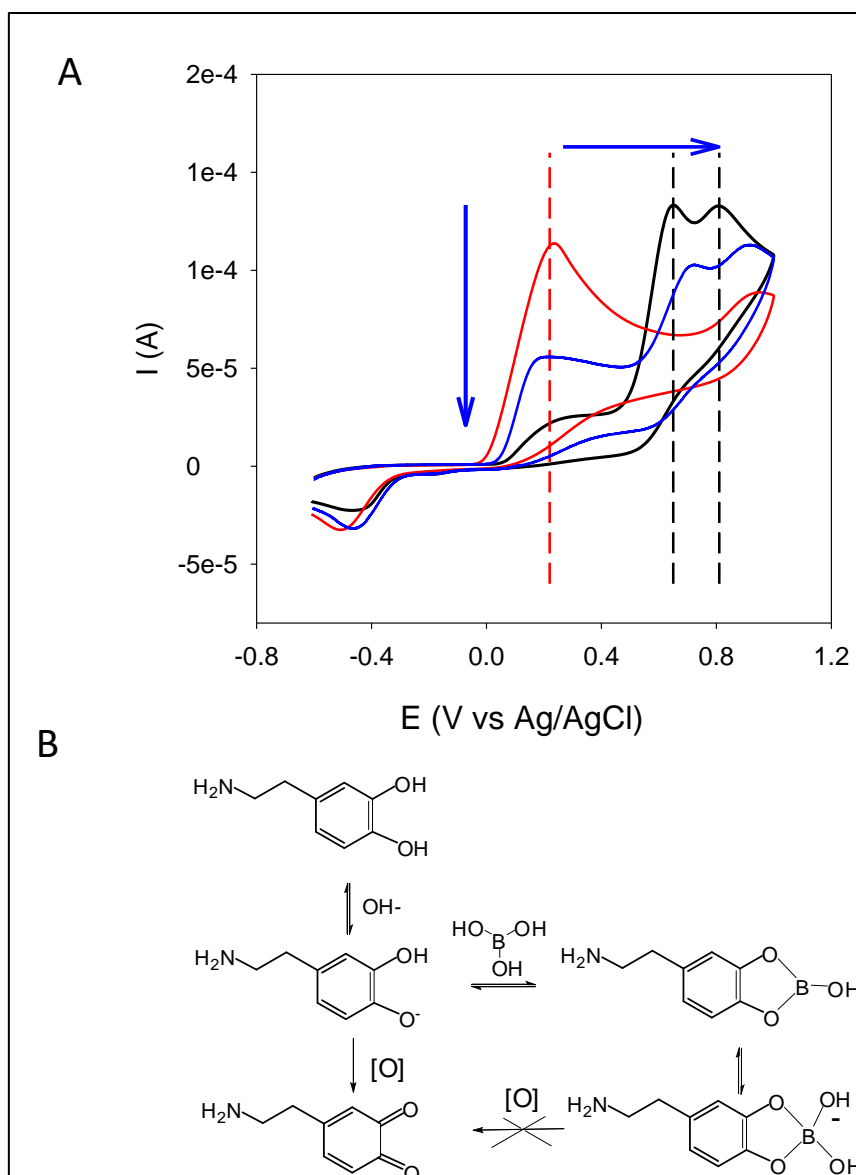


Figure 6: Interaction of boric acid with dopamine and its influence on the electrochemical behavior of dopamine.

A: Cyclic voltammetry of dopamine dissolved at 3.5 mM in Tris buffer at pH = 8.5 (red line) and in the same buffer but in the presence of 43 mM (blue line) and 430 mM (black line) boric acid. The blue arrows indicate the evolution of the cyclic voltammetry curves upon an increase in the boric acid concentration. B: Interaction of dopamine with boric acid and inhibitory effect of complex formation on oxidation to quinone and PDA formation. Modified from ref. (54) with authorization.

A recent study showed that a vast repertoire of oxidants can be used to rapidly prepare polydopamine under aerobic or anaerobic conditions, also in mildly acidic aqueous solutions, and at room temperature (55). Also, the use of strong oxidants such as sodium periodate leads to PDA formation in a much shorter time (56). Another effort to control the size of the PDA@NPs consists in adding either strong free radical scavengers (i.e. edaravone) or stable free radicals (i.e. PTIO) (57) during the synthesis, both resulting in a decrease in the NPs size (Fig 7).

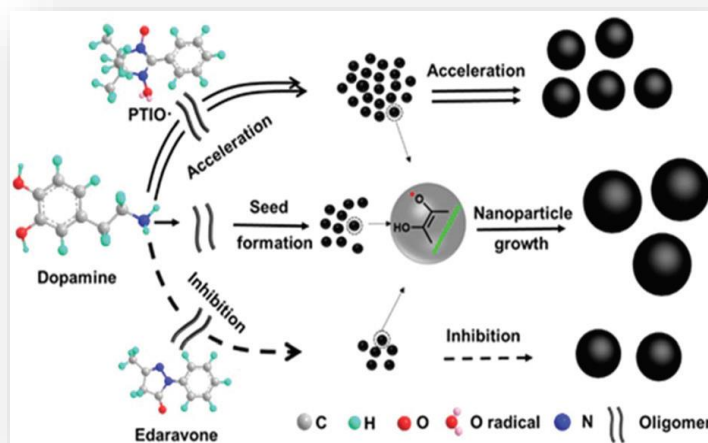


Figure 7: Schematic illustration of the size-controlled synthesis of PDA NPs by using radicalar species. Reproduced from ref. (57) with authorization.

Yet, the problem of the precipitation is still not totally resolved. The size of PDA@NPs can be modulated by changing the amount of dopamine monomers dissolved in a water in oil microemulsion to elaborate pH-activatable nanoparticles with an average diameter from 25 to 43 nm (58).

Inspired by the fact that eumelanin is always surrounded by a layer of proteins (26), a recent study has shown that the whole pool of proteins from the egg white allows to produce a well-controlled and stable eumelanin like material from DHI (59). However, the molecular origin of this controlled oxidation and self-assembly was not investigated, even if many purified enzymes like tyrosinase can play a similar role during the oxidation of L-DOPA (60,61).

Inspired from the proteins present in the skin melanocytes, a specific diad of amino acids in proteins, L-lysine (K) and L-glutamic acid (E), was shown to allow for specific control in the oxidation-self-assembly of dopamine to obtain biocompatible polydopamine@protein nanoparticles. Experiments were performed with single model peptides GKEG, GKGE and GKGE in which the K and E were directly adjacent to each other or separated with one or two Glycine residues. It appeared that K and E have to be adjacent in the amino acid sequence to exert a templating effect in the assembly of PDA particles (62).

Human Serum Albumin (HSA), also containing **KE** diads, was found to increase the rate of PDA formation from dopamine and to allow for the formation of stable, biocompatible nanoparticles [56]. Other proteins that also contain the **KE** diad were found to play a similar role such as Alkaline Phosphatase from bovine intestinal mucosa (63). We will focus on that discovery, made during this PhD work, in chapter 3.

The mechanism by which the two amino acids in the **KE** diad act to modify the oxidation and self-assembly pathways of dopamine has been investigated by means of molecular dynamics simulations. It was found that the residence time of unoxidized dopamine was increased on a **KE** dipeptide in comparison with other dipeptides due to hydrogen bond formation between

the carboxylic group of L-Glutamic acid with the catechol OH groups in synergy with a cation- π interaction between the amino group of L-lysine and the aromatic cycle of the catechol (63).

The **KE** diad plays a clear role in the formation of dopamine based nanomaterials but it is not unique in this effect since tripeptides made from L-phenylalanine, L-aspartic acid and L-tyrosine also strongly affect the structure and the size of the oxidation product of L-tyrosine (64).

Not only molecules like surfactants and peptides but also organic molecules like folic acid allow to direct the shape of PDA based nanostructures to nanofibers (65). π - π interactions are responsible for such a size and morphology control (66).

Interestingly, when resveratrol-dopamine mixtures are oxidized by O_2 in 5:1 water: ethanol mixtures, composite nanocapsules are obtained in the absence of templating agents (67).

4. Applications of polydopamine based nanomaterials

Due to high selectivity and minimal invasiveness, photothermal therapy is emerging as a powerful technique for cancer treatment. Photothermal agents and near-infrared laser exposure allow to target specific tumour sites. A photothermal agent based on dopamine-melanin colloidal nanospheres has been developed for cancer therapy. These nanoparticles have shown good photothermal conversion capability. It was demonstrated that a NIR laser irradiation at 2 W/cm² for 500 seconds of a PDA nanoparticles suspension can produce a significant temperature increase. Compared to pure water as a negative control, the temperature of the PDA suspension increased by 33.6°C instead of 3.2°C for water alone (68). These results pave the way for eumelanin-like nanomaterials as efficient agent for cancer therapy.

Indeed using the control exerted by KE containing proteins (62) on the self-assembly and size control of PDA, we managed to prepare transferrin containing PDA based nanoparticles able to target melanoma cells, to be phagocytosed by them and able to kill them using the photothermal properties of PDA (69).

Using the antioxidant property of PDA (51), an investigation was made to study the use of PDA@NPs as scavengers of reactive oxygen species (ROS) in oxidative stress-induced periodontal diseases. Interestingly, PDA@NPs exhibited particularly good antioxidative performance (70). The antioxidant properties of PDA based nanocolloids are conserved even in the presence of a poly(ethyleneoxide) based capping layer (69).

One of the primary biological role of eumelanin is the protection of the skin against UV-induced nuclear DNA damage. A lack of eumelanin production in humans can cause severe lethal diseases. Thereby, novel synthetic routes to mimic eumelanin-like particles are widely expected. Human epidermal keratinocytes (HEKa), incubated with melanin-like particles, displayed significantly higher viability against UV irradiation than other groups including SiO₂@PDA, PDA@SiO₂, Au@NPs, all similar to melanin-like nanoparticles in size and surface charge (Fig.8) (71).

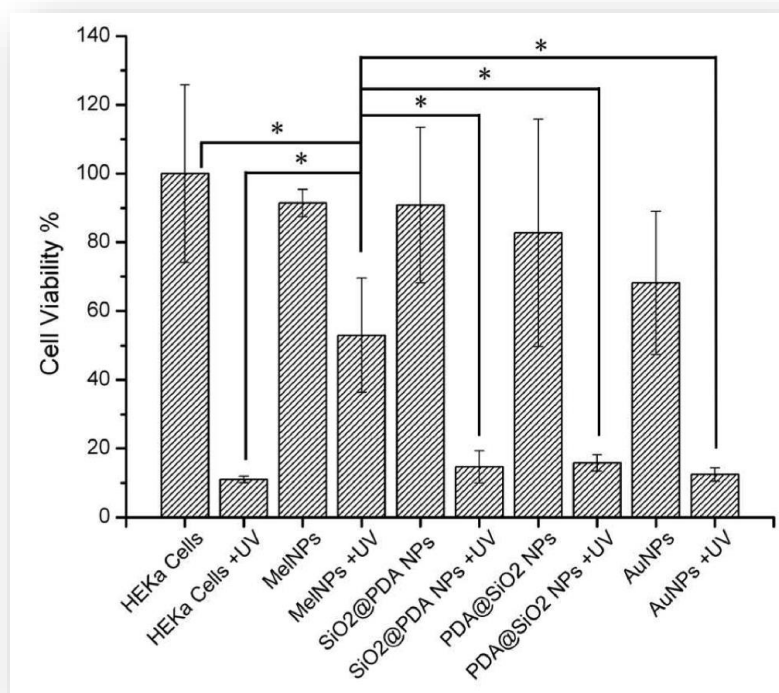


Figure 8: HEKa cell viability with and without UV following a 3 day incubation with melanin-like NPs (MeINPs), SiO₂@PDA core-shell NPs, PDA@SiO₂ core-shell NPs, Au@NPs *p<0.05. Reproduced from ref. (71) with authorization.

Due to the combination of adhesive ability and redox activity, and their strong chelation for metal cations, PDA@NPs are a promising candidate for applications in biomedicine and biodetection fields. For instance, they have been recently used as a support to load functional nanomaterials. Prussian Blue nanoparticles (PB@NPs) are good candidates as peroxidase mimics for electrochemical biosensors thanks to their excellent catalytic activity. They nevertheless have limitations: their aggregation in aqueous solution and their intrinsic color interference. An outcome consists of anchoring dispersed PB nanoparticles on the surface of PDA nanospheres. This resulted in a better dispersion in water and avoidance of the intrinsic color interference. Then the PDA/PB nanocomposites could trigger the coloration/decoloration of several substrates (72).

Because of the increase in bacterial resistance to many antibiotics, it is an urgent challenge to develop new antibacterial materials. In this context, multifunctional chitosan functionalized Chlorin e6 based magnetic polydopamine nanoparticles were constructed to fight methicillin-resistant *Staphylococcus aureus* (MRSA) infection by photodynamic therapy (73). Magnetic PDA nanoparticles prepared by mixing ferric chloride hexahydrate and dopamine, were used to improve the MRSA cells enrichment performance.

Another group demonstrated the therapeutic efficiency of the combined photodynamic and photothermal therapy from Chlorin e6 and PDA under irradiation at 665 nm on bladder cancer

cells (74). In this investigation, PDA was used for its ability to encapsulate and load drugs but also for its photothermal properties.

When PDA is synthesized using $\text{H}_2\text{O}_2\text{-Cu}^{+2}$ as the oxidant, the obtained nanoparticles are fluorescent and can be used as sensors for Al^{3+} (75). Formaldehyde sensing is possible with low interference from other gases like carbon dioxide, hydrogen sulphide, methane, benzene and ammonia when hollow PDA nanotubes are fixed on the surface of a quartz microbalance based gravimetric transducer. The selectivity for formaldehyde originates from the interaction between the aldehyde with -NH- groups present on the surface of PDA (51). The sensor was reversible for at least three exposures to gaseous formaldehyde at 30 ppm. The detection limit for formaldehyde was lower than 100 ppb.

Nanometer sized PDA fluorescent nanoparticles can also be obtained through anodic microplasma electrochemistry (75). This process allows to control the nanoparticles' size through a progressive acidification of the reaction medium to a pH value close to 5 where the spontaneous oxidation of dopamine is not possible anymore. Those nanoparticles have been shown to be sensitive sensors for uranium cations, with a detection limit equal to 2.1 mg/mL (75).

PDA based nanomaterials have been used for energy conversion processes and those applications have already been reviewed (76).

Owing to their strong absorption over the whole UV-vis part of the electromagnetic spectrum, PDA nanoparticles packed as colloidal crystals allow to absorb the scattered light which usually produces milky white colors in colloidal crystals. Centrifugation of PDA nanoparticles produced from the oxidation of dopamine in water/methanol mixtures (4/1 in volume proportion) allows to make films displaying structural colors (77) depending on the particles' diameter (78) as well on the nature of the monomer (79) used to produce the nanoparticles (either L-DOPA, dopamine or norepinephrine). Very recently, the diameter of PDA based nanoparticles and the structural color of PDA based photonic crystals has been modified by grafting poly(hydroxyethyl methacrylate) chains on PDA nanoparticles covered with an atom transfer radical polymerization (ATRP) initiator. Those PDA nanoparticles have been produced in a two-step process first starting from dopamine in the presence of Tris buffer at pH = 8.5 (dissolved O_2 being the oxidant) and following by the addition of 2-bromoisobutyryl bromide (BiBB) modified dopamine, to produce core shell nanoparticles around 220 nm in diameter, where the shell is made from BiBB-PDA acting as the ATRP initiator (80). All this research relies on the fact that PDA is closely related to eumelanin which is the material used to produce the structural colors of the male peacocks' feathers (81).

Finally, chiral PDA nanoribbons were obtained by performing the oxidation of dopamine in the presence of templates made from self-assembled phenylalanine based amphiphiles. The racemic mixture of these two amphiphiles produced flat, achiral tapes after dopamine oxidation (82).

Conclusions

Recent research has shown that PDA and similar compounds obtained through the oxidation of catecholamines appear not only to be **mussel inspired** coatings but also **eumelanin inspired colloids and nanomaterials**.

Up to now **proteins and molecules like folic acid appear to be the best candidates to allow for a fine control, protein**, or folic acid concentration dependent, of the nanoparticles shape and size. Some basic mechanistic aspects of the role of certain specific amino acid sequences (KE for instance) in the controlled oxidation and self-assembly of PDA have been acquired even if an intensive research effort is still required.

Thanks to so many properties, PDA has risen to the rank of a material of choice for surface modification. Not only is this material deposition substrate - independent, but it can itself be studied in the form of a free-standing film or as nanoparticles.

It is in this context that this thesis fits: the **study and control of PDA nanoparticles, also a comparative study of PDA synthesis protocols** and a study of the **influence of PDA in gelatin hydrogels**. The interest of these research efforts is that a better understanding of the structure of the PDA and the control of its properties will lead to a better control of its applications.

References

1. Waite JH, Tanzer ML. Polyphenolic Substance of *Mytilus edulis*: Novel Adhesive Containing L-Dopa and Hydroxyproline. *Science*. 29 mai 1981; 212(4498):1038-40.
2. Waite JH, Qin X. Polyphosphoprotein from the Adhesive Pads of *Mytilus edulis*. *Biochemistry*. 1 mars 2001; 40(9):2887-93.
3. Silverman HG, Roberto FF. Understanding marine mussel adhesion. *Mar Biotechnol N Y N*. déc 2007; 9(6):661-81.
4. Maier GP, Rapp MV, Waite JH, Israelachvili JN, Butler A. BIOLOGICAL ADHESIVES. Adaptive synergy between catechol and lysine promotes wet adhesion by surface salt displacement. *Science*. 7 août 2015; 349(6248):628-32.
5. Lee H, Dellatore SM, Miller WM, Messersmith PB. Mussel-inspired surface chemistry for multifunctional coatings. *Science*. 19 oct 2007; 318(5849):426-30.
6. Ryu JH, Messersmith PB, Lee H. Polydopamine Surface Chemistry: A Decade of Discovery. *ACS Appl Mater Interfaces*. 7 mars 2018; 10(9):7523-40.
7. Iacomino M, Paez JJ, Avolio R, Carpentieri A, Panzella L, Falco G, et al. Multifunctional Thin Films and Coatings from Caffeic Acid and a Cross-Linking Diamine. *Langmuir*. 7 mars 2017 ; 33(9):2096-102.
8. Wei Q, Becherer T, Mutihac R-C, Noeske P-LM, Paulus F, Haag R, et al. Multivalent anchoring and cross-linking of mussel-inspired antifouling surface coatings. *Biomacromolecules*. 11 août 2014; 15(8):3061-71.
9. Vecchia NFD, Avolio R, Alfè M, Errico ME, Napolitano A, d'Ischia M. Building-Block Diversity in Polydopamine Underpins a Multifunctional Eumelanin-Type Platform Tunable Through a Quinone Control Point. *Adv Funct Mater*. 2013; 23(10):1331-40.
10. Liebscher J, Mrówczyński R, Scheidt HA, Filip C, Hädade ND, Turcu R, et al. Structure of polydopamine: a never-ending story? *Langmuir ACS J Surf Colloids*. 20 août 2013; 29(33):10539-48.
11. Hong S, Na YS, Choi S, Song IT, Kim WY, Lee H. Non-Covalent Self-Assembly and Covalent Polymerization Co-Contribute to Polydopamine Formation. *Adv Funct Mater*. 2012; 22(22):4711-7.
12. Hong S, Wang Y, Park SY, Lee H. Progressive fuzzy cation- π assembly of biological catecholamines. *Phys. Chem. A* 2020, 124, 17, 3445–3459.
13. Holcomb NC, Bautista R-M, Jarrett SG, Carter KM, Gober MK, D'Orazio JA. cAMP-mediated regulation of melanocyte genomic instability: A melanoma-preventive strategy. *Adv Protein Chem Struct Biol*. 2019; 115:247-95.
14. Meredith P, Sarna T. The physical and chemical properties of eumelanin. *Pigment Cell Res*. déc 2006; 19(6):572-94.
15. d'Ischia M, Wakamatsu K, Napolitano A, Briganti S, Garcia-Borrón J-C, Kovacs D, et al. Melanins and melanogenesis: methods, standards, protocols. *Pigment Cell Melanoma Res*. sept 2013; 26(5):616-33.
16. Simon JD, Peles DN. The red and the black. *Acc Chem Res*. 16 nov 2010;43(11):1452-60

17. Riesz JJ, Gilmore JB, McKenzie RH, Powell BJ, Pederson MR, Meredith P. Transition dipole strength of eumelanin. *Phys Rev E*. 15 août 2007; 76(2):021915.
18. Ball V. Determination of the extinction coefficient of “polydopamine” films obtained by using NaIO₄ as the oxidant. *Mater Chem Phys*. 15 janv 2017; 186:546-51.
19. Bernsmann F, Ponche A, Ringwald C, Hemmerlé J, Raya J, Bechinger B, et al. Characterization of Dopamine–Melanin Growth on Silicon Oxide. *J Phys Chem C*. 14 mai 2009;113(19):8234-42
20. Meredith P, Riesz J. Radiative relaxation quantum yields for synthetic eumelanin. *Photochem Photobiol*. févr 2004; 79(2):211-6.
21. Chen C-T. Eumelanin and polydopamine: self-assembly, structure, and properties. Thesis: Ph. D., Massachusetts Institute of Technology, Department of Civil and Environmental Engineering, 2016.
22. Chen C-T, Buehler MJ. Polydopamine and eumelanin models in various oxidation states. *Phys Chem Chem Phys*. 14 nov 2018; 20(44):28135-43.
23. Kaxiras E, Tsolakidis A, Zonios G, Meng S. Structural model of eumelanin. *Phys Rev Lett*. 24 nov 2006; 97(21):218102.
24. Chen C-T, Ball V, de Almeida Gracio JJ, Singh MK, Toniazzi V, Ruch D, et al. Self-Assembly of Tetramers of 5,6-Dihydroxyindole Explains the Primary Physical Properties of Eumelanin: Experiment, Simulation, and Design. *ACS Nano*. 26 févr 2013; 7(2):1524-32.
25. Alfieri ML, Micillo R, Panzella L, Crescenzi O, Oscurato SL, Maddalena P, et al. Structural Basis of Polydopamine Film Formation: Probing 5,6-Dihydroxyindole-Based Eumelanin Type Units and the Porphyrin Issue. *ACS Appl Mater Interfaces*. 7 mars 2018; 10(9):7670-80.
26. Clancy CMR, Simon JD. Ultrastructural Organization of Eumelanin from *Sepia officinalis* Measured by Atomic Force Microscopy. *Biochemistry*. 1 nov 2001; 40(44):13353-60.
27. Richardson JJ, Cui J, Björnmalm M, Braunger JA, Ejima H, Caruso F. Innovation in Layer-by-Layer Assembly. *Chem Rev*. 14 déc 2016; 116(23):14828-67.
28. Bain CD, Troughton EB, Tao YT, Evall J, Whitesides GM, Nuzzo RG. Formation of monolayer films by the spontaneous assembly of organic thiols from solution onto gold. *J Am Chem Soc*. 1 janv 1989; 111(1):321-35.
29. Shen B, Xiong B, Wu H. Convenient surface functionalization of whole-Teflon chips with polydopamine coating. *Biomicrofluidics*. juill 2015; 9(4):044111.
30. Talon, I.; Schneider, A.; Ball V.; Hemmerle J. (2020) An original way of biological functionalisation of modified PTFE biomaterial. *J. Surg. Res*. 251, 254-261.
31. Ponzio F, Payamyar P, Schneider A, Winterhalter M, Bour J, Addiego F, et al. Polydopamine Films from the Forgotten Air/Water Interface. *J Phys Chem Lett*. 2 oct 2014; 5(19):3436-40.
32. Gao ZF, Wang XY, Gao JB, Xia F. Rapid preparation of polydopamine coating as a multifunctional hair dye. *RSC Adv*. 25 juin 2019; 9(35):20492-6.
33. Xu Q, Kong Q, Liu Z, Zhang J, Wang X, Liu R, et al. Polydopamine-coated cellulose microfibrillated membrane as high performance lithium-ion battery separator. *RSC Adv*. 20 janv 2014; 4(16):7845-50.

34. Lu Z, Xiao J, Wang Y, Meng M. In situ synthesis of silver nanoparticles uniformly distributed on polydopamine-coated silk fibers for antibacterial application. *J Colloid Interface Sci.* 15 août 2015; 452:8-14.
35. Wei Q, Zhang F, Li J, Li B, Zhao C. Oxidant-induced dopamine polymerization for multifunctional coatings. *Polym Chem.* 12 oct 2010; 1(9):1430-3.
36. Feng Y, Zheng Y, Rahman ZU, Wang D, Zhou F, Liu W. Paper-based triboelectric nanogenerators and their application in self-powered anticorrosion and antifouling. *J Mater Chem A.* 22 nov 2016; 4(46):18022-30.
37. Kim BH, Lee DH, Kim JY, Shin DO, Jeong HY, Hong S, et al. Mussel-inspired block copolymer lithography for low surface energy materials of teflon, graphene, and gold. *Adv Mater Deerfield Beach Fla.* 15 déc 2011; 23(47):5618-22.
38. Thakur VK, Vennerberg D, Kessler MR. Green Aqueous Surface Modification of Polypropylene for Novel Polymer Nanocomposites. *ACS Appl Mater Interfaces.* 25 juin 2014; 6(12):9349-56.
39. You I, Seo YC, Lee H. Material-independent fabrication of superhydrophobic surfaces by mussel-inspired polydopamine. *RSC Adv.* 6 févr 2014; 4(20):10330-3.
40. Ball, V., Del Frari, D., Michel, M. et al. Deposition Mechanism and Properties of Thin Polydopamine Films for High Added Value Applications in Surface Science at the Nanoscale. *BioNanoSci.* 2, 16–34 (2012).
41. Liu Y, Ai K, Lu L. Polydopamine and Its Derivative Materials: Synthesis and Promising Applications in Energy, Environmental, and Biomedical Fields. *Chem Rev.* 14 mai 2014; 114(9):5057-115.
42. Lee YB, Shin YM, Lee J-H, Jun I, Kang JK, Park J-C, et al. Polydopamine-mediated immobilization of multiple bioactive molecules for the development of functional vascular graft materials. *Biomaterials.* nov 2012; 33(33):8343-52.
43. Lee H, Rho J, Messersmith PB. Facile Conjugation of Biomolecules onto Surfaces via Mussel Adhesive Protein Inspired Coatings. *Adv Mater Deerfield Beach Fla.* 26 janv 2009; 21(4):431-4.
44. Moon J, Byun J, Kim H, Jeong J, Lim E-K, Jung J, et al. Surface-Independent and Oriented Immobilization of Antibody via One-Step Polydopamine/Protein G Coating: Application to Influenza Virus Immunoassay. *Macromol Biosci.* 2019; 19(6):e1800486.
45. Ball V, Frari DD, Toniazio V, Ruch D. Kinetics of polydopamine film deposition as a function of pH and dopamine concentration: Insights in the polydopamine deposition mechanism. *J Colloid Interface Sci.* 15 nov 2012; 386(1):366-72.
46. Lin, J.; Daboss, S.; Blaimer, D.; Kranz, C. Micro-Structured Polydopamine Films via Pulsed Electrochemical Deposition. *Nanomaterials.* 2019, 9, 242.
47. Han X, Tang F, Jin Z. Free-standing polydopamine films generated in the presence of different metallic ions: the comparison of reaction process and film properties. *RSC Adv.* 17 mai 2018; 8(33):18347-54.
48. Bridelli MG. Self-assembly of melanin studied by laser light scattering. *Biophys Chem.* 27 juill 1998; 73(3):227-39.
49. Ball V. Impedance spectroscopy and zeta potential titration of dopa-melanin films produced by oxidation of dopamine. *Colloids Surf Physicochem Eng Asp.* 20 juin 2010; 363(1):92-7.

50. Bronze-Uhle E.S, Paulin J.V, Piacenti-Silva M, Battachio C, Rocco M.L.M, de Oliveira Graeff C.F. Melanin synthesis under oxygen pressure. *Polymer International*. Nov 2016; 65(11):1339-1346.
51. Ju K-Y, Lee Y, Lee S, Park SB, Lee J-K. Bioinspired Polymerization of Dopamine to Generate Melanin-Like Nanoparticles Having an Excellent Free-Radical-Scavenging Property. *Biomacromolecules*. 14 mars 2011; 12(3):625-32.
52. Arzillo M, Mangiapia G, Pezzella A, Heenan RK, Radulescu A, Paduano L, et al. Eumelanin Buildup on the Nanoscale: Aggregate Growth/Assembly and Visible Absorption Development in Biomimetic 5,6-Dihydroxyindole Polymerization. *Biomacromolecules*. 13 août 2012; 13(8):2379-90.
53. Ponzio F, Bertani P, Ball V. Role of surfactants in the control of dopamine-eumelanin particle size and in the inhibition of film deposition at solid-liquid interfaces. *J Colloid Interface Sci*. 1 oct 2014; 431:176-9.
54. Schneider A, Hemmerlé J, Allais M, Didierjean J, Michel M, d'Ischia M, et al. Boric Acid as an Efficient Agent for the Control of Polydopamine Self-Assembly and Surface Properties. *ACS Appl Mater Interfaces*. 7 mars 2018; 10(9):7574-80.
55. Salomäki M, Ouvinen T, Marttila L, Kivelä H, Leiro J, Mäkilä E, Lukkari J. Polydopamine Nanoparticles Prepared Using Redox-Active Transition Metals. *J. Phys. Chem. B* 2019, 123, 11, 2513–2524.
56. Ponzio F, Barthès J, Bour J, Michel M, Bertani P, Hemmerlé J, et al. Oxidant Control of Polydopamine Surface Chemistry in Acids: A Mechanism-Based Entry to Superhydrophilic-Superoleophobic Coatings. *Chem Mater*. 12 juill 2016; 28(13):4697-705.
57. Wang X, Chen Z, Yang P, Hu J, Wang Z, Li Y. Size control synthesis of melanin-like polydopamine nanoparticles by tuning radicals. *Polym Chem*. 2019;10(30):4194-200.
58. Liu F, He X, Zhang J, Chen H, Zhang H, Wang Z. Controllable synthesis of polydopamine nanoparticles in microemulsions with pH-activatable properties for cancer detection and treatment. *J Mater Chem B*. 11 août 2015; 3(33):6731-9.
59. della Vecchia NF, Cerruti P, Gentile G, Errico ME, Ambrogi V, D'Errico G, et al. Artificial biomelanin: highly light-absorbing nano-sized eumelanin by biomimetic synthesis in chicken egg white. *Biomacromolecules*. 13 oct 2014; 15(10):3811-6.
60. Strube OI, Büngeler A, Bremser W. Site-specific in situ synthesis of eumelanin nanoparticles by an enzymatic autodeposition-like process. *Biomacromolecules*. 11 mai 2015; 16(5):1608-13.
61. Strube OI, Büngeler A, Bremser W. Enzyme-Mediated In Situ Synthesis and Deposition of Nonaggregated Melanin Protoparticles. *Macromol Mater Eng*. 2016; 301(7):801-4.
62. Bergtold C, Hauser D, Chaumont A, El Yakhlifi S, Mateescu M, Meyer F, et al. Mimicking the Chemistry of Natural Eumelanin Synthesis: The KE Sequence in Polypeptides and in Proteins Allows for a Specific Control of Nanosized Functional Polydopamine Formation. *Biomacromolecules*. 10 2018;19(9):3693-704.
63. El Yakhlifi S, Ihiawakrim D, Ersen O, Ball V. Enzymatically Active Polydopamine @ Alkaline Phosphatase Nanoparticles Produced by NaIO₄ Oxidation of Dopamine. *Biomimetics*. déc 2018; 3(4):36.
64. Lampel A, McPhee SA, Park HA, et al. Polymeric peptide pigments with sequence-encoded properties. *Science*. 2017; 356(6342):1064-1068.

65. Yu X, Fan H, Wang L, Jin Z. Formation of polydopamine nanofibers with the aid of folic acid. *Angew Chem Int Ed Engl*. 10 nov 2014; 53(46):12600-4.
66. Fan H, Yu X, Liu Y, Shi Z, Liu H, Nie Z, et al. Folic acid–polydopamine nanofibers show enhanced ordered-stacking via π – π interactions. *Soft Matter*. 3 juin 2015; 11(23):4621-9.
67. Amin DR, Higginson CJ, Korpusik AB, Gonthier AR, Messersmith PB. Untemplated Resveratrol-Mediated Polydopamine Nanocapsule Formation. *ACS Appl Mater Interfaces*. 2018;10(40):34792-34801.
68. Liu Y, Ai K, Liu J, Deng M, He Y, Lu L. Dopamine-melanin colloidal nanospheres: an efficient near-infrared photothermal therapeutic agent for in vivo cancer therapy. *Adv Mater*. 2013;25(9):1353-1359.
69. Hauser D, Estermann M, Milosevic A, et al. Polydopamine/Transferrin Hybrid Nanoparticles for Targeted Cell-Killing. *Nanomaterials (Basel)*. 2018;8(12):1065.
70. Bao X, Zhao J, Sun J, Hu M, Yang X. Polydopamine Nanoparticles as Efficient Scavengers for Reactive Oxygen Species in Periodontal Disease. *ACS Nano*. 2018;12(9):8882-8892.
71. Huang Y, Li Y, Hu Z, et al. Mimicking Melanosomes: Polydopamine Nanoparticles as Artificial Microparasols. *ACS Cent Sci*. 2017;3(6):564-569.
72. Ma H, He Y, Liu H, Xu L, Li J, Huang M, et al. Anchoring of Prussian blue nanoparticles on polydopamine nanospheres as an efficient peroxidase mimetic for colorimetric sensing. *Colloids Surf Physicochem Eng Asp*. 20 sept 2019; 577:622-9.
73. Lu C, Sun F, Liu Y, Xiao Y, Qiu Y, Mu H, et al. Versatile Chlorin e6-based magnetic polydopamine nanoparticles for effectively capturing and killing MRSA. *Carbohydr Polym*. 15 août 2019; 218:289-98.
74. Poinard B, Neo SZY, Yeo ELL, Heng HPS, Neoh KG, Kah JCY. Polydopamine Nanoparticles Enhance Drug Release for Combined Photodynamic and Photothermal Therapy. *ACS Appl Mater Interfaces*. 27 juin 2018; 10(25):21125-36.
75. Wang Z, Xu C, Lu Y, Wei G, Ye G, Sun T, et al. Microplasma electrochemistry controlled rapid preparation of fluorescent polydopamine nanoparticles and their application in uranium detection. *Chem Eng J*. 15 juill 2018; 344:480-6.
76. Qu K, Wang Y, Vasileff A, Jiao Y, Chen H, Zheng Y. Polydopamine-inspired nanomaterials for energy conversion and storage. *J Mater Chem A*. 13 nov 2018; 6(44):21827-46.
77. Xiao M, Li Y, Allen MC, et al. Bio-Inspired Structural Colors Produced via Self-Assembly of Synthetic Melanin Nanoparticles. *ACS Nano*. 2015;9(5):5454-5460.
78. Kawamura A, Kohri M, Yoshioka S, Taniguchi T, Kishikawa K. Structural Color Tuning: Mixing Melanin-Like Particles with Different Diameters to Create Neutral Colors. *Langmuir*. 18 avr 2017; 33(15):3824-30.
79. Iwasaki T, Tamai Y, Yamamoto M, Taniguchi T, Kishikawa K, Kohri M. Melanin Precursor Influence on Structural Colors from Artificial Melanin Particles: PolyDOPA, Polydopamine, and Polynorepinephrine. *Langmuir*. 2 oct 2018; 34(39):11814-21.
80. Kohri M, Uradokoro K, Nannichi Y, Kawamura A, Taniguchi T, Kishikawa K. Hairy Polydopamine Particles as Platforms for Photonic and Magnetic Materials. *Photonics*. déc 2018; 5(4):36.

81. Zi J, Yu X, Li Y, Hu X, Xu C, Wang X, et al. Coloration strategies in peacock feathers. *Proc Natl Acad Sci.* 28 oct 2003; 100(22):12576-8.
82. Awasthi AK, Bhagat SD, Ramakrishnan R, Srivastava A. Chirally Twisted Ultrathin Polydopamine Nanoribbons: Synthesis and Spontaneous Assembly of Silver Nanoparticles on Them. *Chem – Eur J.* 8 oct 2019; 25(56):12905-10.

List of the figures – Chapter 1

Figure 1: a) Anatomy of <i>M. edulis</i> mussel and byssus structures. b) Location of adhesive-related proteins identified in the byssus of <i>M. edulis</i>	20
Figure 2: : Simplified overall view of main reaction pathways involved in polydopamine formation. A proposed origin of the eumelanin markers, PDCA and PTCA, is highlighted	22
Figure 3: Chemical pathways leading to eumelanin and to pheomelanin and the enzymes (in red characters) implied in the different chemical steps. Modified from ref. [13] with authorization. Nomenclature: DOPA: 3,4-dihydroxyphenylalanine, TRP-1: Tyrosinase related	23
Figure 4: Polydopamine coating method.....	26
Figure 5: A : Rate of PDA formation as followed by UV-vis spectroscopy at $\lambda = 350$ nm as a function of the concentration in SDS B: Evolution of the size of PDA aggregates as a function of the surfactant concentration in the case of SDS.....	28
Figure 6: Interaction of boric acid with dopamine and its influence on the electrochemical behavior of dopamine.....	29
Figure 7: Schematic illustration of the size-controlled synthesis of PDA NPs.....	30
Figure 8: HEKa cell viability without UV following a 3 day incubation with melanin-like NPs.....	32

List of the tables – Chapter 1

Table 1: Exhaustive list of materials that can be modified by PDA.....	25
Table 2: Comparaison of two surface modification methods: LBL versus PDA deposition.....	25

Chapter 2

« In the middle of difficulty lies opportunity »

Albert Einstein

Chapter 2:

Materials and methods

INTRODUCTION	44
1. MATERIALS	45
1.1. MATERIALS FOR NANOPARTICLES SYNTHESIS	45
1.2. MATERIALS FOR FILMS FORMATION	45
1.3. MATERIALS FOR GELS FORMATION	46
2. PREPARATION OF THE SAMPLES	46
2.1. FORMATION OF THE PDA@ALP NANOPARTICLES	46
2.2. FORMATION OF THE (PAH)@PDA FILMS	47
2.3. FORMATION OF THE PDA FILMS	48
2.4. FORMATION OF THE GELATIN@PDA GELS	50
3. SAMPLES CHARACTERIZATION	51
3.1. CHARACTERIZATION OF THE PDA@ALP NANOPARTICLES	51
3.1.1. Ultraviolet-Visible (UV-Vis) spectroscopy	51
3.1.2. Enzymatic activity of the PDA@ALP nanoparticles	52
3.1.3. Transmission electron microscopy (TEM)	53
3.1.4. Atomic force microscopy (AFM)	54
3.1.5. Dynamic light scattering (DLS) – Zeta Potential	54
3.2. CHARACTERIZATION OF THE DOPA/OXIDANT FILMS	54
3.2.1. Atomic force microscopy (AFM)	54
3.2.2. Static contact angle measurements	54
3.2.3. X-Ray photoelectron spectroscopy (XPS)	55
3.2.4. Cyclic voltammetry (CV)	55
3.2.5. Antioxidant analysis of the PDA@oxidant films	55
3.2.6. Matrix-assisted laser desorption mass spectrometry with time of flight analysis	56
3.3. CHARACTERIZATION OF THE GEL@PDA GELS	57
3.3.1. Rheology	57
3.3.2. Scanning electron microscopy (SEM)	57
CONCLUSION	59
REFERENCES	60
LIST OF THE FIGURES – CHAPTER 2	61
LIST OF THE TABLES – CHAPTER 2	61

Chapter 2 :

Materials and methods

Introduction

The aim of this chapter is to list detailed information in order to specify the context of each experiments.

First, the **materials** used during this thesis will be presented.

Then, we will give a description of the **nanoparticle's synthesis** (chapter 3), the **film** (chapter 4) and **gel** (chapter 5) preparation, and their associated **characterization techniques**.

Finally, a detailed **description of the protocols** for the formation of nanoparticles, films and gels will be presented.

1. Materials

All chemicals were purchased and used without further purification.

All solutions were made from ultra-pure water (Milli Plus, Millipore, Billerica, MA, USA) with a resistivity of 18.2 M Ω .cm.

1.1. Materials for nanoparticles synthesis

Dopamine-hydrochloride (Sigma Aldrich, ref. H8502) was used to synthesize polydopamine nanoparticles (PDA@NPs).

Two buffers were used to perform the synthesis of polydopamine nanoparticles (PDA@NPs):

- 50 mM Tris(hydroxymethyl)aminomethane (Euromedex, Schiltigheim, France) at pH 8.5
- 50 mM sodium acetate buffer (Sigma Aldrich, ref. W302406) at pH 5.0

The pH of each buffer was adjusted with concentrated hydrochloric acid, and checked with a Hannah 802 pH meter, calibrated in the pH range between 4.0 and 7.0, or 7.0 and 9.0, for the sodium acetate and Tris buffer, respectively.

Sodium periodate (NaIO₄, Sigma Aldrich, ref. 311448) was used as an oxidant in the case where the synthesis was performed in the presence of sodium acetate buffer.

p-nitrophenyl phosphate (PNP, ref. N7653), and **alkaline phosphatase from bovine intestinal mucosa** (ALP, ref. P7640) were all purchased from Sigma-Aldrich (L'isle D'Abeau Chesnes, France).

Poly(allylamine hydrochloride) (PAH, ref. 283215, MW= 17500 g/mol as measured by gel permeation chromatography) was from Sigma-Aldrich?

Dialysis tubing, with a molecular weight cut-off at 300 kDa, was purchased from Spectrum Labs (Repligen group, Waltham, MA, USA).

1.2. Materials for films formation

Dopamine-hydrochloride, sodium periodate, anhydrous sodium acetate and Tris(hydroxymethyl)aminomethane are the same materials as those described in section 1.1.

Two other oxidants were used for the deposition of PDA films, all purchased from Sigma-Aldrich (L'isle d'Abeau Chesnes, France):

- **ammonium persulfate** ((NH₄)₂ S₂O₈, ref. 1257273)

- **copper (II) sulfate** (CuSO_4 , anhydrous, ref. 61230) mixed with **hydrogen peroxide** (H_2O_2 , ref. H1009)

2,2-diphenyl-1-picrylhydrazyl (Sigma-Aldrich, ref. 257621) was employed for antioxidant analysis.

Films were deposited on gold coated mica wafers for XPS analysis, on quartz slides (4 cm × 1 cm, Thuet, Blodelsheim, France) for characterization by UV-Vis spectroscopy, and deposited on glass slides for AFM, contact angle studies, and for antioxidant investigation.

1.3. Materials for gels formation

Dopamine-hydrochloride, sodium periodate, anhydrous sodium acetate are the same materials as those described in 1.1.

Gelatin B from bovine skin is purchased from Sigma Aldrich (ref. G9382, lot 051M0012V).

The table below gives a summary of all the chemical compounds as well as their abbreviations.

Materials	Abbreviations
Dopamine-HCL	Dopamine
Tris(hydroxymethyl)aminomethane	Tris buffer
Anhydrous sodium acetate	Sodium acetate
Sodium periodate	NaIO_4
Copper (II) sulfate	H_2O_2
Hydrogen peroxide	CuSO_4
Ammonium persulfate	$(\text{NH}_4)_2 \text{S}_2\text{O}_8$
alkaline phosphatase from bovine intestinal mucosa	ALP
<i>p</i> -nitrophenyl phosphate	PNP
Poly(allylamine hydrochloride)	PAH
2,2-diphenyl-1-picrylhydrazyl	DPPH
Gelatin type B	Gelatin

Table 1: Chemicals used in this investigation

2. Preparation of the samples

2.1. Formation of the PDA@ALP nanoparticles

The PDA nanoparticles were prepared by dissolving dopamine at 2mg/mL in sodium acetate buffer, then adding an appropriate volume of NaIO_4 solution at 0.1 mol/L under continuous

stirring, at room temperature (17–20 °C). The final NaIO₄ concentration was equal to 10⁻² mol/L.

Alkaline phosphatase was first dissolved in sodium acetate buffer without any stirring. Then, dopamine was added under continuous stirring to reach a final concentration of 2 mg/mL (10.6 mM). Directly after that, a small amount of NaIO₄ (at 0.1 mol/L) was added, always under continuous stirring (Figure 1). The oxidation of the dopamine + Alp blend was allowed for 6 h at room temperature (17–20 °C). The final concentration of oxidant was 20 mM in all experiments, whereas the ALP concentration was changed from 0 (reference experiment) to 4 mg/mL.

After synthesis, the solution was put in a dialysis tubing and dialyzed against Tris buffer for approximately 24 h, and with three buffer changes. At the end, the solution of PDA particles was either stored at 4 °C in a glass beaker, or immediately used for characterization experiments. Note that dialysis was performed against Tris buffer and not against sodium acetate buffer because the later one is not at the optimal pH for enzymatic assays of ALP having maximal activity at a pH close to 8.

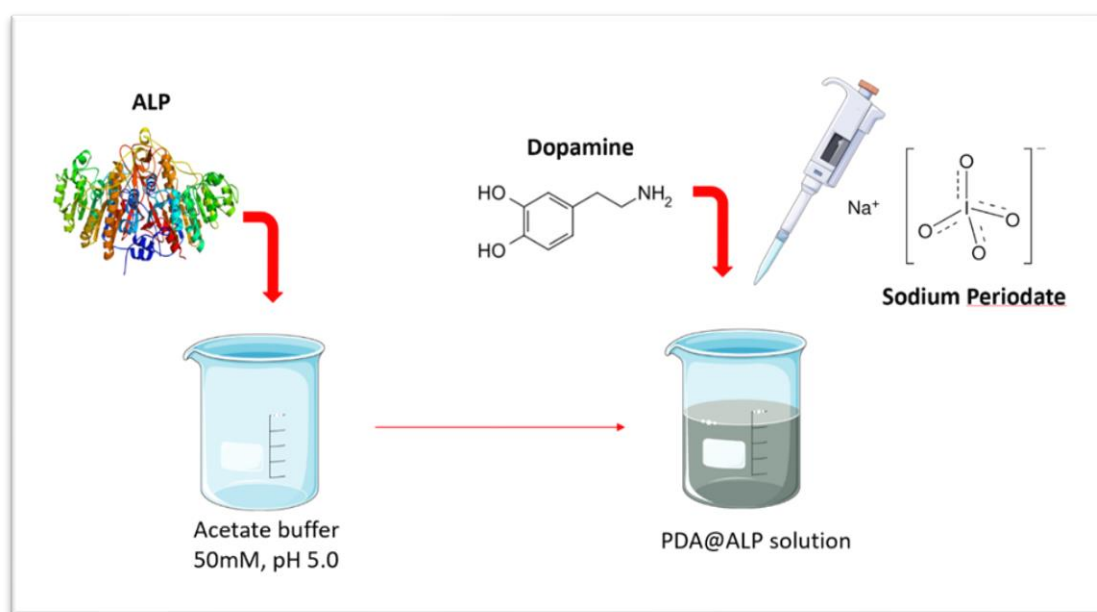


Figure 1: illustration of the PDA@ALP nanoparticles preparation method.

2.2. Formation of the (PAH)@PDA films

The (PAH)@PDA films were prepared with the layer-by-layer method as schematically represented in Figure 2.

The PDA@ALP nanoparticles, obtained in the presence of ALP at 1 mg/mL after 6 h of dopamine oxidation and intensive dialysis against Tris buffer, were used to deposit polyelectrolyte multilayer films (1,2) in alternance with PAH at 1 mg/mL in the same buffer as a polycation.

The films were deposited on plasma-cleaned quartz slides (air plasma, Harrick PDC-32G-2 plasma cleaner) using a deposition time of 5 min per deposition step, and subsequent rinsing with 50 mM Tris buffer.

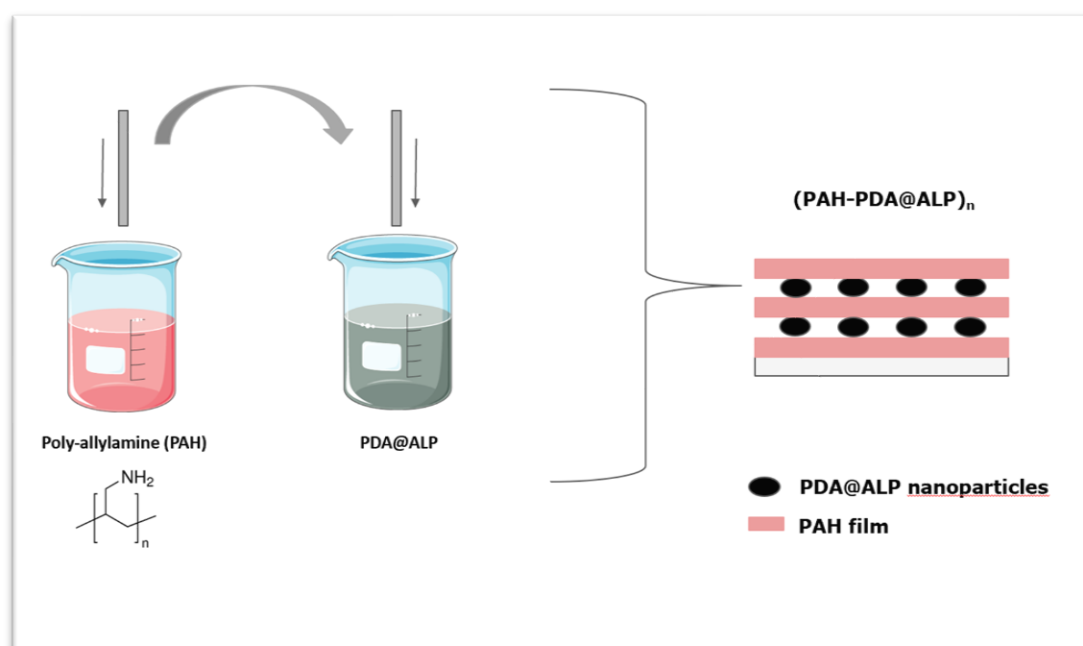


Figure 2: illustration of the (PAH@PDA)_n films preparation using the LBL deposition method.

2.3. Formation of the PDA films

Four different oxidants were used to induce PDA film deposition in order to compare their effect-in relation with their standard redox potential of mechanism of oxidation-on the composition and properties of the obtained films. All the oxidation experiments were conducted at room temperature, (20±1) °C.

Whatever the used oxidant, plasma cleaned (PDC-32G plasma cleaner, Harrick Plasma, USA) glass slides (76 mm x 26 mm) were placed vertically in the dopamine solutions before the addition of the oxidant solutions prepared as described below. In these conditions and in the used flasks, the surface area of the glass slides in contact with the dopamine + oxidant solution was of 45mm x 26mm. To have a good estimation of the influence of the oxidant on the quantitative anti-oxidant effect, it was mandatory to have films deposited on a constant nominal surface area, even if the films roughness may be oxidant dependant and will probably influence the surface density of available anti-oxidant groups.

The deposition process of PDA@oxidant films was stopped after 3 or 8h by removing the glass slides from the reactive solution and intensive rinse with distilled water. Whatever the used oxidant, the final dopamine concentration was equal to 1 mg/mL.

a) Auto-oxidation O₂ with Tris buffer

50 mg of dopamine were dissolved in 50 mL Tris buffer at pH = 8.5 without any additional step.

b) Sodium periodate NaIO_4 and ammonium persulfate $(\text{NH}_4)_2\text{S}_2\text{O}_8$

50 mg of dopamine were dissolved in 45 mL sodium acetate buffer at pH = 5.0

At time $t=0$ of the deposition experiments, 5 mL of the NaIO_4 or $(\text{NH}_4)_2\text{S}_2\text{O}_8$ was added.

The oxidant solution was prepared at 0.1 mol/L, to reach a final oxidant concentration of 10×10^{-3} mol/L by adding 5 mL of the oxidant in the 45 mL of dopamine.

c) Copper sulfate $\text{CuSO}_4 + \text{H}_2\text{O}_2$

In the case of $\text{CuSO}_4 + \text{H}_2\text{O}_2$, the molar ratio of hydrogen peroxide to copper was equal to one.

50 mg of dopamine were dissolved in 25 mL sodium acetate buffer at pH = 8.5.

At time $t=0$ of the deposition experiments, 25 mL of the $\text{CuSO}_4 + \text{H}_2\text{O}_2$ mixture was added.

Hence, in all film deposition experiments (Figure 3) the dopamine concentration was of 1 mg/mL, namely 5.3×10^{-3} mol/L, implying a constant oxidant / dopamine molar ratio of 1.9. This oxidant/dopamine molar ratio is the same as the one used in a previous investigation performed in our laboratory (3).

The same procedures were used for the films analysed by Atomic force microscopy (AFM) and for the antioxidant tests.

For the X-ray photoelectron spectroscopy (XPS) characterization, the PDA films were deposited on a gold covered substrate to avoid the presence of silica in the penetration depth region of the X-ray beam. Indeed, the presence of silica will unavoidably modify the O/C ratio we aim to determine, as well as the C/N ratio to characterize the obtained PDA films.

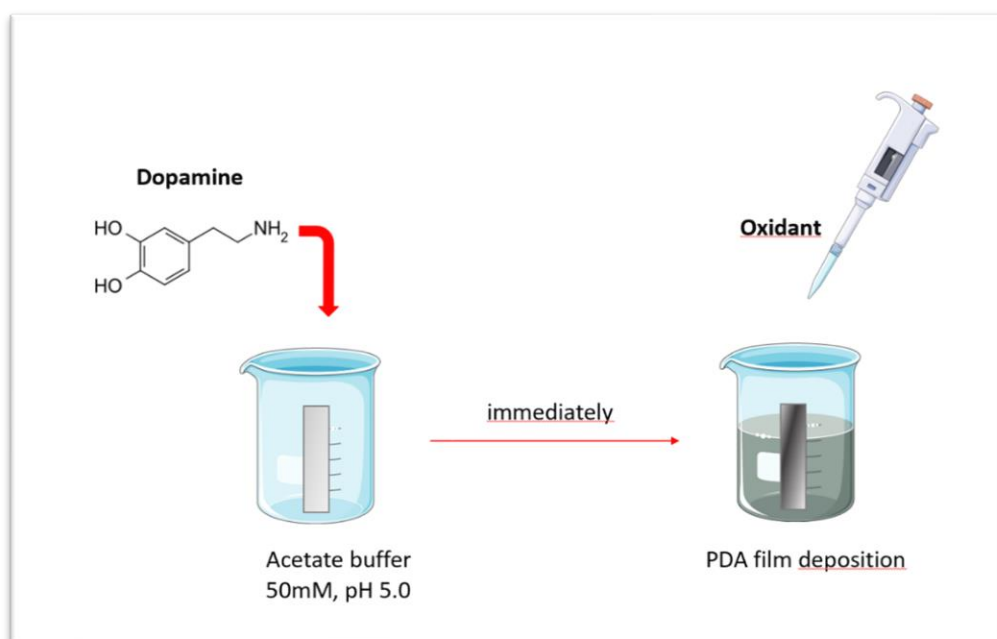


Figure 3: illustration of the PDA films preparation with sodium periodate.

The table below gives an overview of the four oxidants investigated.

dopa/oxidant	Materials	Method
dopa@Tris	<ul style="list-style-type: none"> Dopamine 50mg Tris 50 mM pH 8.5, Volume = 50 mL 	Dissolution of dopamine in Tris buffer in a glass beaker covered by an aluminium with small holes
dopa@NaIO ₄	<ul style="list-style-type: none"> Dopamine 50mg Sodium acetate buffer 50mM pH 5.0, Volume = 45 mL NaIO₄ 100mM Masse = 2,139g Volume = 100 mL buffer 	Dissolution of dopamine in 45 mL buffer then adding of 5 mL NaIO ₄
dopa@ CuSO ₄ +H ₂ O ₂	<ul style="list-style-type: none"> Dopamine 50mg Preparation of CuSO₄+H₂O₂ mixture: Mass (CuSO₄) = 0.399g Volume buffer = 247,5 mL Volume H₂O₂ = 2,5 mL 	Dissolution of dopamine in 25 mL buffer then adding 25 mL of the mixture CuSO ₄ +H ₂ O ₂
dopa@(NH ₄) ₂ S ₂ O ₈	<ul style="list-style-type: none"> Dopamine 50mg (NH₄)₂S₂O₈ 100mM Mass = 1,141g Volume buffer = 50 mL 	Dissolution of dopamine in 45 mL buffer and then adding of 5 mL of (NH ₄) ₂ S ₂ O ₈

Table 2: Summary of the PDA film preparation in the presence of different oxidants.

2.4. Formation of the gelatin@PDA gels

a) Gelatin gel as reference

The reference for comparison of the effect of adding PDA was prepared in this way: 5.0 g of gelatin was dissolved in 50 ml of sodium acetate buffer at 75 °C, to reach a 10% (w/v) concentration.

b) Gelatin@PDA gels

Gelatin (5.0 g) was dissolved in 40 mL of sodium acetate buffer at 75 °C.

Dopamine (weighted to reach the desired concentration) was dissolved in 5 mL sodium acetate buffer at room temperature.

Then, the dopamine solution was added dropwise to the gelatin dissolved solution. Finally, 5 mL of sodium periodate NaIO_4 (100mM) was added in this gelatin-dopamine solution to induce PDA formation, to reach a 10% (w/v) gelatin concentration, and a 10 mM NaIO_4 concentration (Figure 4).

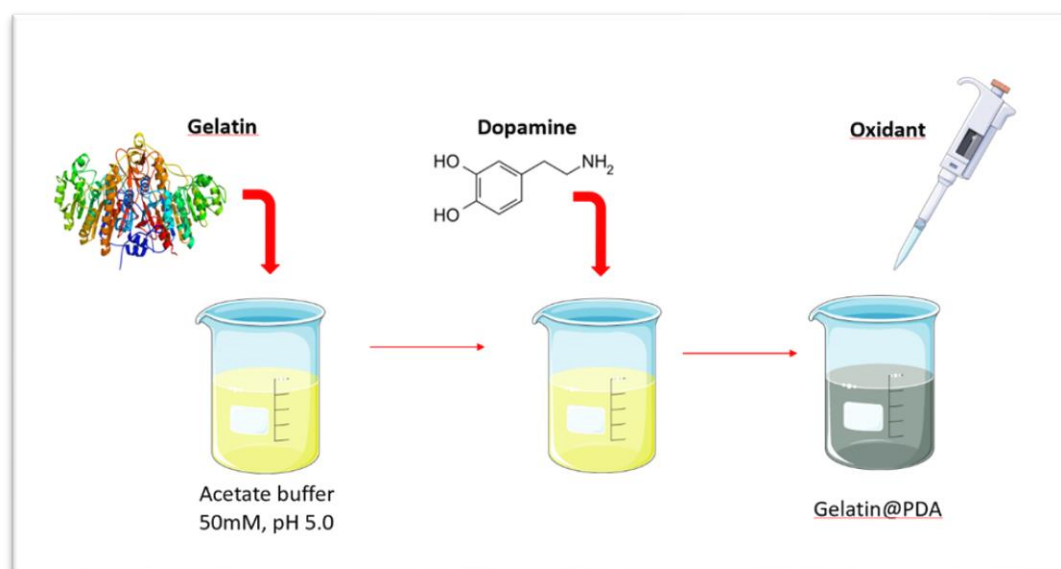


Figure 4: illustration of the gelatin@PDA gel preparation.

3. Samples characterization

3.1. Characterization of the PDA@ALP nanoparticles

3.1.1. Ultraviolet-Visible (UV-Vis) spectroscopy

a) Analysis of PDA@ALP nanoparticles

Since dopamine does not absorb at $\lambda = 500$ nm, and this wavelength is characteristic of the maximal solar emission, we followed the oxidation kinetics of dopamine in the absence or presence of ALP at this particular wavelength using an ultraviolet-visible UV Vis spectrophotometer (SAFAS, Monaco), with the reference cuvette containing either Tris buffer or sodium acetate buffer, depending on the current study.

b) Analysis of the (PAH)@PDA films

The absorption spectrum of the dried (PAH)@PDA films (on quartz slides) was measured with the same spectrophotometer every two layer pairs, using a cleaned quartz slide as the reference, to follow the regular deposition of PDA@ALP nanoparticles and of PAH. The film

deposition always started with the adsorption of the polycation PAH, owing to the negative charge of the quartz substrate under these conditions.

3.1.2. Enzymatic activity of the PDA@ALP nanoparticles

a) Analysis of the PDA@ALP nanoparticles

The enzymatic activity of the solutions containing the PDA@ALP nanoparticles was measured by following the production of *p*-nitrophenol from the hydrolysis of *p*-nitrophenol phosphate. The phosphatase activity is measured using a continuous or single-point spectrophotometric assay based on the ability of phosphatases to catalyze the hydrolysis of PNP to *p*-nitrophenol. The selected wavelength was equal to 405 nm, corresponding to the maximum of the *p*-nitrophenol absorption spectrum.

The mother solution of PNP had a concentration of $(4.6 \pm 0.4) \times 10^{-4}$ mol/L, as determined using a method described elsewhere (4). To determine the activity of the particles, the absorbance of solutions containing PNP and PDA@ALP mixtures was measured with the double-beam UV–vis spectrophotometer at a wavelength of 405 nm, taking an absorbance measurement every 10 s. The reference cuvette contained a mixture of PNP (3 mL) and Tris buffer (1 mL) to account for the spontaneous hydrolysis of PNP. The studied solution was prepared with 3 mL of PNP and 1 mL of nanoparticles (1 mL of buffer in the reference cuvette). The influence of both the substrate concentration and the dilution of the nanoparticles were investigated. The kinetic experiments covered a period of 15 min.

For investigating the evolution of the enzymatic activity with storage time, the suspension of nanoparticles was stored at 4 °C between two successive measurements. As a control experiment, the activity of ALP in the presence of NaIO_4 was investigated. An exponential decrease law was fitted to the experimental kinetics as expected for a reaction of pseudo first-order, with respect to the substrate:

$$A_{405\text{nm}}(t) = A_{\text{max}}[1 - \exp(-kxt)]$$

where A_{max} and k are the maximal measured absorbance (corresponding to consumption of all the substrate) and the rate constant, respectively. From a qualitative point of view, we can observe a color change from transparent to yellow, meaning the presence of an enzymatic activity (Figure 5).

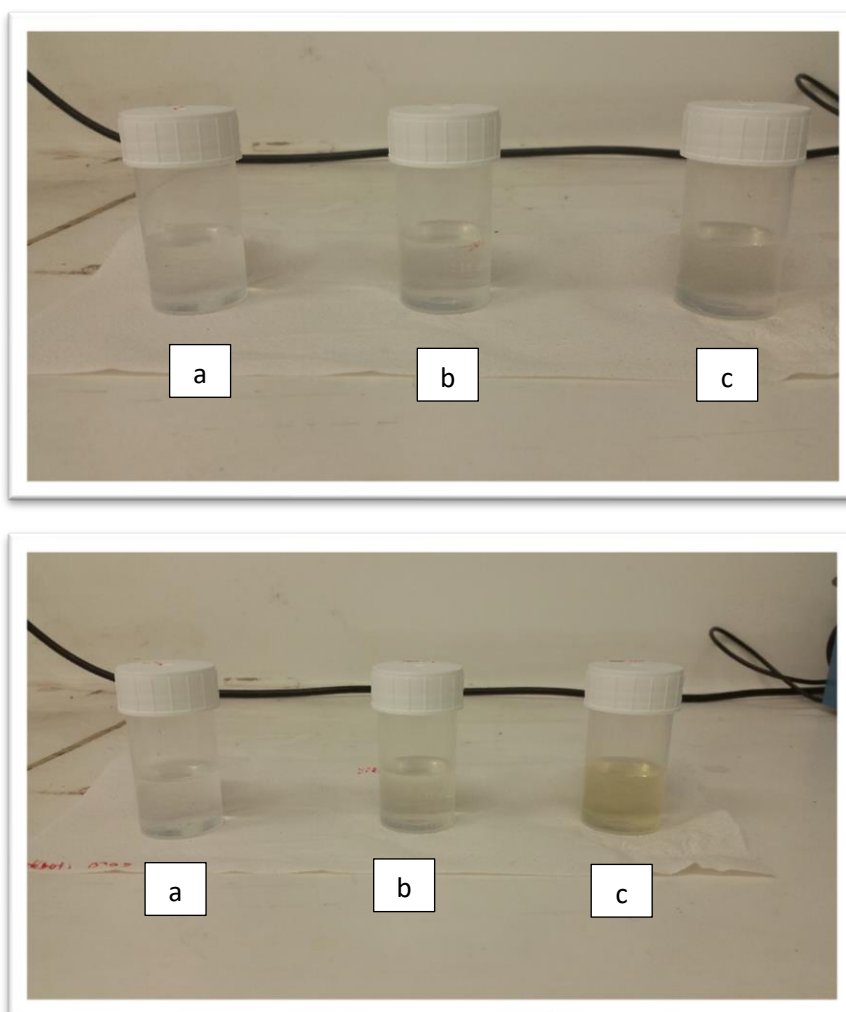


Figure 5: PNP test on PDA solution with and without ALP.

a) Reference: only PNP, b) PNP + PDA diluted 20x c) PNP + PDA@ALP diluted 20x
Top at t=0 and bottom at t=30min

b) Analysis of the (PAH)@PDA films

The enzymatic activity of the multi-layered films was estimated as a function of the number of (PAH-PDA@ALP) layer pairs, by immersing the films in 3 mL of 20-fold diluted PNP solutions. The reference cuvette contained the same PNP solution in Tris buffer at pH 8.5, to compensate for the spontaneous hydrolysis of PNP.

3.1.3. Transmission electron microscopy (TEM)

For cryo-transmission electron microscopy (TEM) characterization, a drop of the dialyzed PDA@ALP solution was deposited onto an electron microscopy grid covered by a hydrophobic carbon membrane. The drop size was progressively reduced, in order to obtain a thin film covering the whole membrane. The grid was subsequently plunged into ethane at the temperature of liquid nitrogen. By maintaining the specimen at this temperature, the grid was transferred on the cryo-holder, and inserted in the column of the electron microscope. These

grids were analysed by scanning transmission electron microscopy (STEM) (JEOL 2100F, Akishima, Japan) working at 200 kV, and equipped with a probe aberration corrector, an electron energy loss (EELS) spectrometer (Gatan Tridiem, Pleasanton, CA, USA), and an energy dispersive X-ray (EDX) spectrometer based on a Si(Li) detector. This set-up allows reaching resolutions of 2 and 1.1 Å under TEM and STEM modes, respectively. For limiting the irradiation damage, the images were acquired using a low-density electron beam.

TEM analysis were carried out at the Institut de Physique et de Chimie des Matériaux IPCMS – CNRS in collaboration with Prof. Ovidiu Ersen and Dr. Dris Ihawakarim.

3.1.4. Atomic force microscopy (AFM)

The morphology of the (PAH-PDA@ALP)_n films was investigated in the dry state by contact mode atomic force microscopy (AFM) (Nanoscope III, Bruker, Mannheim, Germany), using an MLCT-C cantilever (nominal spring constant: 0.01 N·m⁻¹).

3.1.5. Dynamic light scattering (DLS) – Zeta Potential

The colloidal stability of the nanoparticles was investigated as a function of their storage time at 4°C, after dialysis with a NanoZS device (Orsay, France) to measure their electrophoretic mobility. The electrophoretic mobility was subsequently converted in a zeta potential value using the Smoluchowski approximation. This approximation is justified, *posteriori*, for nanoparticles with a diameter larger than 30 nm in the sodium acetate buffer having an ionic strength of 32 mM at pH 5.0.

3.2. Characterization of the dopa/oxidant films

3.2.1. Atomic force microscopy (AFM)

The morphology and the thickness of the PDA films deposited on glass slides were analysed with a Catalyst AFM (Bruker Inc, Santa Barbara, USA) using the scan assist fluid method. To determine the film thickness, a scratch using a sterile syringe tip was made on each slide. The roughness and thickness were then calculated with the Gwyddion software. The average roughness of the films was also determined on image sizes of 2 x 2 μm², 5x5 μm² and 10x10 μm².

3.2.2. Static contact angle measurements

The static contact angle of water droplets (5 μL) deposited on the PDA-oxidant films was measured with an Attension Theta goniometer (Biolin Scientific, Vastra Frolunda, Sweden). The given values correspond to the average (± one standard deviation) over three measurements performed on regularly spaced locations along the major axis of the coated glass plates.

3.2.3. X-Ray photoelectron spectroscopy (XPS)

X-ray photoelectron spectroscopy on PDA@oxidant films was performed to compare their chemical composition. Au (111) substrates, which consist of a flame annealed layer of Au (200 nm) evaporated on mica, were previously treated by a plasma cleaner during 10 min. and were placed in each dopa/oxidant solution (same protocol as for glass slides). Then, XPS analysis of carbon, oxygen and nitrogen were carried out using a Thermo Scientific photoelectron spectrometer equipped with an aluminium X-ray source (AlK α ray, energy 1.4866 keV) under ultra-high vacuum (pressure of 10^{-8} – 10^{-9} mbar in the main chamber). The X-ray spot size was settled at 400 μ m. Survey spectra were recorded as result of 10 scans with a pass energy of 200.00 eV and a step size of 1 eV. High-resolution spectra were an average of 10 scans with a pass energy of 50.00 eV and a step size of 0.1 eV. The spectra were calibrated respectively to the binding energy of the adventitious carbon.

XPS analyzes were conducted at the Institut de Sciences et d'Ingénierie Supramoléculaire (ISIS) in collaboration with Prof. Arthur CIESIELSKI and his PhD student, Matilde Eredia.

3.2.4. Cyclic voltammetry (CV)

The cyclic voltammetry measurements were carried out with CHI604B three electrode setup (CHI Instruments, Houston, Texas) in order to identify different redox moieties in the PDA@oxidant films. The PDA films were deposited from the dopamine@oxidant blends on a carbon working electrode. Just before the deposition step (8h), the carbon electrode was polished with aluminium oxide slurries (1 μ m and at 0.1 μ m in diameter). Then, each electrode was placed in a water containing beaker for ultrasound treatment for 20 minutes (repeated 2 times). To check the surface state of the working electrode, potassium ferrocyanide was used at 1mM in the presence of either sodium acetate or Tris buffer. A CV cycle performed between -1.0 and +0.7V versus the reference electrode was then performed at a potential sweep rate of 100 mV/s. The electrode was used for film deposition if the oxidation and reduction peak potential were separated by less than 80 mV, the theoretical value for a one electron process being of 59 mV at 298 K. Otherwise, the electrode was repolished. After having measured the CV capacitive curve of the polished electrode in presence of sodium acetate buffer or Tris buffer, the electrode was placed in a mixture of dopamine and oxidant. After 8 hours of reaction, the electrode was rinsed with the same buffer as for the film deposition and voltammetry measurements were carried out again in the presence of buffer and at a potential sweep rate of 100 mV/s.

3.2.5. Antioxidant analysis of the PDA@oxidant films

The antioxidant activity of the films was investigated by the DPPH decoloration method. DPPH is a well-known radical and a trap ("scavenger") for other radicals. Because of a strong absorption band centred at about 520 nm, the DPPH radical has a deep violet color in solution, and it becomes colorless or pale yellow when neutralized (5) (figure 6).

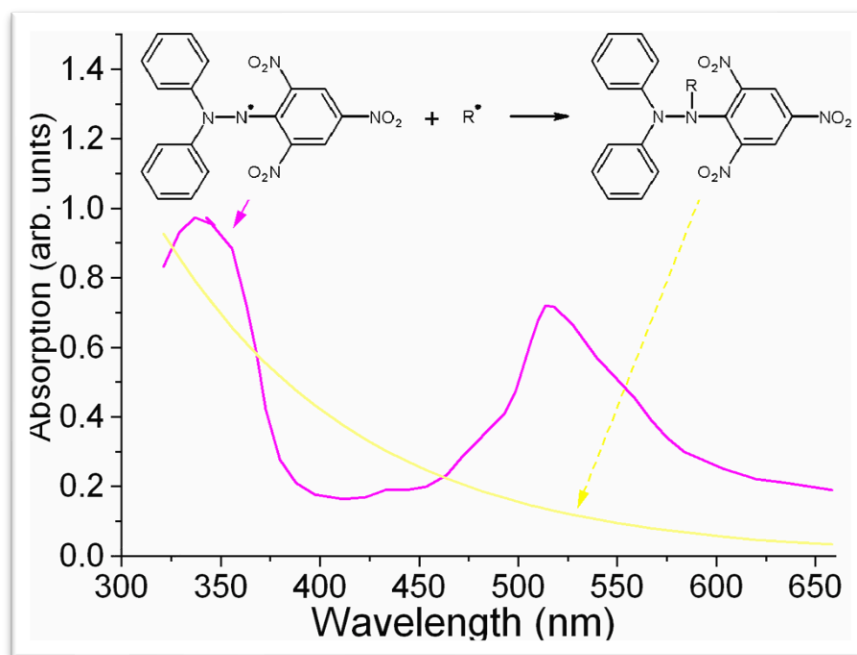


Figure 6: DPPH molecules and the effect of a scavenging reaction on their absorption spectrum (5)

The change in absorbance of ethanol solubilized DPPH was measured with an mc² UV-Vis spectrophotometer (SAFAS, Monaco). The PDA@oxidant-3h and PDA@oxidant-8h coated glass slides were placed in a beaker containing 50mL of DPPH (10^{-4} mol/L in pure ethanol) and allowed to react with DPPH for 2 hours in the absence of external light. Great care was taken to use the same surface area of the film and the same volume of DPPH solution in all experiments. Then, the absorbance of each DPPH solution in contact with the PDA@oxidant films was measured at 516nm, the reference cuvette containing DPPH alone. This reference DPPH solution was prepared in the same condition as the DPPH solution in contact with the films to account for spontaneous discoloration of the dye in the presence of dissolved O₂. The radical scavenging efficiency was calculated according to:

$$Efficiency = \left(1 - \frac{A_f}{A_i}\right) \times 100$$

where A_i and A_f are the absorbance of the initially used DPPH solution and of the same solution exposed during 2h to the PDA/oxidant-xh films, respectively.

3.2.6. Matrix-assisted laser desorption mass spectrometry with time of flight analysis

MALDI-MS spectra were recorded on a AB Sciex TOF/TOF 4800 instrument. The laser was operated at 3.700 Hz in the positive reflection mode. PDA@O₂-8h and PDA@NaIO₄ films that adhered on the surface of the MALDI target plate were carefully washed with distilled water, air-dried and analyzed. The mass spectrometer parameters were set as recommended by the manufacturer and adjusted for optimal acquisition performance. The laser spot size was set at medium focus (B50 mm laser spot diameter). The mass spectra data were acquired over a mass range of m/z 100-4.000, and each mass spectrum was collected from the accumulation of 10.000 laser shots from randomly chosen spots per sample position. Raw data were analyzed

using the computer software provided by the manufacturer and reported as monoisotopic masses.

One mL of a dimethylsulfoxide suspension of each sample (1 mg/mL) homogenized with a glass/glass potter was premixed with 1 mL of the matrix (2,5-dihydroxybenzoic acid at 1 % in water) in a centrifuge tube, and then 2 μ L of the resulting mixture were pipetted on the MALDI target plate and air-dried for MALDI-ToF MS analysis.

All the parameters, condition described above are the same also for the solid sample.

Maldi-Toff analysis were carried out at the University of Naples, Italy, in collaboration with Prof. Marco d'Ischia and his PhD student Maria Laura Alfieri.

3.3. Characterization of the gel@PDA gels

3.3.1. Rheology

The gelation kinetics and the adhesion strength of the gels were analysed with a Kinexus ultra rheometer (Malvern).

For dynamic rheometric measurements, the gelatin@dopamine solutions were mixed over the lower plate to immediately start the measurement of the gelation kinetics. All rheology experiments were performed in the kinetic mode to measure the gelation kinetics over 3h with time resolution of 30s. For all rheological measurements, 1.2 mL of gelling material was deposited on the lower plate of the rheometer just after mixing of all the gel components and the measurements were started 1 min after the end of the mixing process. These gelation kinetics were performed with an upper cone with 4cm in diameter and an apex angle of 176°. The tacking tests made to investigate the adhesion strength of the gelatin@PDA based gels were performed using an upper plate disk 2 cm in diameter. The as deposited gel was aged for 3h with a space of 1mm between the two steel disks of the rheometer. Before starting the test, the gel was compressed under a force of 1 N during 10s. The retraction speed was equal to 10, 100 or 1000 μ m/s. Water was placed in the surroundings of the rheometer plates to slow down water evaporation from the gel which could severely modify its adhesion properties.

The work of adhesion was calculated by integrating the area under the force versus distance curves, the distance being proportional to time with the retraction speed as the proportionality factor.

3.3.2. Scanning electron microscopy (SEM)

The SEM was used to study the cross sections of the gel and to see how the PDA@NPs are distributed inside.

Two mL of each investigated gel was placed on a plastic coverslip. The samples were set at 4°C for 3 hours. After 3 hours of waiting, the samples were fixed by using a solution of 0.05 M Glutaraldehyde in 4% Cacodylate buffer for 8 hours. After that, the samples were rinsed by

using 4 % Cacodylate buffer for three times of 5 min. The samples were dehydrated in graded series of ethanol (35%, 50%, 70%, 95% and 100%) for 3 min each. After the graded series of ethanol solution, the samples were dried by using a chemical drying agent, Hexamethyldisilazane (HMDS). The samples were transferred from 100% ethanol into 1:1 solution of HMDS for 10 min, then transferred into 100% HMDS for two treatments each one lasting over 10 min. All HMDS steps needed to be carried out in the fume hood, as it is highly toxic.

After dehydration steps, the samples were sectioned sagittally using a diamond wire saw (Walter Ebner, Le Locle, Switzerland) and mounted on 45°/90° SEM stubs in order to observe the sectioned surfaces.

The sectioned samples were sputter-coated with gold-palladium alloys (20/80) using a Hummer JR sputtering device (Technics, CA, USA). Later, a Quanta 250 FEG scanning electron microscope SEM (FEI Company, Eindhoven, The Netherlands) functioning with an accelerating voltage of the electrons of 10 kV was used for the observation of all coated specimens.

Conclusion

The purpose of this chapter was to present the list of the materials used during this thesis and the different characterization techniques used for materials investigation.

Another goal was to describe the formation of PDA@ALP nanoparticles, the (PAH)@PDA films, the PDA@films and finally the gelatin@PDA hydrogels.

References

1. Decher G. Fuzzy Nanoassemblies: Toward Layered Polymeric Multicomposites. *Science*. 29 août 1997; 277(5330):1232-7.
2. Borges J, Mano JF. Molecular Interactions Driving the Layer-by-Layer Assembly of Multilayers. *Chem Rev*. 24 sept 2014; 114(18):8883-942.
3. Ponzio F, Barthès J, Bour J, Michel M, Bertani P, Hemmerlé J, et al. Oxidant Control of Polydopamine Surface Chemistry in Acids: A Mechanism-Based Entry to Superhydrophilic-Superoleophobic Coatings. *Chem Mater*. 12 juill 2016; 28(13):4697-705.
4. Ball V. Activity of alkaline phosphatase adsorbed and grafted on « polydopamine » films. *J Colloid Interface Sci*. 1 sept 2014; 429:1-7.
5. Abuin E, Lissi E, Ortiz P, Henriquez C. URIC ACID REACTION WITH DPPH RADICALS AT THE MICELLAR INTERFACE. *Bol Soc Chil Quím*. juin 2002;47(2):145-9

List of the figures – Chapter 2

Figure 1: illustration of the PDA@ALP nanoparticles preparation method.	47
Figure 2: illustration of the (PAH@PDA) _n films preparation using the LBL deposition method.....	48
Figure 3: illustration of the PDA films preparation with sodium periodate.	49
Figure 4: illustration of the gelatin@PDA gel preparation.	51
Figure 5: PNP test on PDA solution with and without ALP.	53
Figure 6: DPPH molecules and the effect of a scavenging reaction on their absorption spectrum.	56

List of the tables – Chapter 2

Table 1: Chemicals used in this investigation.....	46
Table 2: Summary of the PDA film preparation in the presence of different oxidants.	50

Chapter 3

« There are literally as many ideas as there are organisms »

Janine Benqus

Chapter 3:

Formation of enzymatically active size-controlled polydopamine nanoparticles

INTRODUCTION	64
1. RECENT ADVANCES IN THE CONTROL OF PDA NANOPARTICLES AT INSERM 1121	65
1.1. CONTROL OF THE SIZE OF PDA NANOPARTICLES	65
1.1.1. Influence of the addition of Human Serum Albumin during dopamine oxidation	65
1.1.2. Influence of the KE sequence in PDA formation	66
1.2. OXIDATION CONTROL OF THE PDA FORMATION	67
1.3. OUR STRATEGY	68
2. FORMATION OF SIZE-CONTROLLED PDA NANOPARTICLES	69
2.1. OXIDATION OF DOPAMINE WITH SODIUM PERIODATE	69
2.1.1. Color change during oxidation	69
2.1.2. Reproducibility	69
2.2. INFLUENCE OF THE ADDITION OF ALP IN DOPAMINE SOLUTION	70
2.2.1. Kinetics of PDA@ALP formation analyzed by UV Vis spectroscopy	70
2.2.2. Influence of the dopamine/protein ratio on the PDA nanoparticles' size	71
2.2.3. Structure of the PDA@ALP nanoparticles	72
3. ENZYMATIC ACTIVITY OF THE PDA@ALP NANOPARTICLES	74
3.1. ANALYSIS OF THE ENZYMATIC ACTIVITY WITH PNP METHOD	74
3.2. KINETICS REACTION	76
4. APPLICATION OF THE PDA@ALP NANOPARTICLES	78
4.1. FORMATION OF MULTILAYERS FILMS	78
CONCLUSION	81
REFERENCES	82
LIST OF THE FIGURES – CHAPTER 3	83
LIST OF THE TABLES – CHAPTER 3	83

Chapter 3:

Formation of enzymatically active size-controlled polydopamine nanoparticles

Introduction

Inspired by the structural analogies between PDA and eumelanin and the homogeneous hierarchical size distribution of the eumelanin grains of the skin, a special attention was paid to produce **size-controlled and colloidally stable PDA-based nanoparticles**, instead of amorphous precipitates.

First, we will investigate the **influence of adding proteins** during polydopamine nanoparticles formation in acidic conditions ($\text{pH} = 5.0$), where spontaneous auto-oxidation of dopamine is suppressed, using **sodium periodate** as the oxidant and a protein, like **alkaline phosphatase (ALP)**, as a templating agent.

Then we will focus on the **enzymatic properties** of these PDA@ALP nanoparticles.

Finally, we will explore how the PDA@ALP nanoparticles can be **engineered in polyelectrolyte multilayered films** to potentially design model biosensors

1. Recent advances in the control of PDA nanoparticles at INSERM 1121

1.1. Control of the size of PDA nanoparticles

1.1.1. Influence of the addition of Human Serum Albumin during dopamine oxidation

Proteins seem good candidates to modify the formation of PDA owing to the presence of free amino groups on the surface of most of them. It has been shown that human serum albumin (HSA) increases the rate of PDA formation of stable and biocompatible nanoparticles and that the size of those nanoparticles was dependent on the initial protein/dopamine molar ratio and, simultaneously, to the formation of 30 nm diameter nanoparticles (1). By analyzing the absorbance of the dopamine-HSA in Tris containing solution (absorbance at 350 nm where usually dopamine does not absorb) as a function of time, in the absence and in the presence of HSA at different concentration, it appears that when HSA is added in the solution up to a concentration of 2 mg/mL the absorbance intensity increases more rapidly, meaning an increase of the formation rate. It also appears that a certain concentration (0.2 mg/mL) is sufficient to reach a constant enhancement in the PDA formation rate. However, the addition of HSA slows down the deposition kinetics of PDA on solid surface in contact with this solution, resulting in the preventing of the PDA deposit on the wall of the beakers (fig1.).



Figure 1: Picture of the bottom of the reaction vessel into which PDA synthesized (during 96 h) in the presence of HSA at 1 mg/mL (left) and without HSA (right) was stored during 3 months. (1)

Moreover, those PDA nanoparticles offer promising biocompatible properties since human gingival fibroblasts display good viability, either in presence or in absence of the HSA proteins.

1.1.2. Influence of the KE sequence in PDA formation

Eumelanin grains are always surrounded by a tightly bound protein layer (2) Melanosomal proteins, the organelle where eumelanin is synthesized, allow for increasing the rate of eumelanin formation and association with the obtained particles (3) However, we have seen in the first chapter, that PDA has structural similarities with the black-brown pigment of the skin. Then, these findings motivated the effort to form PDA nanoparticles in the presence of proteins.

Some proteins were found to play a similar role, and the presence of a solvent-accessible dyad of two amino acids, namely L-lysine and L-glutamic acid (KE sequence), was found to play a crucial role in the formation of PDA nanoparticles (4).

In this study, it was demonstrated that different proteins containing at least on KE sequence allow to inhibit the systematic deposition of PDA on the walls of the reaction beakers and to reduce the size of PDA particles in a protein/dopamine dependent ratio. The authors performed some experiments to study the role of KE : they analyzed different model single peptides in which K and E were directly adjacent to each other, or separated with one or two glycine residues (G), glycine as a spacer amino acid (fig.2). After incubation of those peptides with dopamine, only the peptide with KE being adjacent to each other could control PDA aggregation. It appears that even a single G residue was critical to produce PDA stable suspensions (4).

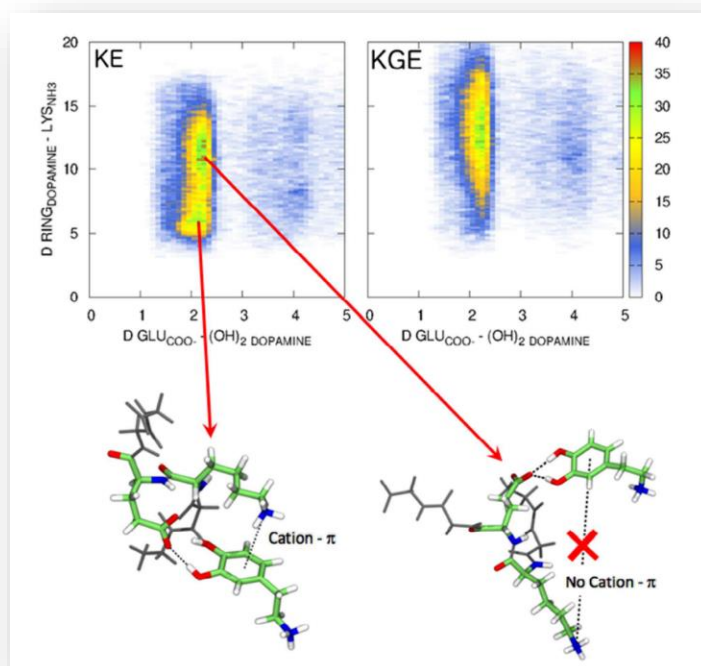


Figure 2: Population analysis in the case of KE directly adjacent or KE separated by G (KGE) as a function of the distance between the center of mass of the benzene ring and the N atom of the NH_3^+ group of the lysine residue and between the C atom of the COO^- of the glutamic acid residue and the center of mass of both -OH groups of dopamine. Colored regions: green = population often observed, blue = population seldomly observed and white = population never observed (4)

By using molecular dynamics simulations, they investigated the specific interactions between the dopamine molecule and the various peptides. It appeared that the hydrogen bond formation between the –OH or –NH₃⁺ protons of the dopamine molecule with the different carboxylic functions of the peptides situated either on the central E or D residues or on the C-terminus.

However, those nanoparticles were all produced at pH 8.5, by oxygen-triggered auto-oxidation of dopamine, a slow reaction mechanism.

1.2. Oxidation control of the PDA formation

It has been reported that sodium periodate, a strong oxidant ($E^\circ = +1.55 \text{ V}$ vs NHE), yields a faster deposition rate of PDA formation than dissolved O₂ at pH 8.5 or other strong oxidants as copper sulfate and ammonium peroxodisulfate at pH 5.0 (5). The addition of sodium periodate induces complete conversion of dopamine to the o-quinone and allows for the formation of dopaminochrome from dopamine through a two-electron oxidation process, a much simpler reaction mechanism than in the presence of O₂ as the oxidant (table 1).

Techniques	PDA - O ₂	PDA – SP
¹³ C-MAR NMR: Carboxylic groups (177 ppm band)	Absent	Present
¹³ C-MAR NMR: Aliphatic chain Carbon (20-50 ppm bands)	Low intensity or absent	High intensity
FTIR: Carbonyl/Carboxyl groups (1715 cm ⁻¹)	Absent	Strong band

Table 1: comparison between powders of PDA formed by auto-oxidation (PDA – O₂) and PDA formed with sodium periodate as oxidant (PDA-SP)

In conclusion, all characterization techniques used in this study highlighted that PDA-SP is richer in C=O groups and/or quinoid structures and undergoes partial loss of Carbon. Also, compared to copper sulfate and ammonium peroxodisulfate, sodium periodate allows for efficient cyclisation to aminochrome and subsequent conversion to indole-type units.

1.3. Our strategy

Based on the previous findings, our strategy to form enzymatically active and size-controlled PDA nanoparticles, implies to select the best oxidant to produce PDA with a rapid and unique kinetic pathway (fig. 2, Chapter 1). Thus, we decided to pursue our research by using exclusively sodium periodate as the oxidant to induce faster nanoparticles formation.

In particular, we investigated the conservation of the templating role of alkaline phosphatase (ALP) in the presence of this latter oxidant at pH at 5.0 instead of O_2 at pH at 8.5 in Tris buffer. We also analyzed if those new nanoparticles keep the enzymatic property of the protein. Finally, we studied the use of this particle system to produce polyelectrolyte multilayers films.

2. Formation of size-controlled PDA nanoparticles

2.1. Oxidation of dopamine with sodium periodate

2.1.1. Color change during oxidation

PDA is known as a typically dark black material due to optic intrinsic property. However, the color of dopamine solution changes during the synthesis. This color change reflects the different chemical steps of the PDA formation. The speed of the darkness of the solution can be an indication of the speed of the formation of PDA.

In the case of sodium periodate (fig. 3), the color of the dopamine solution turned immediately to yellow when the oxidant is added. Then after only 20 minutes the color changed to red, which is typical of the dopaminochrome formation. And finally, the solution became black after few hours. In comparison, dopamine in presence of Tris buffer at pH 8.5 became black after a much longer time.



Figure 3: Color change of the dopamine solution in presence of sodium periodate as a function of time

2.1.2. Reproducibility

The reproducibility of the production of PDA nanoparticles was strongly dependent on the rate of the sodium periodate addition. We worked with concentrated solutions of sodium periodate that we titrated in the dopamine solution. The consequence is that locally the concentration of the oxidant was higher than expected according to the color change kinetics and homogeneity of the solution. This happened so fast that even continuous stirring could not avoid it. This may affect the whole particle formation process. For these reasons, we report the data from different particles batches with different symbols in the next figures.

2.2. Influence of the addition of ALP in dopamine solution

2.2.1. Kinetics of PDA@ALP formation analyzed by UV Vis spectroscopy

We investigated the kinetics of the formation of PDA nanoparticles in the absence and in the presence of ALP by UV-Vis spectroscopy.

It appears that the addition of ALP at 0.5, 1 or 2 mg/mL can produce PDA aggregates faster than in the absence of the enzyme, from a 2 mg/mL dopamine solution. The absorbance of the dopamine containing solutions was followed as a function of time in the absence as well as in the presence of ALP at different concentrations. It appears that the absorbance at 500 nm increases more rapidly with time when ALP is present in solution (fig. 4A). However, at longer reaction times the absorbance versus time curves reach a plateau which seems independent from the protein concentration. The fact that a constant absorption is reached certainly implies that a constant conversion of dopamine into PDA is reached and is independent on the presence or not of ALP since we could obtain a plateau in both cases.

The absorbance of the dopamine containing solutions was also followed as a function of different concentrations of ALP. It appears that the absorbance at 500 nm increases with the increase of the enzyme concentration (fig. 4B).

These results are similar to those obtained for dopamine in the presence of ALP at pH 8.5 in Tris buffer (4). This increase in the oxidation rate of dopamine in the presence of ALP is also similar to the influence found for HSA, but at pH 8.5 in the presence of dissolved oxygen as the oxidant (1).

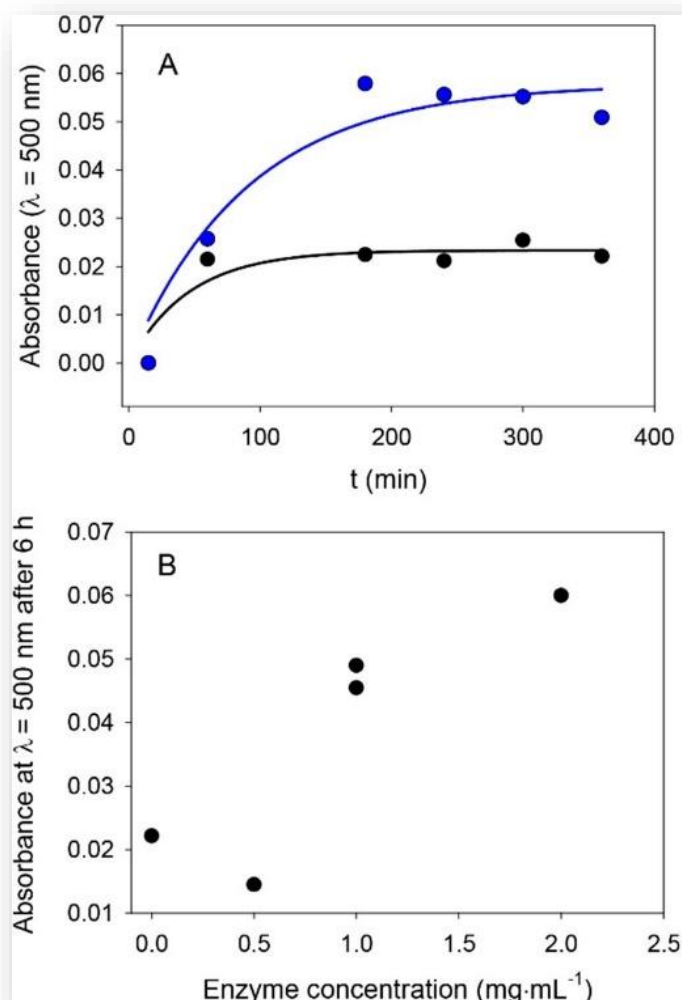


Figure 4: Investigation of the influence of ALP on dopamine oxidation. (A) Evolution of the absorbance at 500 nm at pH 5.0 in the presence of 20 mM NaIO₄ in the absence of enzyme (•) and in the presence of ALP at 1 mg·mL⁻¹ (•). The initial dopamine concentration was equal to 2 mg·mL⁻¹ in all cases. The solid lines correspond to an exponential decay fit to the data with rate constants of $(2.3 \pm 0.3) \times 10^{-2} \text{ min}^{-1}$ and $(5.8 \pm 0.6) \times 10^{-2} \text{ min}^{-1}$ in the absence and in the presence of ALP at 1 mg·mL⁻¹, respectively. (B) Evolution of the absorbance after 6 h of dopamine oxidation (2 mg·mL⁻¹ at pH 5.0) as a function of the concentration of initially added ALP. Each data point corresponds to an individual curve as those described in (A).

2.2.2. Influence of the dopamine/protein ratio on the PDA nanoparticles' size

The size distribution of the nanoparticles obtained after 6 hours of oxidation and subsequent dialysis (against Tris buffer at pH 8.5) of the reaction medium was obtained by TEM analysis (fig. 5). It appears, clearly, that an increase in protein concentration induces a significant reduction in the average size of the PDA nanoparticles. The particles go from an average size of 90 nm without protein, to a size of around 38 nm in the presence of 1mg/mL of ALP.

We also measured the hydrodynamic diameter distribution of the particles with a dynamic Light scattering instrument, but the distribution was too inhomogeneous and not precise enough (results not shown here). However, we did note the protein's ability to significantly reduce the particle size.

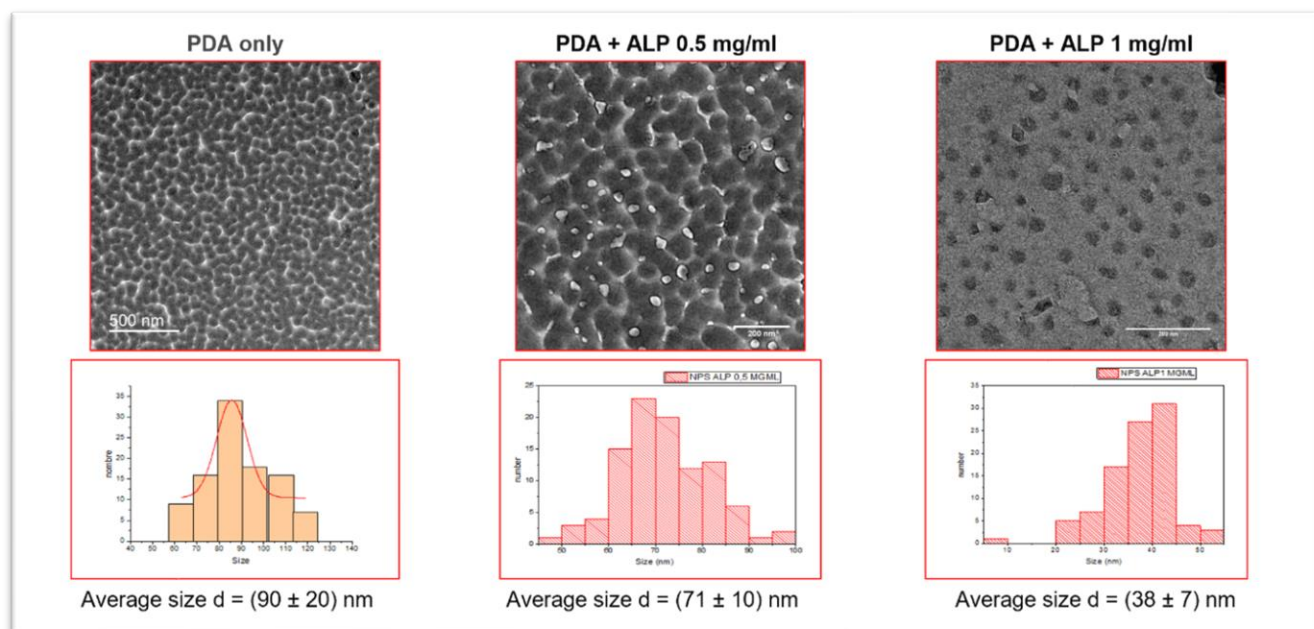


Figure 5: Representative TEM micrographs of polydopamine nanoparticles. (Top) Representative TEM micrographs of polydopamine nanoparticles produced after 6 h of oxidation in the presence of 20 mM NaIO_4 from the dopamine solutions (10.6 mM) after the subsequent dialysis against Tris buffer, as a function of the added concentration in ALP. (Bottom) Size distribution of the particles obtained by analyzing 100 particles.

In the presence of 20 mM NaIO_4 as the oxidant, the effect of the enzyme is, however, less pronounced than in the case of PDA synthesized at pH 8.5 using dissolved O_2 as the oxidant. In this latter case, the average particle size was reduced from about 500 to 50 nm when the ALP concentration was increased from 0 to $2 \text{ mg} \cdot \text{mL}^{-1}$ (4). The fact that the PDA particles are smaller when synthesized in the presence of NaIO_4 versus O_2 may originate from the fact that NaIO_4 not only allows 5,6-indolequinone to be produced in a single chemical pathway, but may also degrade the obtained polydopamine (5).

Regardless, it appears that oxidation of dopamine in the presence of ALP in acidic conditions and using NaIO_4 as the oxidant allows the small nanoparticles to be produced in a much faster way than at pH 8.5 under auto-oxidation conditions.

2.2.3. Structure of the PDA@ALP nanoparticles

The TEM micrographs obtained at higher resolution show the presence of an external corona less dense than the core of the particles, suggesting that the composition of the external part of the particles is richer in protein than the core (fig. 6).

From the zeta potential we can see that the charge of the PDA nanoparticle changes when adding ALP. Indeed, PDA is positively charged at pH 5.0, but in the presence of ALP the nanoparticles becomes negatively charged. ALP has an isoelectric point of 4.4 – 5.8, but since we dialyzed the nanoparticles samples against Tris buffer at pH 8.5, the protein was negatively charge at this acidic condition reaching a zeta potential value of (-25 ± 5) mV (fig. 7). The difference in charge in the absence and presence of the enzyme supports the hypothesis of a high concentration of the enzyme on the surface.

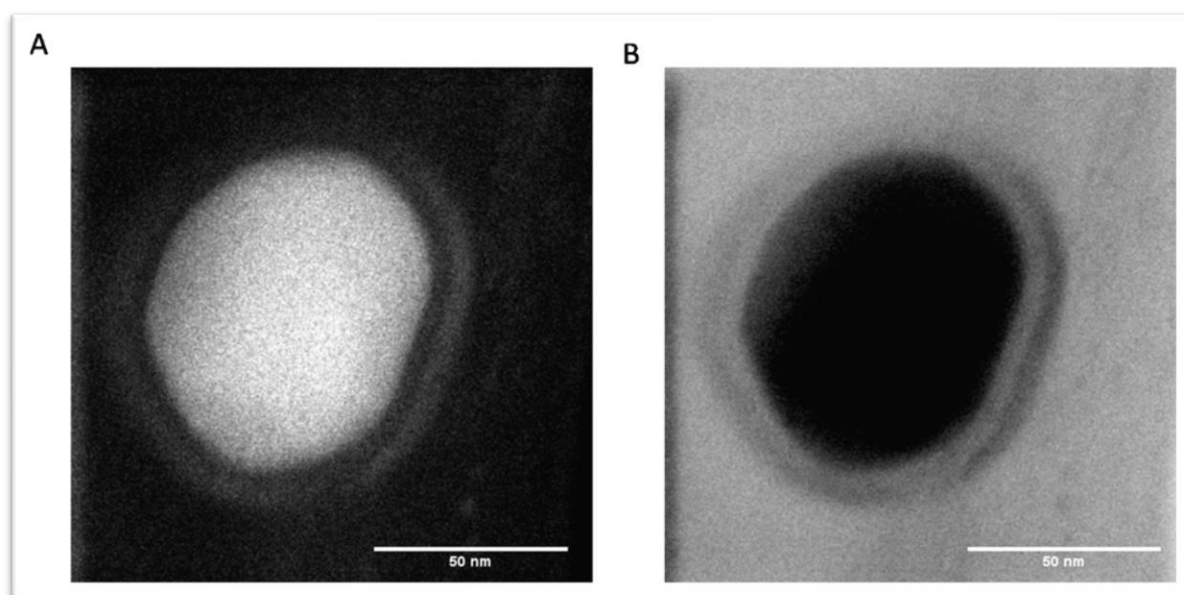


Figure 6: High-resolution STEM images acquired simultaneously in (A) high-angle annular dark field and (B) bright field modes of PDA@ALP nanoparticles obtained after 6 h of oxidation of a 10 mM dopamine solution + 1 mg·mL⁻¹ ALP in the presence of 20 mM NaIO₄.

Nevertheless, we do not have definitive proof that the obtained PDA@ALP nanoparticles are of the core–shell type. It seems that the corona of the particles may just be richer in protein than the core. However, owing the preparation method of the nanoparticles, just by mixing dopamine and the enzyme, we cannot exclude that proteins are also present in the core of the particles. More experiments are still needed to confirm this proposition.

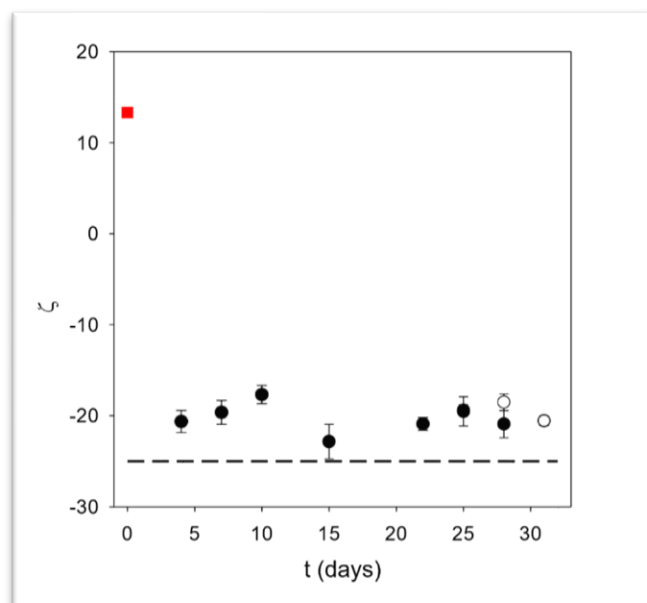


Figure7: Zeta potential of PDA particles obtained after 6 h of oxidation of a $2 \text{ mg}\cdot\text{mL}^{-1}$ dopamine solution in the presence of 20 mM NaIO_4 without added enzyme (\square) and in the presence of ALP at $1 \text{ mg}\cdot\text{mL}^{-1}$ (two independent syntheses: \circ , \bullet). The particle suspension was dialyzed against Tris buffer as described in the Materials and Methods section. Each data point corresponds to the average over three measurements on a same batch of particles, and the error bar corresponds to one standard deviation. The dashed line corresponds to the zeta potential of a $1 \text{ mg}\cdot\text{mL}^{-1}$ solution of the enzyme in Tris buffer, namely $(-25 \pm 5) \text{ mV}$.

Otherwise, this is a major advantage provided that the obtained nanoparticles are stable and are of use for biological applications. Indeed, the PDA@ALP nanoparticles were stable from a colloidal point of view, with no sedimentation during weeks, as observed visually, and a stable zeta potential during storage time at 4°C (fig. 7).

3. Enzymatic activity of the PDA@ALP nanoparticles

3.1. Analysis of the enzymatic activity with PNP method

The possible core-shell aspect of PDA@ALP nanoparticles invited us to wonder if the presence of proteins on the surface affords the nanoparticles with an enzymatic activity. The optimum pH for enzymatic activity of ALP is around pH 8-10 and the enzyme is stable at pH 7.5-9.5, but this stability can change upon substrate, substrate concentration or ionic concentration even if the enzyme seems to be pretty stable according to some FTIR analysis (6,7). However, during the formation of nanoparticles, ALP could lose its enzymatic properties. A first step therefore consisted in verifying if it keeps this attracting property under such synthesis conditions.

According to UV Vis spectroscopy (fig.8), the same and constant absorbance strongly suggest that the oxidant does not affect the enzymatic activity of the enzyme itself, at least when using

sodium periodate, and this is reflected by the fact that the PDA@ALP nanoparticles keep the enzymatic activity expected for ALP after oxidative synthesis in the presence of sodium periodate and subsequent dialysis against Tris buffer at pH 8.5.

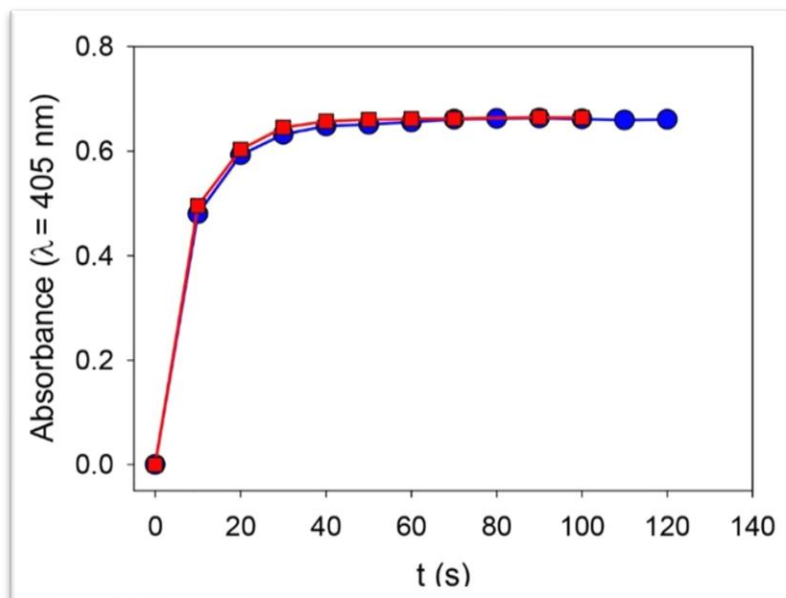


Figure 8: Enzymatic activity of ALP ($0.1 \text{ mg} \cdot \text{mL}^{-1}$) in the presence of 50 mM Tris buffer (□) and in the presence of 50 mM Tris buffer with 20 mM NaIO₄ (●).

All the particles prepared in the presence of ALP at different concentrations display the expected enzymatic activity. More so, the higher the concentration of enzyme, the higher the enzymatic activity is. This may simply reflect an increase in the area/volume ratio of the smaller particles obtained when the oxidation of dopamine is performed in the presence of a higher concentration in enzyme.

Those obtained nanoparticles progressively loosed their enzymatic activity upon storage at 4°C (between two successive measurements) (fig. 9A). This loss in activity cannot be attributed to ALP desorption from the particle's surface because we measured the activity of the particles in the presence of their supernatant buffer after appropriate dilution by a factor of 20. In addition, this progressive loss in activity is reproducible in at least two independent particle batches (fig. 9B). It may represent a slow and progressive enzyme denaturation when grafted on the surface of the nanoparticles.

The most challenging problems in the elucidation of the mechanism of action of this enzyme remain the explanation of the step controlling the rate of phosphorylation of the enzyme by the substrate. According to some studies (8,9), the presence of Tris during hydrolysis of PNP by ALP (from *E. Coli*) at pH 8 increased the rate of 4-nitrophenol liberation with concomitant phosphorylation of Tris. It has been found that even the concentration of Tris buffer plays a role in the enzymatic activity.

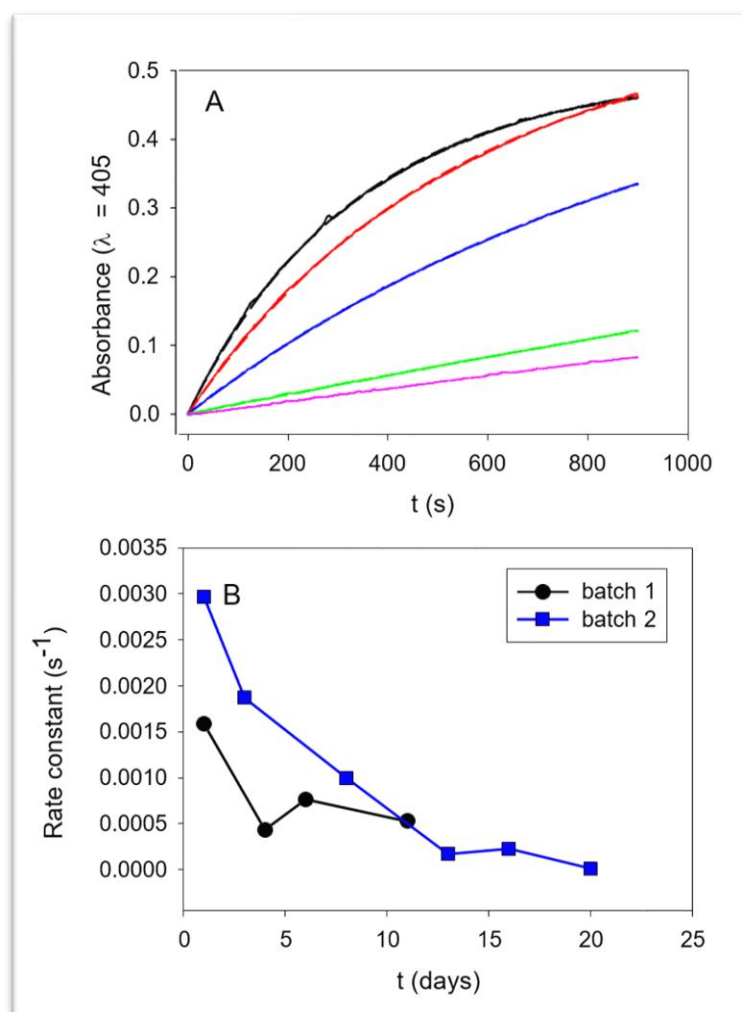


Figure 9: Influence of the substrate concentration and storage time on the enzymatic activity of a 10-fold diluted PDA@ALP nanoparticle suspension. (A) Evolution of the enzymatic activity of a 10-fold diluted PDA@ALP nanoparticle suspension in the presence of a 20-fold diluted PNP solution at day 1 (—), 3 (—), 8 (—), 14 (—), and 20 (—) after the end of the particles dialysis step against Tris buffer at pH 8.5. (B) Evolution of the rate constant of the enzymatic hydrolysis kinetics shown in (A) for a first batch of particles (corresponding to the kinetics displayed in Figure 7 A (■)) and for an independent batch of particles (●).

3.2. Kinetics reaction

Taking these results into account, we investigated the influence of both the nanoparticle relative concentration (expressed as the nanoparticle dilution in the following) and the substrate concentration on the enzymatic activity of PDA@ALP nanoparticles immediately at the end of the dialysis step against Tris buffer.

The influence of the dilution in nanoparticles for a constant concentration in PNP (10-fold diluted mother solution, corresponding to an effective concentration of $(4.6 \pm 0.4) \times 10^{-4}$ mol/L), is given in Figure 10. The obtained linear relationship demonstrates that the PNP

hydrolysis is a first-order process with respect to the concentration in nanoparticles and, hence, also to the enzyme concentration available on the surface of the nanoparticles, as expected.

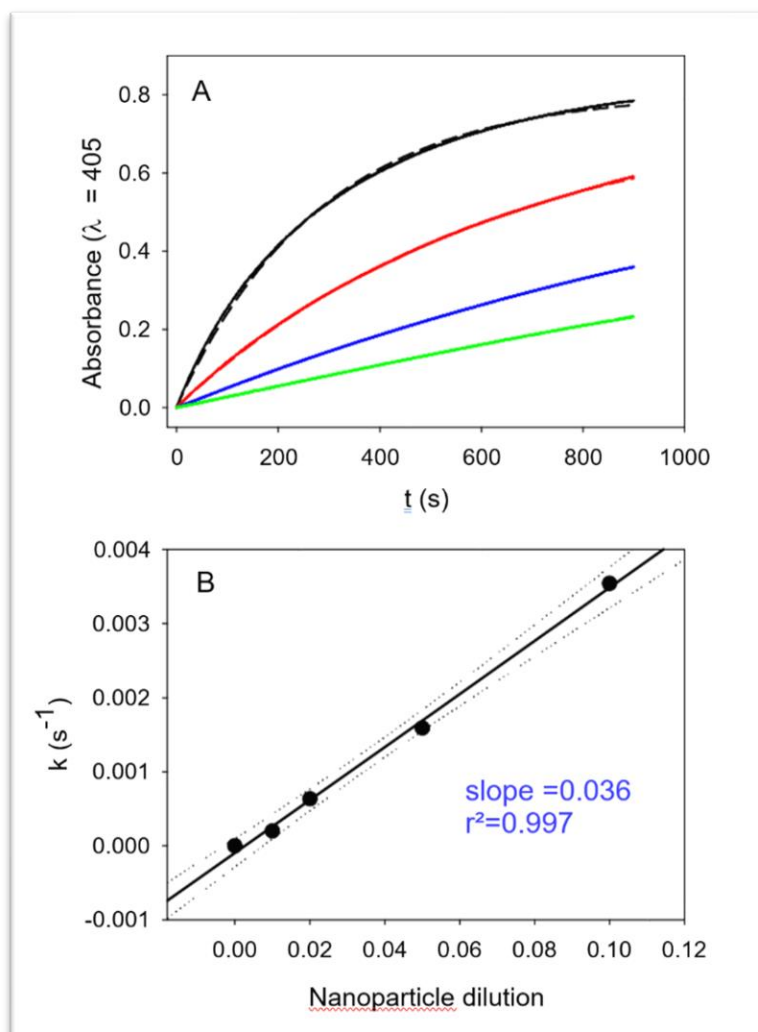


Figure 10: Influence of the dilution of PDA@ALP nanoparticles on their enzymatic activity. (A) Hydrolysis of 10-fold diluted PNP solutions in the presence of PDA@ALP nanoparticles at different dilutions: mother suspension issued from the synthesis and dialysis-diluted 10-fold (—), 20-fold (—), 50-fold (—), and 100-fold (—). The solid lines correspond to the experimental data, whereas the dashed lines correspond to the fit of an exponential decay function to the experimental data. (B) Rate constant obtained by fitting an exponential decay function to the experiments displayed in (A) versus the nanoparticle dilution factor.

The same kinds of experiments were performed but changing the concentration of the substrate at a given concentration of the PDA@ALP nanoparticles. The results are shown in Figure 11.

For all the investigated particle batches, the rate constant for the hydrolysis of PNP decreases with the substrate concentration, which proves that immobilized ALP on PDA nanoparticles is inhibited by its substrate.

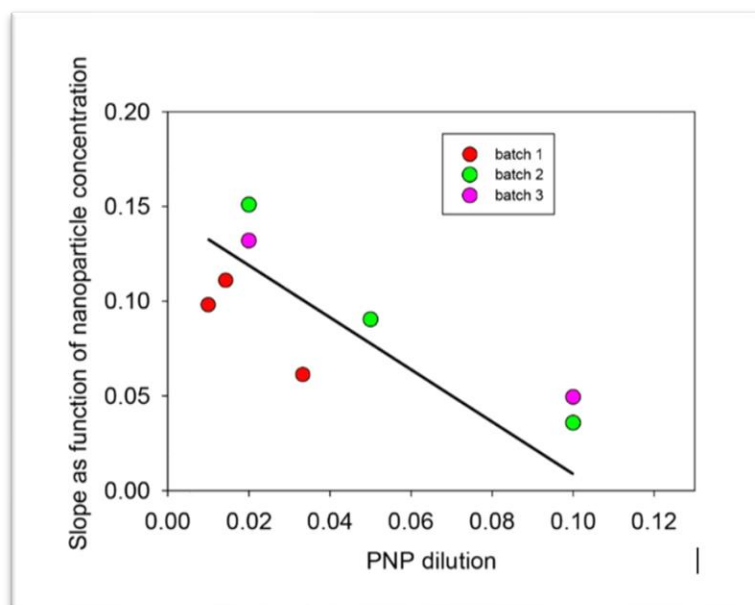


Figure 11: Evolution of the slope of the curves shown in Figure 9B as a function of the PNP dilution (mother solution at $(4.6 \pm 0.4) \times 10^{-4} \text{ mol}\cdot\text{L}^{-1}$) for three independent batches of PDA@ALP nanoparticles. The solid line does not correspond to a fit but is aimed to guide the eye.

4. Application of the PDA@ALP nanoparticles

4.1. Formation of multilayers films

Using the finding that the PDA@ALP nanoparticles keep the enzymatic activity of the grafted enzyme, we thought to use such particles as active components in thin films which, by using other more relevant enzymes, can be useful for the design of biosensors. Layer-by-layer deposited films (10,11) offer the advantage to allow for a progressive increase in the surface concentration of active compounds, owing to a regular growth process with the number of deposition steps.

The $(\text{PAH-PDA@ALP})_n$ films grow regularly with the number of deposition cycles n (fig. 12A), and the obtained films reflect the presence of nanoparticles close to about 100–400 nm in diameter, as inferred by AFM imaging (fig. 12B), and as expected for films made from PDA@ALP nanoparticles prepared in the presence of ALP at $1 \text{ mg}\cdot\text{mL}^{-1}$. This size is in relative agreement with the particles' size determined by TEM (fig. 5). In the immobilized state, the particles may become closer than in solution and aggregate.

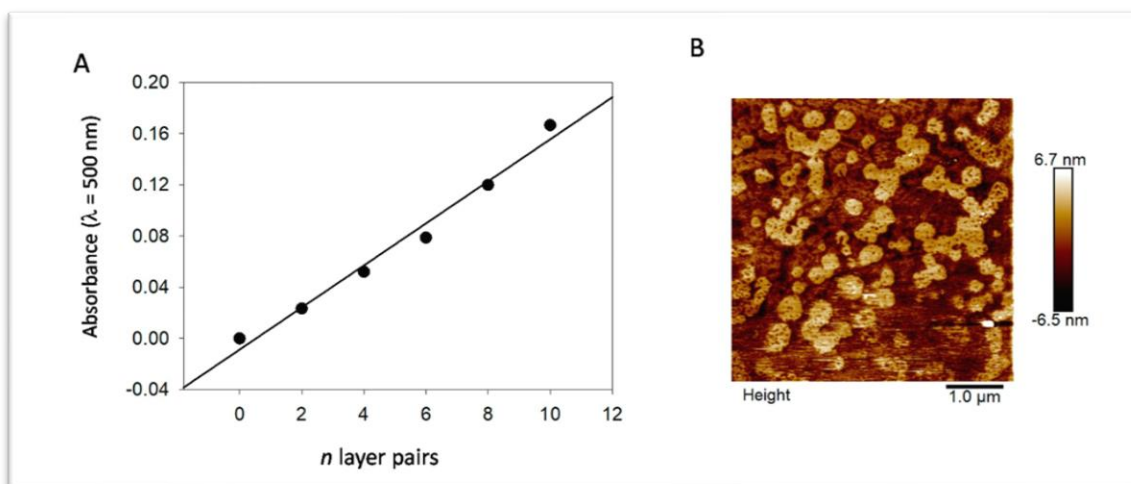


Figure 12: Incorporation of PDA@ALP nanoparticles in layer-by-layer films. (A) Evolution of the absorbance at $\lambda = 500$ nm (where PAH does not absorb light) of $(\text{PAH-PDA@ALP})_n$ films with the number of deposited layer pairs, n . (B) Film morphology of a $(\text{PAH-PDA@ALP})_6$ film as investigated by means of contact mode AFM.

The enzymatic activity of the $(\text{PAH-PDA@ALP})_n$ films was then measured as function of the number of deposited layer pairs, n , and some representative kinetics are given in figure 13. For reaction times as short as 15 min, and for very low enzyme amounts present in the films, contrarily to the experiments performed in bulk the kinetics are linear. Such a linear regime corresponds, of course, to the first part of an exponential curve. The slope of those straight lines represents the rate of PNP hydrolysis which was then plotted as a function of the number of layer pairs in figure 14. It appears that the hydrolysis rate of PNP scales proportionally with n , namely, with the film thickness (fig.14). This means that all enzymes on the PDA@ALP nanoparticles are accessible to the substrate.

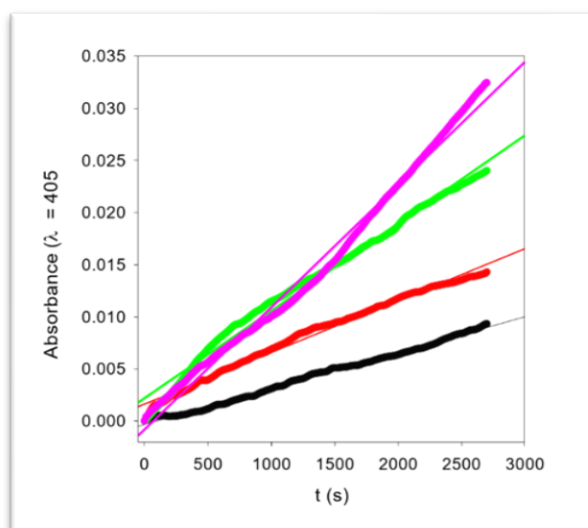


Figure 13: Enzymatic kinetics for $(\text{PAH-PDA@ALP})_n$ films put in contact with a 20-fold diluted PNP solution as a function of the number of deposited layer pairs: $n = 3$ (\bullet), $n = 6$ (\bullet), $n = 12$ (\bullet), and $n = 15$ (\bullet). The data points correspond to the experimental data, whereas the solid lines correspond to linear regressions of the data.

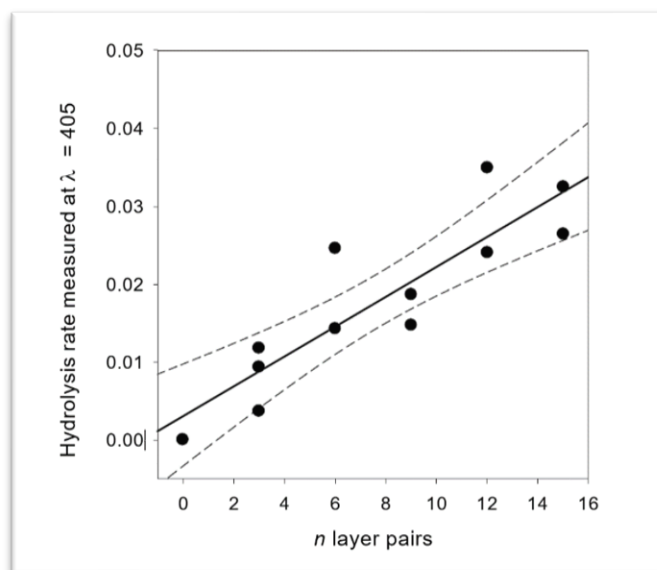


Figure 14: Evolution of the hydrolysis rate of (PAH-PDA@ALP) n films as a function of the number of deposited layer pairs. The solid line corresponds to a linear regression of the data points, whereas the dashed lines correspond to the limit of the 95% confidence interval.

Conclusion

The oxidation of dopamine by sodium periodate in the presence of alkaline phosphatase **allows to produce stable nanoparticles of controlled size** in a much shorter time than by auto-oxidation at pH 8.5.

Those nanoparticles **keep the enzymatic activity of the used enzyme** and seem to be **enriched in enzyme on their corona with respect to their core**.

Owing to their negative charge, **they can be immobilized in polyelectrolyte multilayer films** with PAH as a polycation to produce reactors with an activity proportional to the film thickness.

The major challenge of this research remains to determine the accurate distribution of the enzyme in the nanoparticle to better understand the mechanism by which the enzyme controls nanoparticle formation.

In addition, even if we demonstrated the possibility to produce enzymatically active PDA@ALP nanoparticles, **some research effort is still required to improve the reproducibility** of their preparation method. In particular, the rate of oxidant addition to the dopamine and enzyme containing solution should be automatized specially since these materials can be used in 3D printing.

References

1. Chassepot A, Ball V. Human serum albumin and other proteins as templating agents for the synthesis of nanosized dopamine-eumelanin. *J Colloid Interface Sci.* 15 janv 2014; 414:97-102.
2. Guo S, Hong L, Akhremitchev BB, Simon JD. Surface elastic properties of human retinal pigment epithelium melanosomes. *Photochem Photobiol.* juin 2008; 84(3):671-8.
3. Wagh S, Ramaiah A, Subramanian R, Govindarajan R. Melanosomal proteins promote melanin polymerization. *Pigment Cell Res.* déc 2000; 13(6):442-8.
4. Bergtold C, Hauser D, Chaumont A, El Yakhlifi S, Mateescu M, Meyer F, et al. Mimicking the Chemistry of Natural Eumelanin Synthesis: The KE Sequence in Polypeptides and in Proteins Allows for a Specific Control of Nanosized Functional Polydopamine Formation. *Biomacromolecules.* 10 2018; 19(9):3693-704.
5. Ponzio F, Barthès J, Bour J, Michel M, Bertani P, Hemmerlé J, et al. Oxidant Control of Polydopamine Surface Chemistry in Acids: A Mechanism-Based Entry to Superhydrophilic-Superoleophobic Coatings. *Chem Mater.* 12 juill 2016; 28(13):4697-705.
6. Latner AL, Parsons M, Skillen AW. Isoelectric focusing of alkaline phosphatases from human kidney and calf intestine. *Enzymologia.* 1971;40(1):1-7.
7. de La Fournière L, Nosjean O, Buchet R, Roux B. Thermal and pH stabilities of alkaline phosphatase from bovine intestinal mucosa: a FTIR study. *Biochim Biophys Acta.* 27 avr 1995; 1248(2):186-92.
8. Trentham DR, Gutfreund H. The kinetics of the reaction of nitrophenyl phosphates with alkaline phosphatase from *Escherichia coli*. *Biochem J.* janv 1968; 106(2):455-60.
9. Dayan J, Wilson IB. THE PHOSPHORYLATION OF TRIS BY ALKALINE PHOSPHATASE. *Biochim Biophys Acta.* 9 mars 1964; 81:620-3.
10. Decher G. Fuzzy Nanoassemblies: Toward Layered Polymeric Multicomposites. *Science.* 29 août 1997; 277(5330):1232-7.
11. Borges J, Mano JF. Molecular Interactions Driving the Layer-by-Layer Assembly of Multilayers. *Chem Rev.* 24 sept 2014; 114(18):8883-942.

List of the figures – Chapter 3

Figure 1: Picture of the bottom of the reaction vessel into which PDA synthesized (during 96 h) in the presence of HSA at 1 mg/mL (left) and without HSA (right) was stored during 3 months. (1)	65
Figure 2: Population analysis in the case of KE directly adjacent or KE separated by G (KGE) as a function of the distance between the center of mass of the benzene ring and the N atom of the NH_3^+ group of the lysine residue and between the C atom of the COO^- of the glutamic acid residue and the center of mass of both -OH groups of dopamine.....	66
Figure 3: Color change of the dopamine solution in presence of sodium periodate as a function of time ...	69
Figure 4: Investigation of the influence of ALP on dopamine oxidation.. ..	71
Figure 5: Representative TEM micrographs of polydopamine nanoparticles.	72
Figure 6: High-resolution STEM images acquired simultaneously in (A) high-angle annular dark field and (B) bright field modes of PDA@ALP nanoparticles obtained after 6 h of oxidation of a 10 mM dopamine solution + 1 mg·mL ⁻¹ ALP in the presence of 20 mM NaIO ₄	73
Figure 7: Zeta potential of PDA particles obtained after 6 h of oxidation.....	74
Figure 8: Enzymatic activity of ALP (0.1 mg·mL ⁻¹) in the presence of 50 mM Tris buffer and in the presence of 50 mM Tris buffer with 20 mM NaIO ₄	75
Figure 9: Influence of the substrate concentration and storage time on the enzymatic activity.....	76
Figure 10: Influence of the dilution of PDA@ALP nanoparticles on their enzymatic activity	77
Figure 11: Evolution of the slope of the curves shown in Figure 9B as a function of the PNP dilution for three independent batches of PDA@ALP nanoparticles.	78
Figure 12 : Incorporation of PDA@ALP nanoparticles in layer-by-layer films	79
Figure 13: Enzymatic kinetics for (PAH-PDA@ALP) _n films	79
Figure 14: Evolution of the hydrolysis rate of (PAH-PDA@ALP) _n films as a function of the number of deposited layer pairs.	80

List of the tables – Chapter 3

Table 1: comparison between powders of PDA formed by auto-oxidation (PDA – O ₂) and PDA formed with sodium periodate as oxidant (PDA-SP)	67
--	----

Chapter 4

« Nothing is to be feared. It is only to be understood. »

Marie Curie

Chapter 4:

Influence of different oxidants on the physico-chemical characteristics of Polydopamine coatings

INTRODUCTION	86
1. MORPHOLOGY OF THE DOPA/OXIDANT FILMS	87
1.1. FILMS ROUGHNESS	87
1.2. FILMS THICKNESS	88
2. CHEMICAL COMPOSITION OF THE DOPA/OXIDANT-XH FILMS	91
2.1. UV VIS ANALYSIS	91
2.2. XPS ANALYSIS	93
3. ELECTROCHEMICAL BEHAVIOR OF THE DOPA/OXIDANT-XH FILMS.....	98
4. PROPERTIES OF THE DOPA/OXIDANT-XH FILMS	99
4.1. ANTIOXIDANT PROPERTIES.....	99
4.1.1. Basic features of antioxidants	99
4.1.2. Antioxidant activity of the PDA/oxidant-xh films.....	100
CONCLUSIONS.....	103
REFERENCES	104
LIST OF THE FIGURES – CHAPTER 4:	105
LIST OF THE TABLES – CHAPTER 4:.....	105
SUPPORTING INFORMATION	106
AFM SURFACE TOPOGRAPHIES.....	106
XPS SPECTRA	109
CYCLIC VOLTAMMETRY	110

Chapter 4:

Influence of different oxidants on the physico-chemical characteristics of Polydopamine coatings

Introduction

Polydopamine can be formed in various shapes including nanoparticles as we just have seen in the previous chapter. However, many applications require PDA as thin layer or films. It is well known that polydopamine offers a **promising route to produce multifunctional coatings**. Thus, different strategies to produce polydopamine from dopamine oxidation have been proposed these last years. However, the influence of these different techniques on the physico-chemical properties of polydopamine has not been studied deeply enough. **Several parameters can play a huge role on the PDA formation** as the pH and the nature of the used buffer (1), the duration of the oxidation, and the choice of the oxidant. Autoxidation of dopamine in basic solutions allows the deprotonation of the amino group and then facilitates the intramolecular Michael addition. Oxidation salts or redox active transition metals in weakly acidic conditions can also be used.

Therefore, during this thesis, we were interested in studying **the role of different PDA coating methods**. In this chapter, we will focus on **four oxidants** used to produce polydopamine films from dopamine : oxidation with **oxygen** dissolved in Tris(hydroethyl)aminomethane (O_2) which is the most commonly used method and serves as a kind of reference, **sodium periodate** ($NaIO_4$), a mixture of **copper sulfate and hydrogen peroxide** ($CuSO_4 + H_2O_2$), and **ammonium peroxodisulfate** ($(NH_4)_2S_2O_8$). The obtained films are referred to as PDA/oxidant-xh for materials produced in the presence of the cited oxidant for x hours of oxidation.

We will explore the role that these oxidants have on **the thickness, roughness, and chemical composition** of polydopamine films using atomic force microscopy, UV Vis spectrophotometry and X-ray photoelectron spectroscopy.

Attention is then focused on the study of **electrochemical behavior** of the produced films using cyclic voltammetry.

Finally, **the antioxidant properties** of those coatings have been compared and related to their morphological and chemical attributes.

1. Morphology of the dopa/oxidant films

1.1. Films roughness

The morphology of the PDA films is remarkably influenced by the oxidant used to produce them. In agreement with previous findings (2), the PDA@O₂-8h films are smoother than the highly granular PDA@NaIO₄ -8h films (fig. 1A), as well at 3h but less pronounced (fig. 1B and fig. S1 and S2 of the supporting information at the end of this chapter) according to our AFM images. An intermediate scenario between the PDA@O₂ films and the PDA@NaIO₄ film is observed when films are produced in the presence of CuSO₄+H₂O₂ and (NH₄)₂S₂O₈ (fig.1A).

From a quantitative viewpoint, the film roughness increases following the order:

$$\text{PDA@O}_2 < \text{PDA@}(\text{NH}_4)_2\text{S}_2\text{O}_8 < \text{PDA@CuSO}_4+\text{H}_2\text{O}_2 < \text{PDA@NaIO}_4 \text{ (fig. 2)}$$

and depends markedly on the image size in the case of the very rough films. This finding is not unexpected for granular films, and it is consistent with the observation that the grain size of the particles on the PDA@ NaIO₄ -8h films is in the 500nm-1 μ m size range (fig. 1A), being smaller than the films produced with the other oxidants.

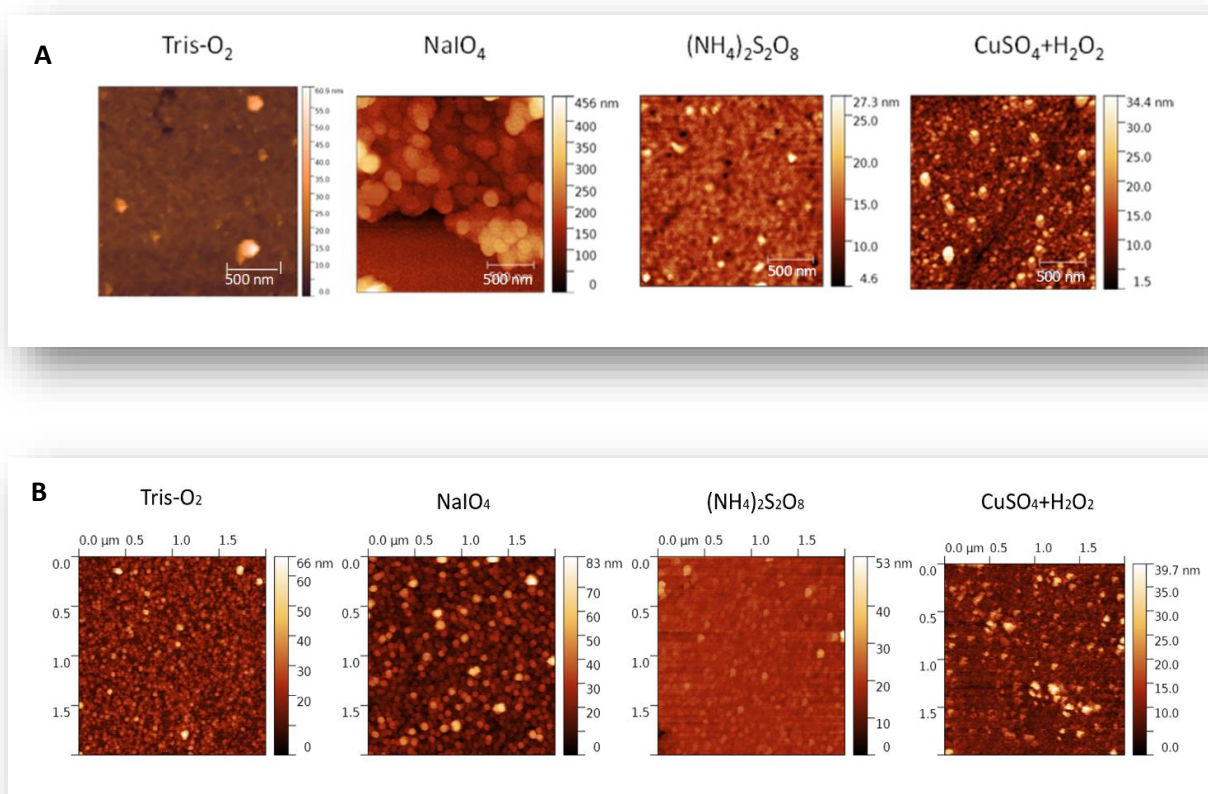


Figure 1: 2 μm x 2 μm AFM surface topographies of PDA/oxidant -8h (A) and PDA/oxidant -3h films (B).

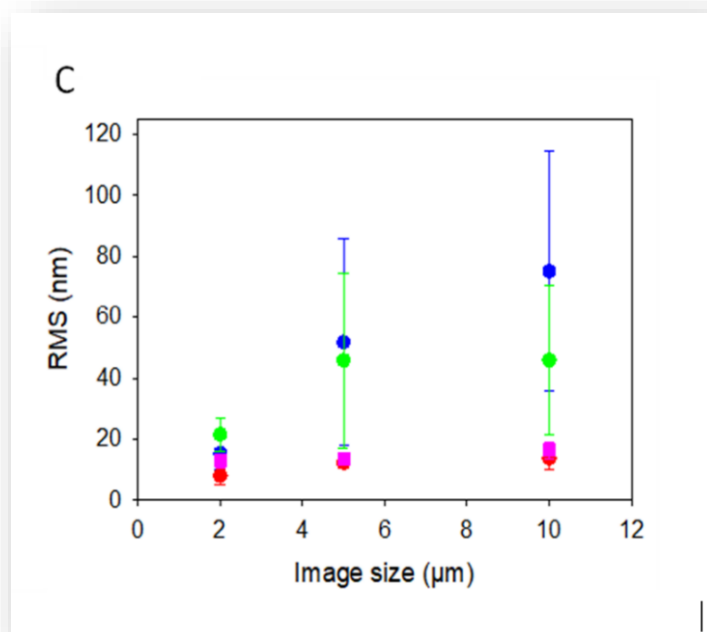


Figure 2: Dependence of the PDA/oxidant -8h films root-mean square roughness as a function of the image size. PDA@Tris-xh (●), PDA@NaIO₄-xh (●), PDA-CuSO₄+H₂O₂-xh (●) and PDA@(NH₄)₂S₂O₈-xh (●) films. These data correspond to 5 measurements \pm one standard deviation.

1.2. Films thickness

As a reminder, during the oxidation of dopamine, we can observe with the naked eye a color change of the solution or of the material on which the PDA is deposited. For example, the films deposited on quartz slides for UV analyzes have become black (fig.3). Even if it is not accurate- because of light scattering effects- the intensity of the color change is a nice indicator of the amount of PDA deposited on the slides, thus an indicator of the film thickness.

We could already see with the naked eye, notable differences between the four oxidants. The color of the slides on which PDA@NaIO₄ and PDA@CuSO₄+H₂O₂ were deposited change faster than the others. After only 1h30 the slides supporting the PDA@NaIO₄ and PDA@CuSO₄+H₂O₂ coatings already started to darken.

We found that the film thickness, as determined by topographic AFM imaging, is higher for the PDA@NaIO₄-8h films and for the CuSO₄+H₂O₂-8h films compared to PDA-(NH₄)₂S₂O₈ -8h and PDA@O₂-8h films (fig. 4A). The same trend holds true after 3 h of deposition (fig. 4B) but in a less marked manner. Concerning the films produced with NaIO₄ (65 nm after 1 h in the presence of 20 mM NaIO₄ (2)) and CuSO₄+H₂O₂ (43 nm in 1h (3)) our findings are consistent with those in previous reports. Regardless the used oxidant, the film thickness is almost independent on the image size, indicating a conformal coating.

Coating methods	1h30 - 8h oxidation
PDA@O ₂	
PDA@NaIO ₄	
PDA@CuSO ₄ +H ₂ O ₂	
PDA@(NH ₄) ₂ S ₂ O ₈	

Figure 3: color change of the PDA/oxidant-xh films on quartz slides after 1h30 and 8h oxidation.

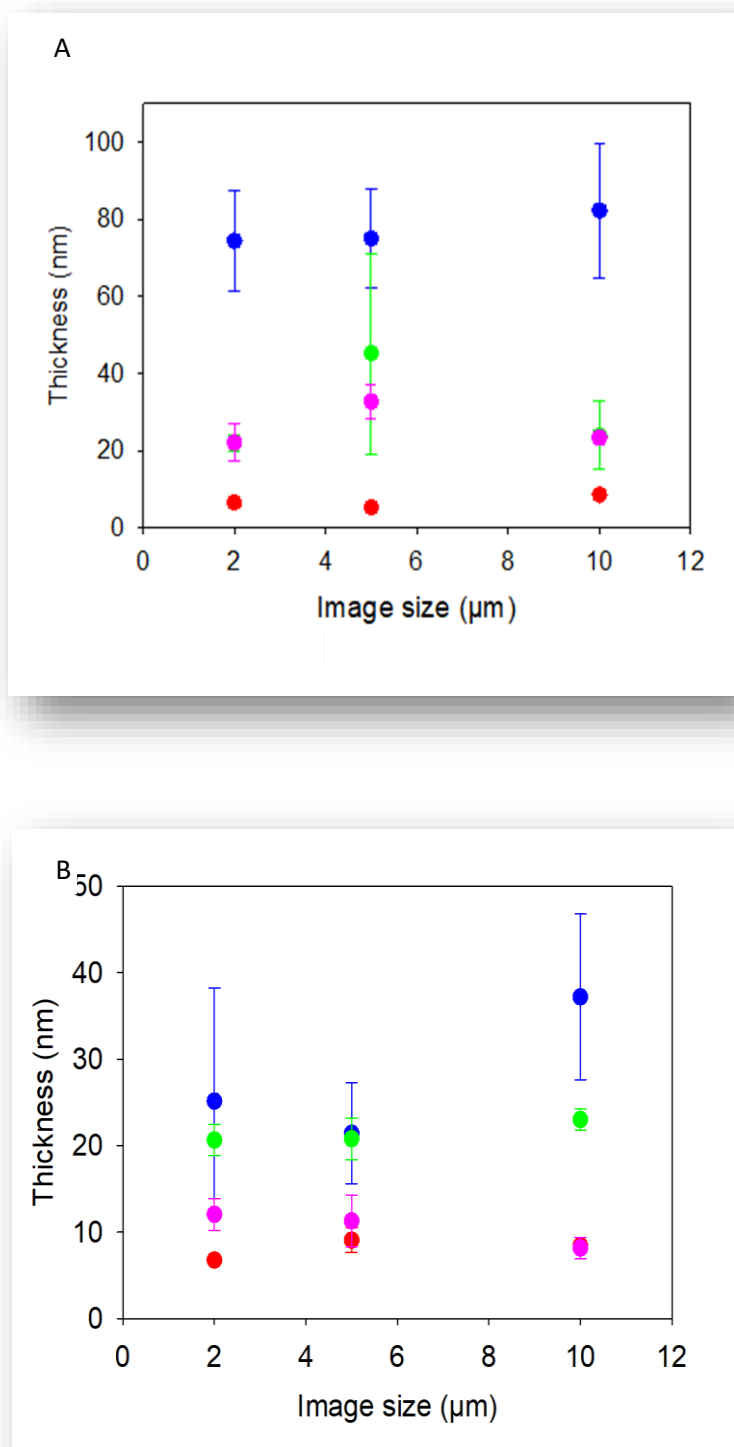


Figure 4: Evolution of the film thickness as a function of the image size for PDA/oxidant-8h (A) and PDA/oxidant-3h (B) samples. The data have been determined from topographical profiles in AFM images and the error bars correspond to \pm one standard deviation over $n = 5$ measurement. PDA@Tris-xh (●), PDA@NaIO₄-xh (●), PDA-CuSO₄+H₂O₂-xh (●) and PDA@(NH₄)₂S₂O₈-xh (●) films.

The large standard deviations on the films' thickness (Fig. 4) and roughness (Fig. 2) are obviously increasing with the granular morphology of the films, in direct relationship with the heterogeneous nature of PDA and related eumelanin like materials.

It is worth noting that the films morphology, thickness, and roughness, are not a monotonous function of the oxidant's strength. This is expected on the basis of kinetic effects : even if $(\text{NH}_4)_2\text{S}_2\text{O}_8$ is the strongest investigated oxidant (the standard redox potentials are listed in Table 1) the formation kinetics of the oxidizing sulfate through decomposition of peroxydisulfate is a much slower process than the direct dopamine oxidation using the two electron oxidant NaIO_4 (4).

It has to be noted also that the presence of CuSO_4 alone induces a slow film deposition mainly through Cu^{2+} - catechol coordination (5) and that H_2O_2 only induces a yellow coloration of the dopamine solution and no measurable film deposition in agreement with the known reaction mechanism of catecholamines with H_2O_2 (6). Indeed, hydrogen peroxide induces oxidation of dopamine to a quinone or semi quinone but the forthcoming intramolecular addition, leading normally to leucodopaminechrome is then precluded by an epoxidation as manifested by the obtention of a stable yellowish solution.

2. Chemical composition of the dopa/oxidant-xh films

2.1. UV Vis analysis

To better understand the influence of the oxidants on the PDA formation, we compared the chemistry of films and solutions after 1h30 and 8h oxidation time. The oxidation process of the four oxidants were monitored using UV Vis spectrophotometry (more details on the protocol are given in chapter 2, section 3.1.1). Absorbance spectra showed dissimilarities between not only the oxidants but also between films and solutions (fig. 5). These findings highlight the complexity of the PDA chemistry.

The initial steps leading to PDA formation can be resumed as following: dopamine > dopamine semiquinone > dopaminequinone > leucodopaminechrome > dopaminechrome > DHI > PDA materials. More details and schemes were already given in chapter 1, figure 2.

Concerning PDA@NaIO_4 -1h30 solution, we could observe a rapid transformation of the dopamine into the yellow dopaminequinone (300 and 480 nm). Indeed, when adding sodium periodate into the dopamine containing solution, we could immediately see the transparent initial solution turning to yellow, then, after 1h30 the solutions became orange which is in accordance with the presence of the large band around 475 nm identified as the orange aminochrome. After 8h, these peaks are no longer observed, indicating several structural changes during the synthesis, and the replacement by a shoulder at 295 nm identified as leucodopaminechrome. Another intermediate species, namely dopaminechrome, was present (300 – 480 nm).

The PDA@ $(\text{NH}_4)_2\text{S}_2\text{O}_8$ presented only one peak at 280 nm due to dopamine at the beginning of the oxidation, but at 8h we observed a flattened peak around 475 nm (aminochrome). These results are like the experimental observation: at 8h the PDA@ $(\text{NH}_4)_2\text{S}_2\text{O}_8$ solution appeared very orange.

Even if we could see some similarities between PDA@ O_2 and $(\text{NH}_4)_2\text{S}_2\text{O}_8$ in terms of roughness and thickness, they presented different UV spectra which underlines the difficult challenge of bringing out a very precise model of each oxidant. However, from the UV Vis spectra we could notice a decrease of the absorption peak at 280 nm (dopamine) after 8h oxidation revealing a transformation of the initial material. PDA formation by dissolved oxygen in Tris buffer usually takes 24h synthesis, thus 1h30 or even 8h are too short time for this oxidant since all experiments were made at room temperature.

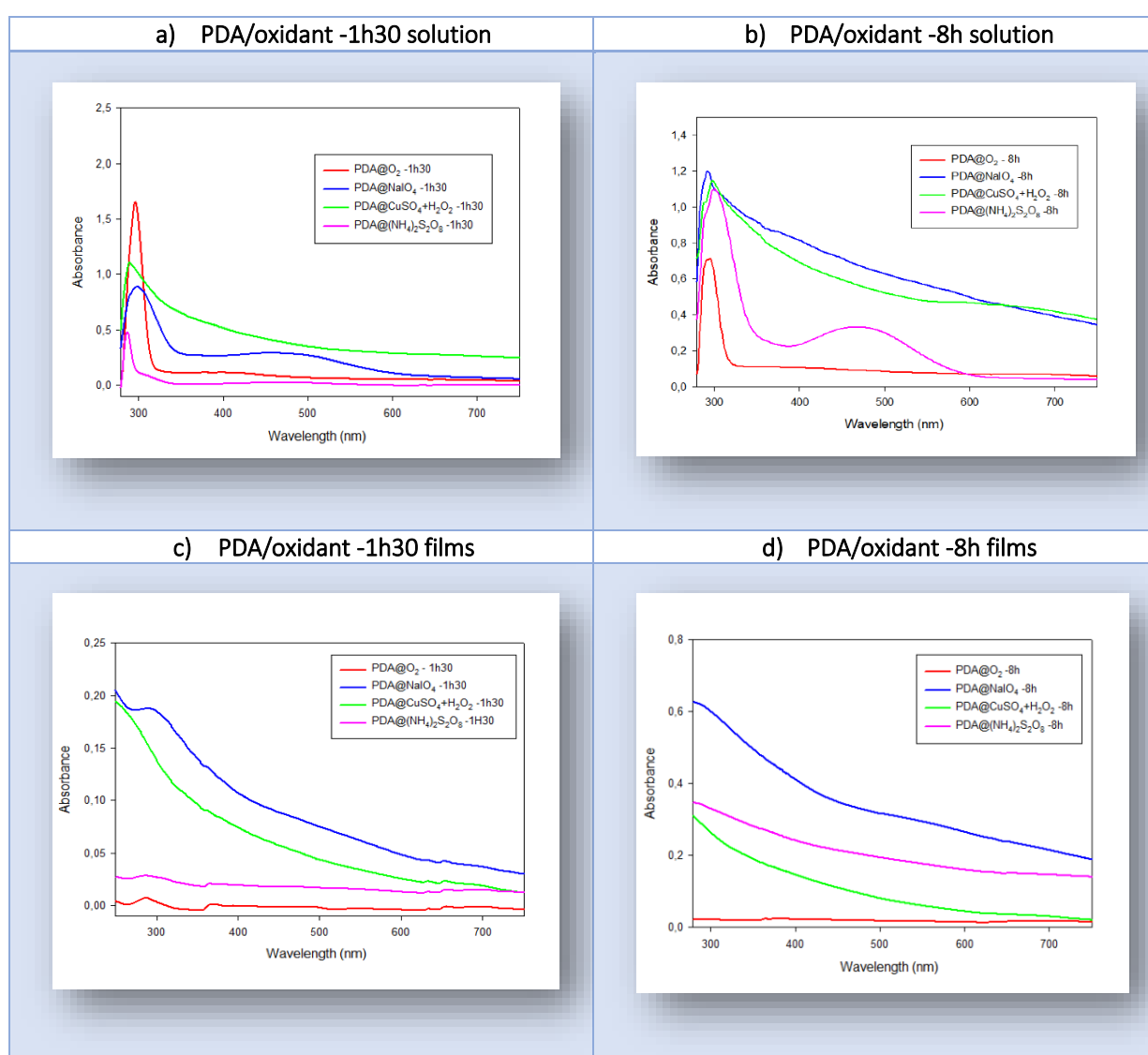


Figure 5: Absorbance spectra of the PDA/oxidant-xh in suspension (a,b) diluted 20x with references as Tris buffer for PDA@ O_2 and sodium acetate buffer for the three other oxidants and in films (c,d).

2.2.XPS analysis

The C1S XPS spectra of dopa/oxidant-8h (fig.6) evidence a difference of composition and structures. The O1S and N1S XPS spectra are given in the fig. S4 and S5 of the supporting information respectively at the end of this chapter.

The XPS survey spectra of the films were analyzed, taking the Scofield sensitivity parameters into account, to determine the composition of the films (Table 1). It is interesting to note that gold was never detected, within the uncertainty of the data ($\pm 1\%$), after 8h of deposition. This suggests-in agreement with the AFM (fig.1) and electrochemical data (fig. 8), that the obtained films are conformal without regions of the substrate accessible to the X-ray beam, characterized by a penetration depth of a few nanometers. However, the PDA@CuSO₄+H₂O₂ - 8h films contain about 2.7 % Cu (Table 1) in agreement with previous data (5) and with the cyclic voltammetry curve (fig.8) of the corresponding film.

Element or elemental ratio in %	O ₂	NaIO ₄ $E_{IO_4^-/IO_3^-}^\circ$ = 1.55 V	CuSO ₄ +H ₂ O ₂ $E_{H_2O_2/H_2O}^\circ$ = 1.78 V, $E_{Cu^{2+}/Cu}^\circ$ = 0.34 V	(NH ₄) ₂ S ₂ O ₈ $E_{S_2O_8^{2-}/HSO_4^-}^\circ$ = 2.12V	Dopamine (calculated)
C	71.5±0.5	68.4±0.3	65.1±0.9	70.5 ± 0.3	62.7
N	8.2 ± 1.0	8.0±0.2	8.2±0.4	7.8 ± 0.2	9.1
O	20.3 ± 0.7	22.3±0.5	23.4±0.4	21.2 ± 0.3	20.9
Au	0.0	0.0	0.0	0.0	/
Cu	0.0	0.0	2.7±0.2	0.0	/
N/C	0.11±0.02	0.12±0.01	0.13±0.01	0.11±0.01	0.12
O/C	0.28±0.01	0.33±0.01	0.36±0.01	0.30 ± 0.01	0.25

Table 1: Elemental composition (in % and average N/C and O/C ratios for the PDA/oxidant-8h films as obtained by XPS on n = 3 samples. All data are given \pm one standard deviation.

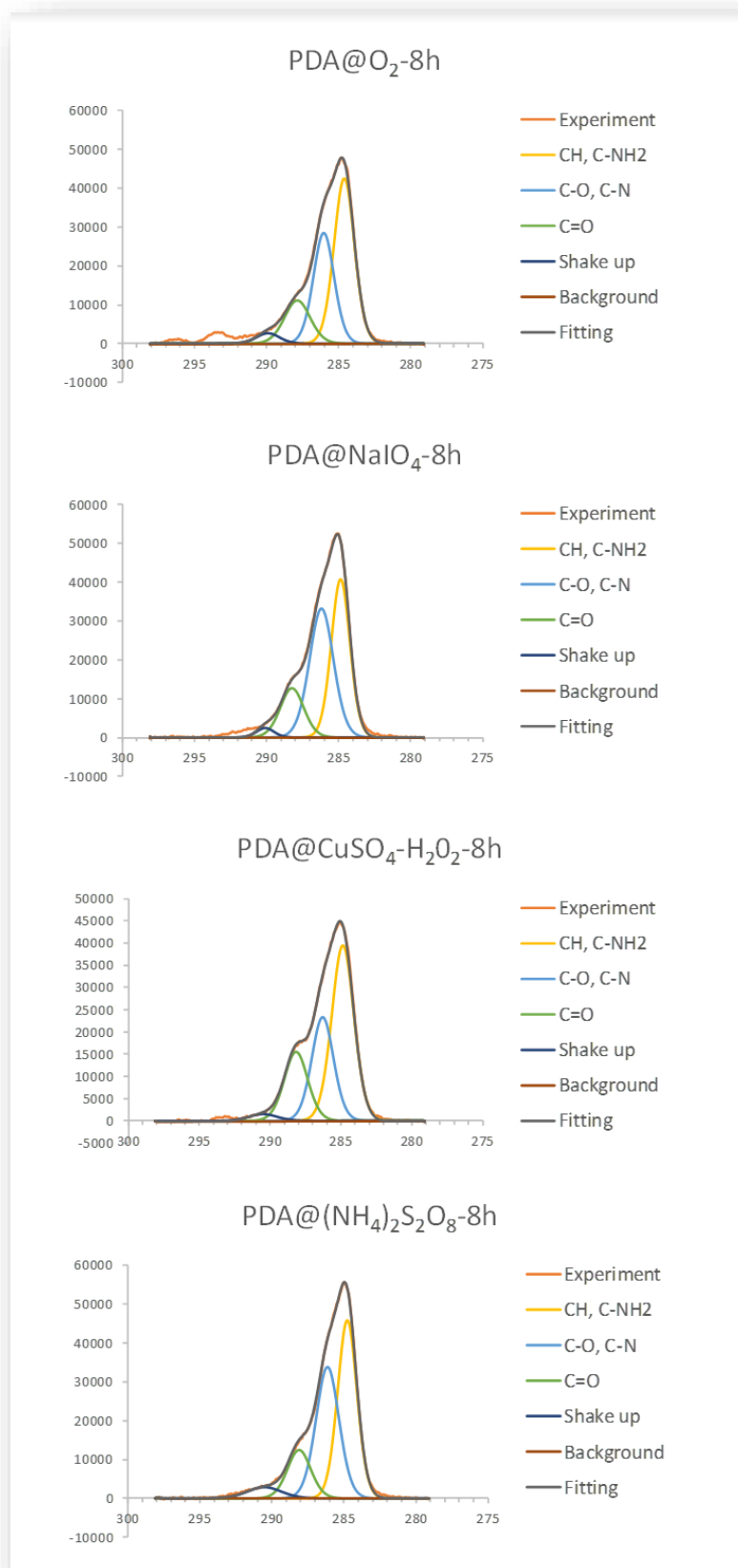


Figure 6: Representative XPS spectra in the C1s region of PDA/oxidant-8h films. The colored lines correspond to the spectral deconvolution with the corresponding chemical assignments on the right.

From the table 1, we can see that we have a remarkably similar N/C ratio when comparing the different oxidants, but also similar to dopamine alone (monomer). This suggests conservation of the aliphatic chains with no detectable loss of amine group. However, the O/C ratio shows that the PDA samples displays structural modifications. As expected, the O/C ratio is higher for all the PDA/oxidant films produced in the presence of strong oxidants, with a value of 0.28 for O_2 , 0.33 for $NaIO_4$, 0.36 for $CuSO_4+H_2O_2$ and 0.30 for $((NH_4)_2S_2O_8)$. These values are significantly higher than the O/C ratio of dopamine, that is 0.25. The highest O/C ratio is obtained for the films prepared with $CuSO_4+H_2O_2$. In the case of PDA- O_2 -8h films, the O/C ratio was only slightly higher than that for monomer dopamine indicating minimal structural alteration caused by synthetic and post-synthetic oxygenation/oxidative breakdown.

All PDA samples seems to contain newly oxygenated units which may arise from various mechanisms depending on the oxidation process, including epoxidation (in the case of H_2O_2 - containing media, pathway a in fig. 7) and hydroxylation of the o-quinone ring (1 O atom per unit, pathway b in fig. 7) and muconic-type fission of quinone rings (2 O atoms per unit, pathway c in fig. 7). It is thus reasonable to suggest that variable proportions of the aforementioned units account for the incorporation of oxygen via the above oxidant-dependent mechanisms, as illustrated in fig 8.

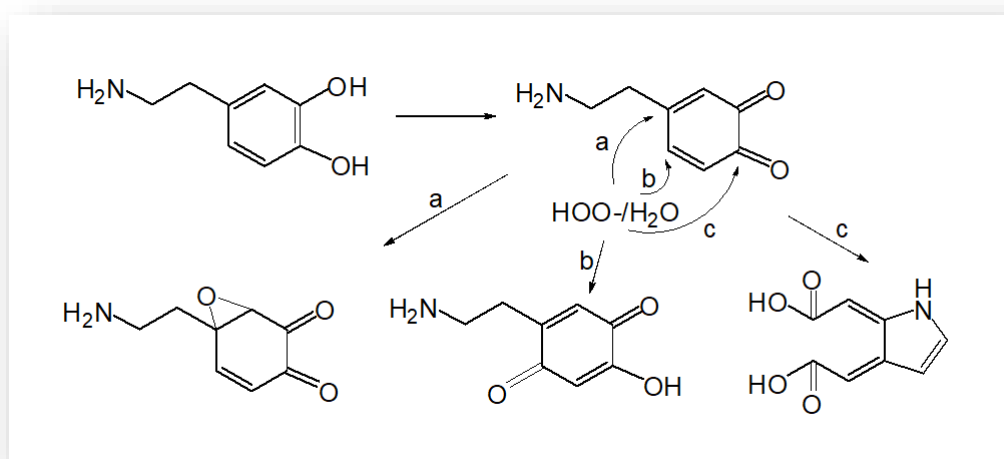


Figure 7: Possible mechanism of oxygenation of dopamine units during PDA formation and film deposition. The different pathways correspond to epoxidation (a), hydroxylation (b) and muconic cleavage (c). This schema was designed and thought with close collaboration of Prof. Marco d'Ischia (University of Naples, Italy)

It can be concluded that all oxidants can induce oxidative degradation of the PDA films to a variable degree, depending both on their redox potential and their mechanism of action, i.e. via electron transfer ($(NH_4)_2S_2O_8$) or ester formation ($NaIO_4$) as the dominant mechanistic step, in agreement with previous observations in the case of PDA@ $NaIO_4$ films (2). Consistent with this view, milder oxidation conditions, i.e. PDA@ O_2 -8h films, produce minimal oxygenation/oxidative breakdown modifications, which can be estimated in the order of 24% and can be attributed to the generation of low levels of H_2O_2 by electron transfer from the catechol ring to molecular oxygen. $(NH_4)_2S_2O_8$, $NaIO_4$ and $CuSO_4+H_2O_2$ caused the most

significant modification to the original level of oxygenation. This observation is in line with the known formation of complexes between Cu^{2+} salts and catecholamines, which may evolve in an aerobic/oxidizing environment with partial electron transfer generating Cu(I) species capable of interacting with H_2O_2 to induce oxidative breakdown and oxygenation. Copper is a well-documented promoter of dopamine oxidation with concomitant formation of reactive species, such as $\cdot\text{O}_2^-$ and hydroxyl radicals via Fenton type chemistry

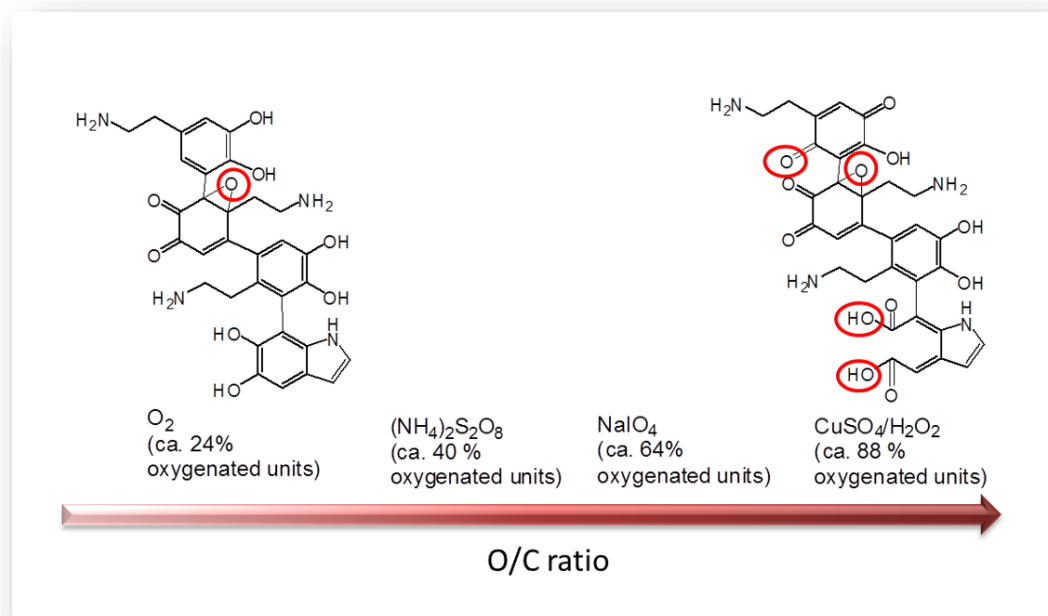


Figure 8: Proposed structures for PDA samples incorporating low (on the left) to high (on the right) levels of additionally oxygenated units. Epoxide moieties can be regarded as markers of H_2O_2 nucleophilic reactivity. This schema was designed and thought with close collaboration of Prof. Marco d'Ischia (University of Naples, Italy)

Comparative analysis of the N/C and O/C ratios as indices of structural integrity allowed to conclude that $(\text{NH}_4)_2\text{S}_2\text{O}_8$ and $\text{CuSO}_4+\text{H}_2\text{O}_2$ caused the most significant modifications to the original dopamine skeleton, the former through partial amine-containing chain degradation and the latter apparently through more extensive decarboxylation/oxygenation pathways. This conclusion is supported by the known formation of complexes between Cu^{2+} salts and catecholamines, which may evolve in an aerobic/oxidizing environment with partial electron transfer generating Cu(I) species capable of interacting with H_2O_2 to induce oxidative breakdown and oxygenation. Copper is a well-documented promoter of dopamine oxidation and partial deamination with concomitant formation of reactive species, such as $\cdot\text{O}_2^-$ and hydroxyl radicals via Fenton type chemistry (7).

We do not focus on the O/C and N/C ratios for the films obtained on gold coated mica substrates after 3 h of contact with dopamine + oxidant blends because most of them (with exception of the PDA@ NaIO_4 -1.5h films) are not conformal, with XPS spectra still displaying the presence of a few % of Au. However, the deconvolution of the XPS spectra shows that the distribution of chemical C-O and C-N groups changes with time in the case of films produced with $\text{CuSO}_4+\text{H}_2\text{O}_2$ and $(\text{NH}_4)_2\text{S}_2\text{O}_8$ (fig.9). Those films produced in the presence of the strongest

oxidant undergo some additional oxidation with time (fig. 9C), however the chemical composition of the films produced in the presence of O₂ is pretty stable with time (fig. 9A).

The N1s and O1s spectra of those films as well as the corresponding high resolution spectra of the purified PDA precipitates subsequently spin coated on gold coated substrates will be analyzed in detail in a forthcoming work aimed at getting deeper insight into the formation mechanism of PDA on surfaces and in the precipitate form. The UV-vis spectra shown in fig. 5 suggest that PDA deposited of quartz slides is different from PDA produced in solution. This assumption deserves future fundamental investigations.

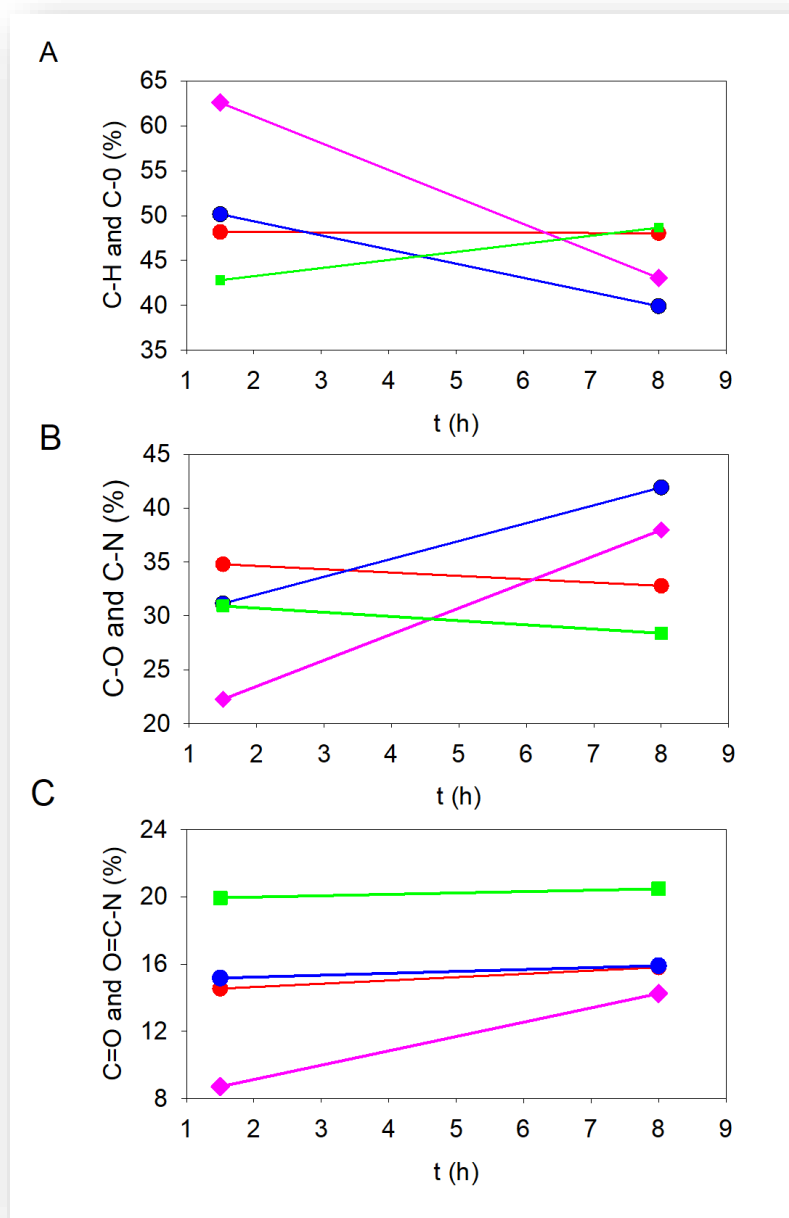


Figure 9: Evolution of the different components of the C1s XPS spectra with deposition time for the PDA@Tris-xh (●), PDA@NaIO₄-xh (●), PDA-CuSO₄+H₂O₂-xh (■) and PDA@(NH₄)₂S₂O₈-xh (◆) films.

3. Electrochemical behavior of the dopa/oxidant-xh films

All the PDA/oxidant-8h films contain electroactive groups as revealed by measuring their cyclic voltammetry curves as measured in the absence of a redox probe added in the buffer solution put in the presence of the film (fig.10).

The area under such curves represent the electrochemical capacity of the films which is related to their thickness and the surface area in contact with the solution which is modulated by the films' roughness. The area under the capacitive curves increases following the order of the $\text{PDA@O}_2 < \text{PDA@}(\text{NH}_4)_2\text{S}_2\text{O}_8 < \text{PDA@CuSO}_4\text{-H}_2\text{O}_2 < \text{PDA@NaIO}_4$ films (fig.10) and this ranking is in qualitative agreement with the thickness of the deposits (fig. 4) thereby emphasizing again that the strongest oxidant (table 1) is not the most efficient in the deposition of PDA films.

The most important information from the electrochemical experiments is however the clear evidence that the cyclovoltamograms of the PDA films depend on the oxidant used to oxidize dopamine (fig.10).

Films produced in the presence of NaIO_4 display not only a high oxidation current but also a broad distribution of oxidation peaks.

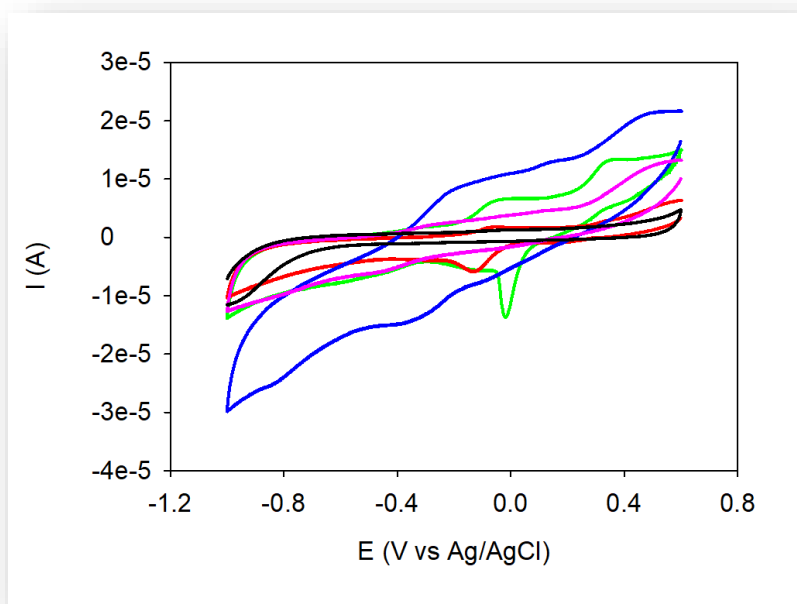


Figure 10: Cyclic voltammetry curves in the presence of the same buffers (sodium acetate or Tris) used for the film deposition : polished electrode (●, sodium acetate buffer), $\text{PDA@O}_2\text{-8h}$ (●, Tris buffer), $\text{PDA@NaIO}_4\text{-8h}$ (●, sodium acetate buffer), $\text{PDA@CuSO}_4\text{-H}_2\text{O}_2\text{-8h}$ (●, sodium acetate buffer) and $\text{PDA@}(\text{NH}_4)_2\text{S}_2\text{O}_8\text{-8h}$ (●, sodium acetate buffer).

The reduction peak observed at about -0.05 V vs Ag/AgCl in the case of $\text{PDA@CuSO}_4\text{-H}_2\text{O}_2$ may well be due to the presence of Cu^{2+} cations in the films, in accordance with XPS measurements made on PDA films using CuSO_4 alone as an oxidant (5).

In all cases, when successive oxidation-reduction cycles are performed, the total charge (proportional to the area under the cyclovoltamogram) progressively decreases implying irreversible chemical processes taking place in the part of the films accessible to the conductive amorphous carbon electrode (fig. S6 of the supporting information, in the particular case of PDA@ $(\text{NH}_4)_2\text{S}_2\text{O}_8$ films).

This observation is in very good agreement with previous results based on gate current measurements on aqueous suspensions of a synthetic eumelanin sample indicating a well detectable hysteretic response, attributed to electron transfer from the eumelanin polymer to the Pt-electrode caused by redox active catechol/quinone components, and a gradual decrease in gate current and areas of the hysteretic loops over repeated cycles, suggesting a far-from-the-equilibrium redox state of the polymer evolving toward a more stable electronic arrangement (8).

In addition, the obtained films are conformal since the hexacyanoferrate redox probe is not oxidized -reduced anymore when put in presence of the PDA/oxidant films deposited on the amorphous carbon working electrode (fig. S7 of the supporting information, in the particular case of PDA@ $(\text{NH}_4)_2\text{S}_2\text{O}_8$ films).

4. Properties of the dopa/oxidant-xh films

Differences in composition and morphology most likely lead to differences in terms of properties as these are related to the structure. In this section, we will see the influence of the oxidant on wettability and antioxidant properties of the PDA/oxidant films. A special focus will be given to the latter one due to the numerous potential applications of the PDA in the biomedical field.

4.1. Antioxidant properties

4.1.1. Basic features of antioxidants

Free radicals derived from oxygen, nitrogen and sulfur containing molecules are small, highly active and can easily react with other molecules due to their unpaired electrons. An excess of those molecules can attack bases in nucleic acids, amino acids side chains in proteins and double bonds in unsaturated fatty acids (9).

Antioxidants are compounds that can decrease the oxidative damage by neutralizing free radicals by accepting or donating electrons to eliminate the unpaired electrons of the radical. Indeed, many antioxidants have aromatic ring structures and are able to delocalize these unpaired electrons. Different mechanism can occur depending on the nature of the antioxidant. Synthetic antioxidants have been widely used in the food industry to avoid lipid oxidation. Such

antioxidant cannot be used for health use because of their toxicity. Then, some research effort has been conducted to identify natural compounds with antioxidant properties.

Several studies have demonstrated that eumelanin has an antioxidant activity. Due to the chemical structure similarities between eumelanin and PDA, the hypothesis that PDA also acts as an antioxidant came naturally.

We have seen in the previous section that PDA is redox-active and can accept and donate electrons. This electron donating-accepting ability depends on its redox state but also on external factors as near-infrared irradiation or metal ion binding. Taking all our results into account, we decided to investigate the antioxidant properties of polydopamine films. More precisely, we analyzed the influence of the oxidant used during polydopamine coatings.

4.1.2. Antioxidant activity of the PDA/oxidant-xh films

The method including the use of DPPH as a stable free radical is widely used to measure the radical scavenging activity of materials. More details about the protocol used are given in chapter 2, section 3.2.5. Even if the antioxidant properties of PDA are little known, few investigations have been done to study antioxidant of PDA films.

As expected, [32-34], all the PDA/oxidant-xh films display some antioxidant activity as evidenced by the discoloration of DPPH. Surprisingly, owing of the strong oxidation of those films (Table 1), the PDA@NaIO₄ films display the most efficient effect (fig. 11A). The DPPH scavenging efficiency-calculated (according to the equation in chapter 2 section 3.2.5) of the PDA@O₂, the PDA@NaIO₄ and the PDA@CuSO₄-H₂O₂ films slightly decreases with the deposition time (fig. 11B) whereas the film thickness continues to increase (fig.4A and 4B). This is not the case for the PDA@(NH₄)₂S₂O₈ films which have a constant scavenging efficiency upon an only slight increase in film thickness from 3 to 8 h of deposition (fig. 11B). Taken together, these data show that the antioxidant activity of the films is not an increasing function of the film thickness. This result is not surprising since DPPH is a large pretty hydrophobic molecule which should not diffuse deeply in the hydrophilic PDA/oxidant coatings. We have shown that even a small hydrophilic redox probe like hexacyanoferrate is not able to cross the PDA/oxidant films (fig. S7 in the supplementary information).

The slight decrease in antioxidant activity of the PDA@O₂, the PDA@NaIO₄ and the PDA@CuSO₄-H₂O₂ films with the deposition time (fig. 11B) may be attributed to a progressive oxidation of the surface catechol groups, even if this should also occur in the case of the PDA@(NH₄)₂S₂O₈ films. One would have expected the highest anti-oxidant effect for the films containing the highest fraction of catechol groups and displaying the lowest O/C ratio, i.e. the less oxidized films, namely those produced in the presence of O₂ dissolved in Tris buffer (Table 1). It must be noticed also that, at first glance, the scavenging efficiency of the PDA/oxidant films appears pretty low-less than 25%. This is however due to the low surface area (45 mm × 26 mm on each side of the glass slide) to volume (50 mL) ratio in the performed experiments. Hence, the most important observation from fig. 11B is the apparent higher scavenging

efficiency of the PDA@NaIO₄ films with respect to the other films which appear similar from this point of view.

Interestingly, when the antioxidant activity is normalized by the film roughness (fig. 2) it appears that it is almost independent on the nature of the used oxidant (fig. 12)/

In addition, despite the chemical expectation of a loss of antioxidant functionalities, the films produced in the presence of strong oxidants are remarkably efficient with respect to this property (fig. 9). Indeed, a reduction in the surface concentration of reducible functionalities is partially compensated by an increase in the surface area accessible to the solvent. This increase in surface area is estimated as the film roughness in this case (fig. 2). However, the relative antioxidant activity of the films decreases with the deposition time (fig. 12) following the same general trend as the antioxidant activity itself, suggesting again that prolonged exposure to oxidants reduces the antioxidant activity of the PDA/oxidant films.

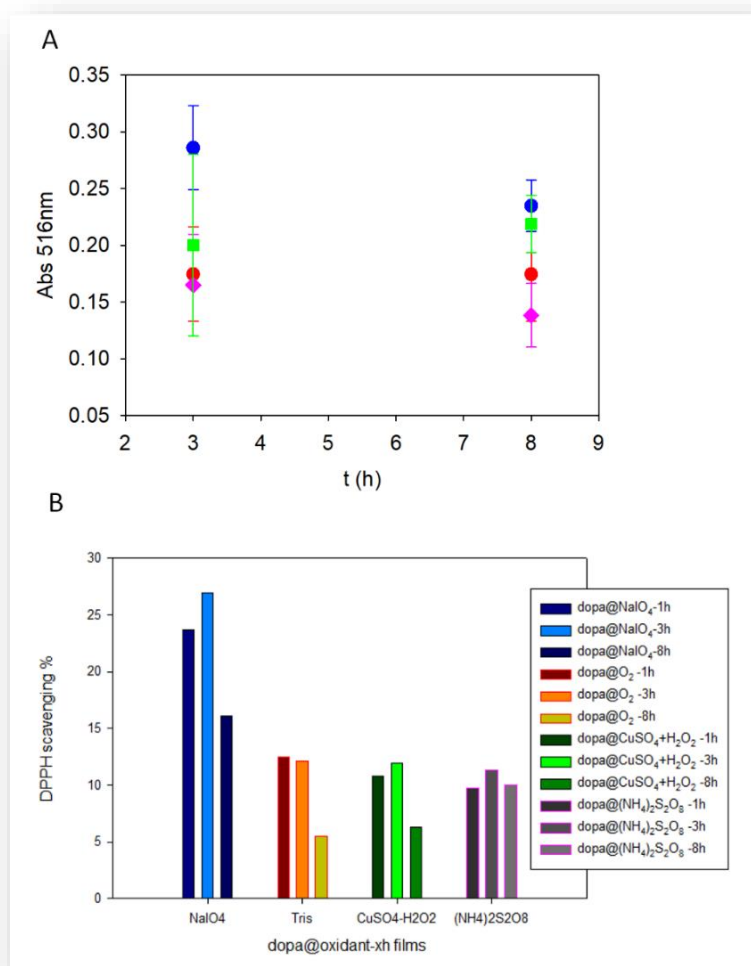


Figure 11: A): Absorbance of the PDA/oxidant films after 3h and 8h deposition time on glass slides and after 2h immersion in a DPPH solution: (●) PDA@O₂, (●) PDA@NaIO₄, (■) PDA@CuSO₄-H₂O₂; (◆) PDA@(NH₄)₂S₂O₈. B): DPPH scavenging efficiency of the PDA/oxidant-xh films as indicated in the inset. The scavenging efficiency is quantified as the reduction in absorbance at $\lambda=516$ nm divided by the initial absorbance of the DPPH solution (10^{-4} M in all experiments).

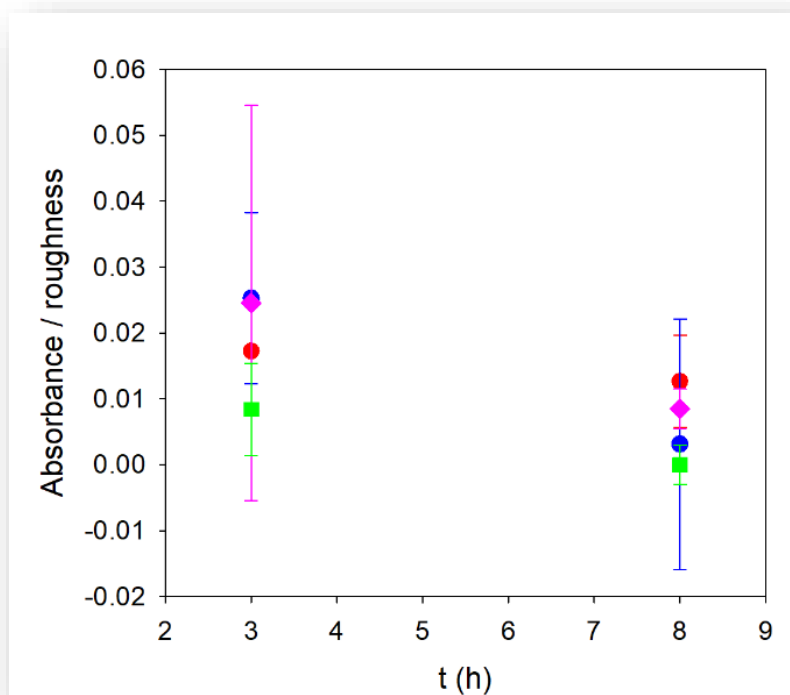


Figure 12: Relative anti-oxidant activity, as quantified by the ratio of the absorbance peak at 516 nm by the film roughness (as determined on $2\ \mu\text{m} \times 2\ \mu\text{m}$ AFM topographic images) for each PDA@ oxidant film as a function of the deposition time. The significance of the colored symbols is: (●) PDA@Tris, (●) PDA@NaIO₄, (■) PDA@CuSO₄-H₂O₂; (◆) PDA@(NH₄)₂S₂O₈.

Hence, the PDA@NaIO₄ films feature numerous advantages with respect to the films prepared in the presence of the other used oxidants, not only due their faster deposition kinetics but also in term of conservation of antioxidant properties, which is due to a compensation of a lost in the catechol surface density (due to oxidation) by an increase in the film's roughness.

Conclusions

The morphology, electrochemical behavior and the composition of PDA films prepared by the oxidation of dopamine are **markedly dependent on the used oxidant**.

All PDA films exhibit some **antioxidant properties**, reflecting the presence of non-oxidized catechol groups even in the presence of strong oxidants like NaIO_4 and $(\text{NH}_4)_2\text{S}_2\text{O}_8$. Surprisingly, the antioxidant activity seems the strongest on the PDA@NaIO_4 films which have undergone strong oxidation, but similar to that of the $\text{PDA@CuSO}_4+\text{H}_2\text{O}_2$ and $\text{PDA@}(\text{NH}_4)_2\text{S}_2\text{O}_8$ films. This result could be rationalized after normalization of the antioxidant activity by the roughness of the films yielding to an almost oxidant independent behavior.

The findings presented in this report highlight the **great diversity of PDA films** in their morphology, structure, and composition as well as in their properties. Such fundamental knowledge should pave the way to improve the already numerous applications of polydopamine films.

References

1. Salomäki M, Marttila L, Kivelä H, Ouvinen T, Lukkari J. Effects of pH and Oxidants on the First Steps of Polydopamine Formation: A Thermodynamic Approach. *J Phys Chem B*. 21 juin 2018; 122(24):6314-27.
2. Ponzio F, Barthès J, Bour J, Michel M, Bertani P, Hemmerlé J, et al. Oxidant Control of Polydopamine Surface Chemistry in Acids: A Mechanism-Based Entry to Superhydrophilic-Superoleophobic Coatings. *Chem Mater*. 12 juill 2016; 28(13):4697-705.
3. Wei Q, Zhang F, Li J, Li B, Zhao C. Oxidant-induced dopamine polymerization for multifunctional coatings. *Polym Chem*. 12 oct 2010; 1(9):1430-3.
4. Weidman SW, Kaiser ET. The Mechanism of the Periodate Oxidation of Aromatic Systems. III. A Kinetic Study of the Periodate Oxidation of Catechol. *J Am Chem Soc*. 1 déc 1966; 88(24):5820-7.
5. F B, V B, F A, A P, M M, Jj G, et al. Dopamine-melanin film deposition depends on the used oxidant and buffer solution. *Langmuir ACS J Surf Colloids*. 18 févr 2011; 27(6):2819-25.
6. Manini P, Panzella L, Napolitano A, d'Ischia M. A novel hydrogen peroxide-dependent oxidation pathway of dopamine via 6-hydroxydopamine. *Tetrahedron*. 24 mars 2003; 59(13):2215-21.
7. Bisaglia M, Bubacco L. Copper Ions and Parkinson's Disease: Why Is Homeostasis So Relevant? *Biomolecules*. févr 2020;10(2):195
8. Tarabella G, Pezzella A, Romeo A, D'Angelo P, Coppedè N, Calicchio M, et al. Irreversible evolution of eumelanin redox states detected by an organic electrochemical transistor: en route to bioelectronics and biosensing. *J Mater Chem B*. 17 juill 2013; 1(31):3843-9.
9. Lü J-M, Lin PH, Yao Q, Chen C. Chemical and molecular mechanisms of antioxidants: experimental approaches and model systems. *J Cell Mol Med*. avr 2010; 14(4):840-60.
10. Liu Y, Ai K, Ji X, Askhatova D, Du R, Lu L, et al. Comprehensive Insights into the Multi-Antioxidative Mechanisms of Melanin Nanoparticles and Their Application To Protect Brain from Injury in Ischemic Stroke. *J Am Chem Soc*. 18 2017; 139(2):856-62.
11. Ju K-Y, Lee Y, Lee S, Park SB, Lee J-K. Bioinspired Polymerization of Dopamine to Generate Melanin-Like Nanoparticles Having an Excellent Free-Radical-Scavenging Property. *Biomacromolecules*. 14 mars 2011; 12(3):625-32.
12. Liu H, Qu X, Tan H, Song J, Lei M, Kim E, et al. Role of polydopamine's redox-activity on its pro-oxidant, radical-scavenging, and antimicrobial activities. *Acta Biomater*. 01 2019; 88:181-96.

List of the figures – chapter 4:

Figure 1: AFM surface topographies of PDA/oxidant -8h (A) and PDA/oxidant -3h films (B).	87
Figure 2: Dependence of the PDA/oxidant -8h films root-mean square roughness as a function of the image size.	88
Figure 3: color change of the PDA/oxidant-xh films on quartz slides after 1h30 and 8h oxidation.	89
Figure 4: Evolution of the film thickness as a function of the image size for PDA/oxidant-8h (A) and PDA/oxidant-3h (B) samples.	90
Figure 5: Absorbance spectra of the PDA/oxidant-xh in suspension (a,b) diluted 20x with references as Tris buffer for PDA@O ₂ and sodium acetate buffer for the three other oxidants and in films (c,d).	92
Figure 6: Representative XPS spectra in the C1s region of PDA/oxidant-8h films.....	94
Figure 7: Possible mechanism of oxygenation of dopamine units during PDA formation and film deposition.	95
Figure 8: Proposed structures for PDA samples.....	96
Figure 9: Evolution of the different components of the C1s XPS spectra with deposition time	97
Figure 10: Cyclic voltammetry curves.	98
Figure 11: A): Absorbance of the PDA/oxidant films after 3h and 8h deposition time	101
Figure 12: Relative anti-oxidant activity, as quantified by the ratio of the absorbance peak at 516 nm by the film roughness	102

List of the tables – Chapter 4:

Table 2: Elemental composition (in % and average N/C and O/C ratios for the PDA/oxidant-8h films as obtained by XPS on n = 3 samples..	93
---	----

Supporting information

AFM surface topographies

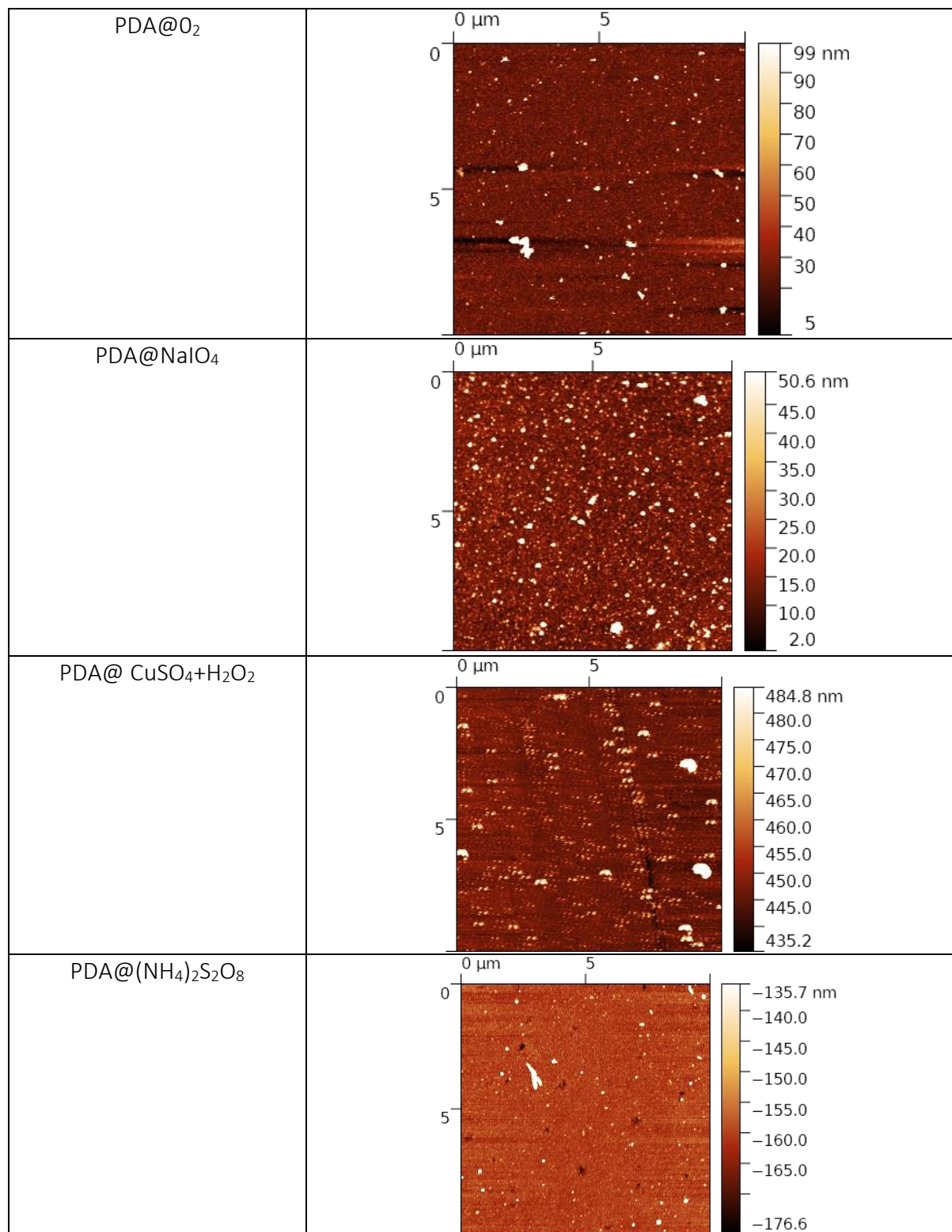


Fig. S1: AFM surface topographies, on 10 μm x 10 μm images for PDA/oxidant-3h films.

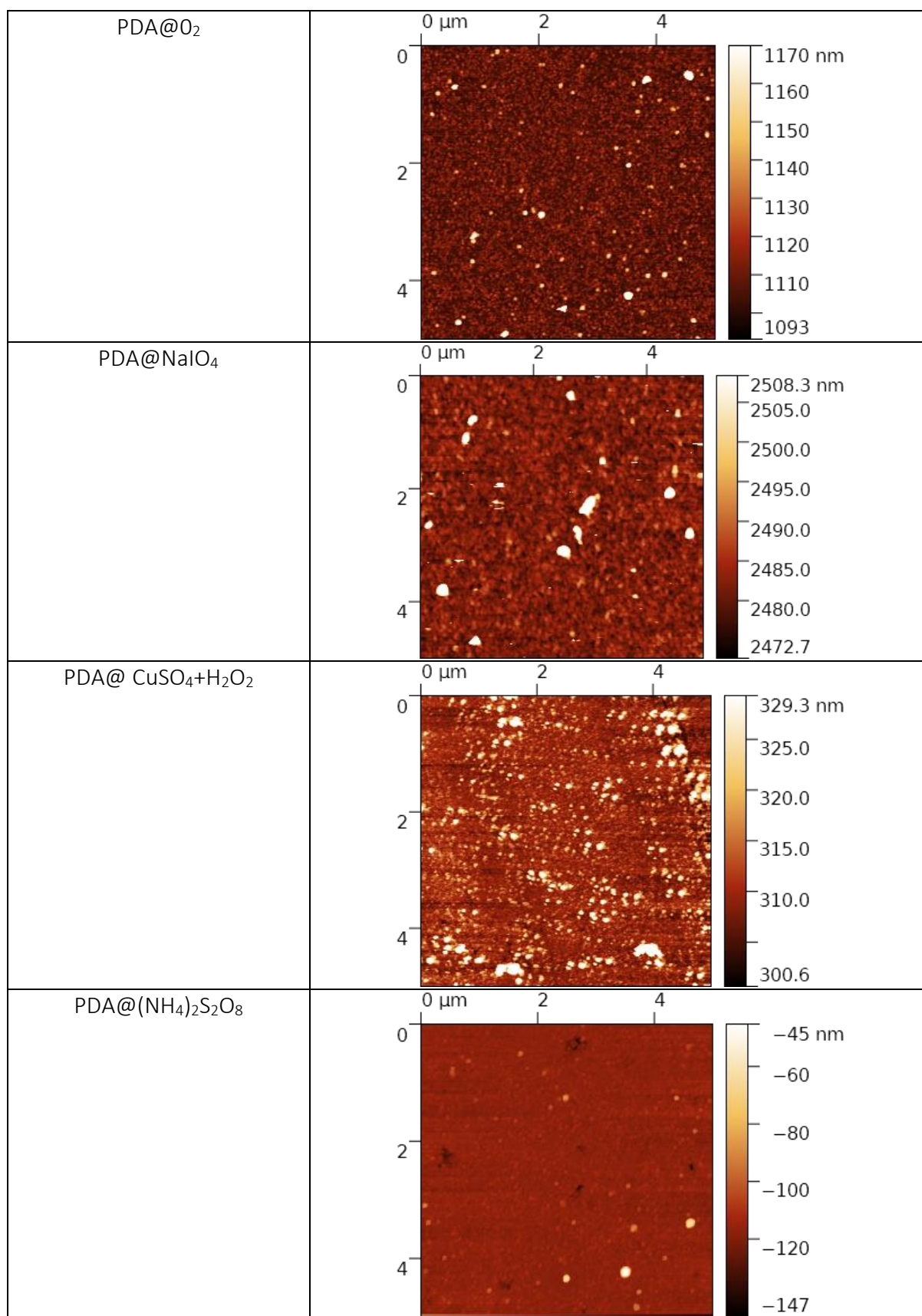


Fig. S2: AFM surface topographies, on 5 μm x 5 μm images for PDA/oxidant-3h films.

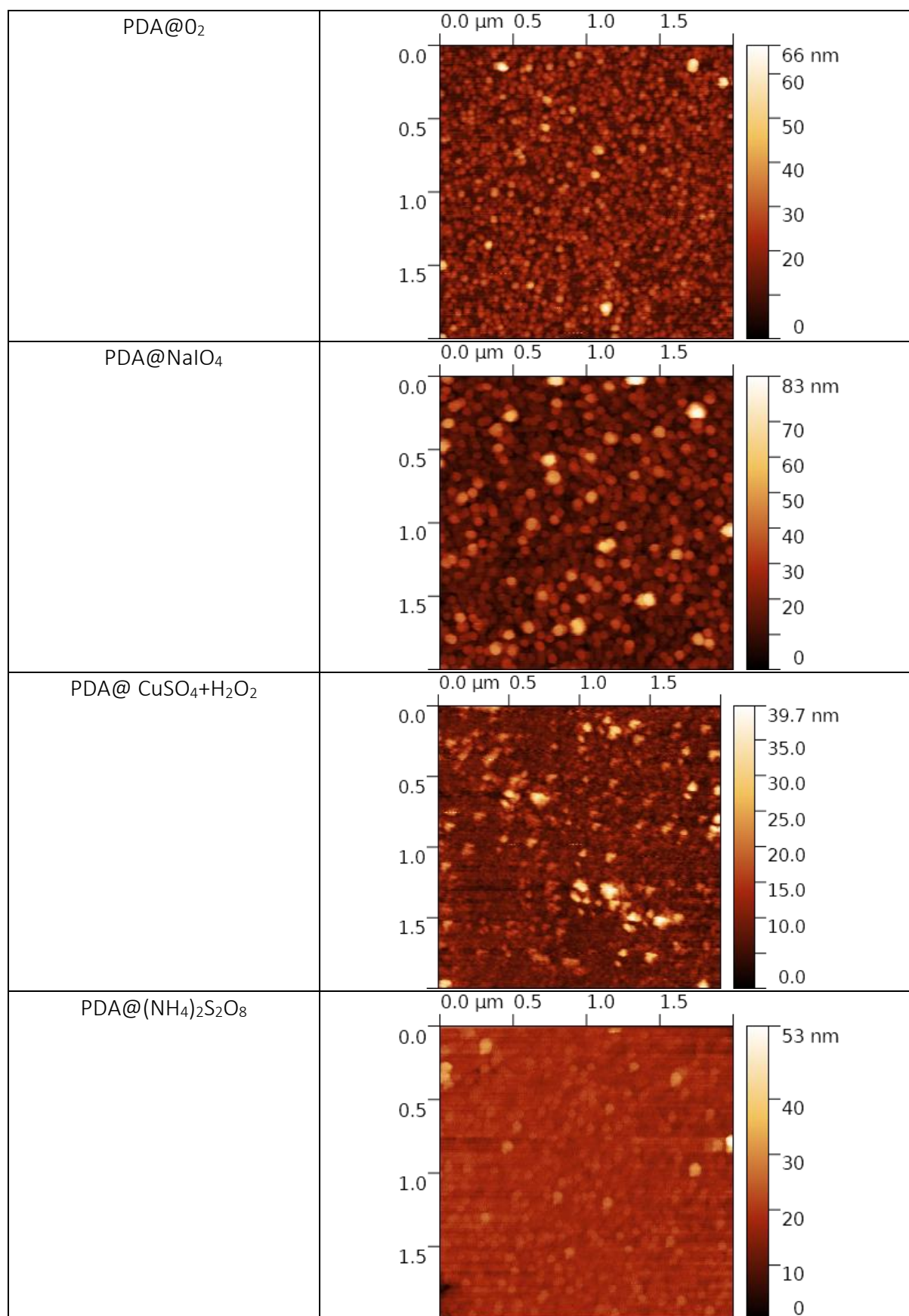


Fig. S3: AFM surface topographies, on 2 μm x 2 μm images for PDA/oxidant-3h films.

XPS spectra

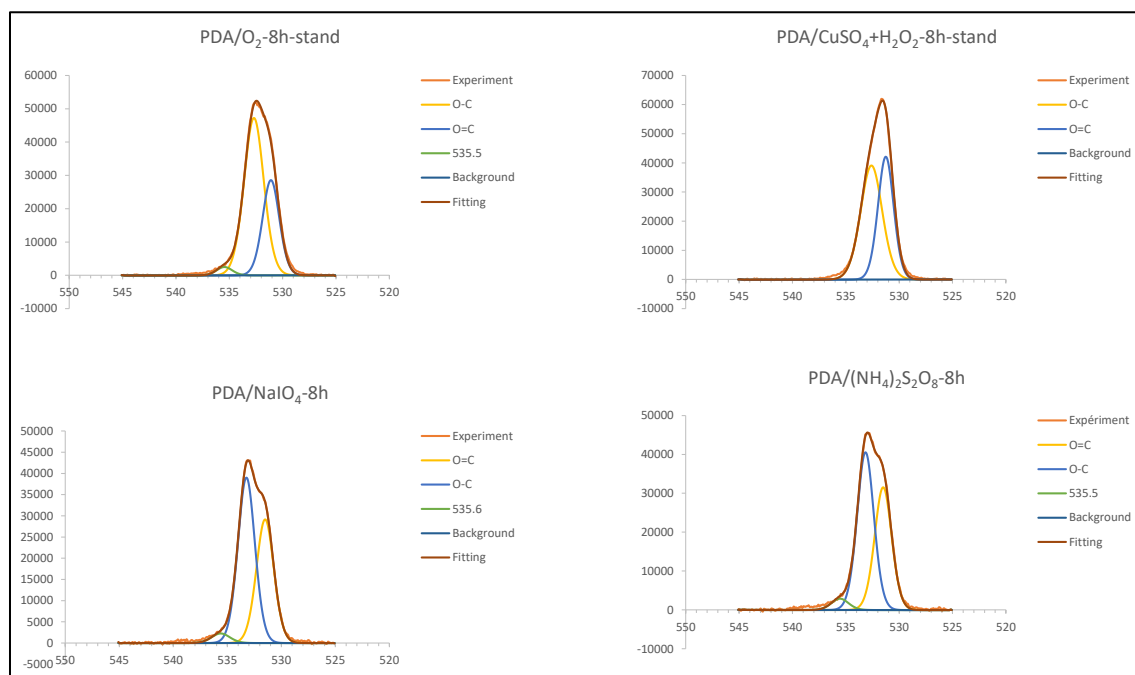


Fig. S4: O1S XPS spectra of PDA/oxidant-8h films deposited on gold coated mica slides. The deconvolution of the spectra in their constitutive chemical components are indicated with colored lines.

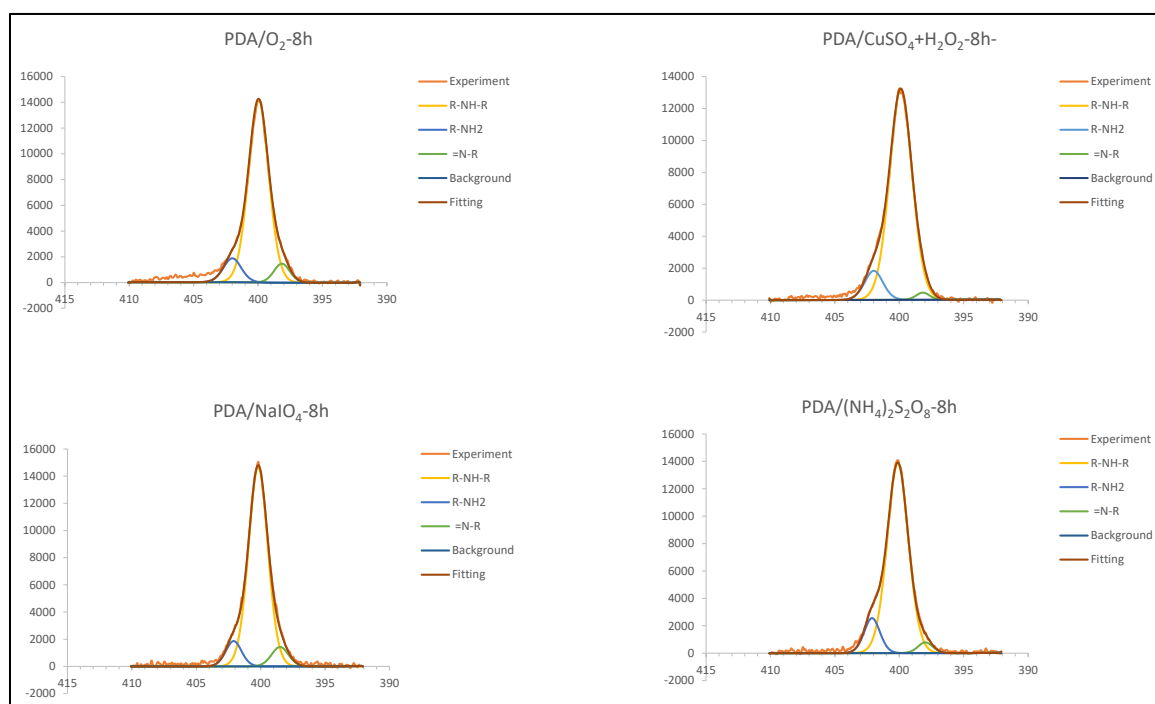


Fig. S5: N1S XPS spectra of PDA@oxidant-1h 30 films deposited on gold coated mica slides. The deconvolution of the spectra in their constitutive chemical components are indicated with colored lines.

Cyclic voltammetry

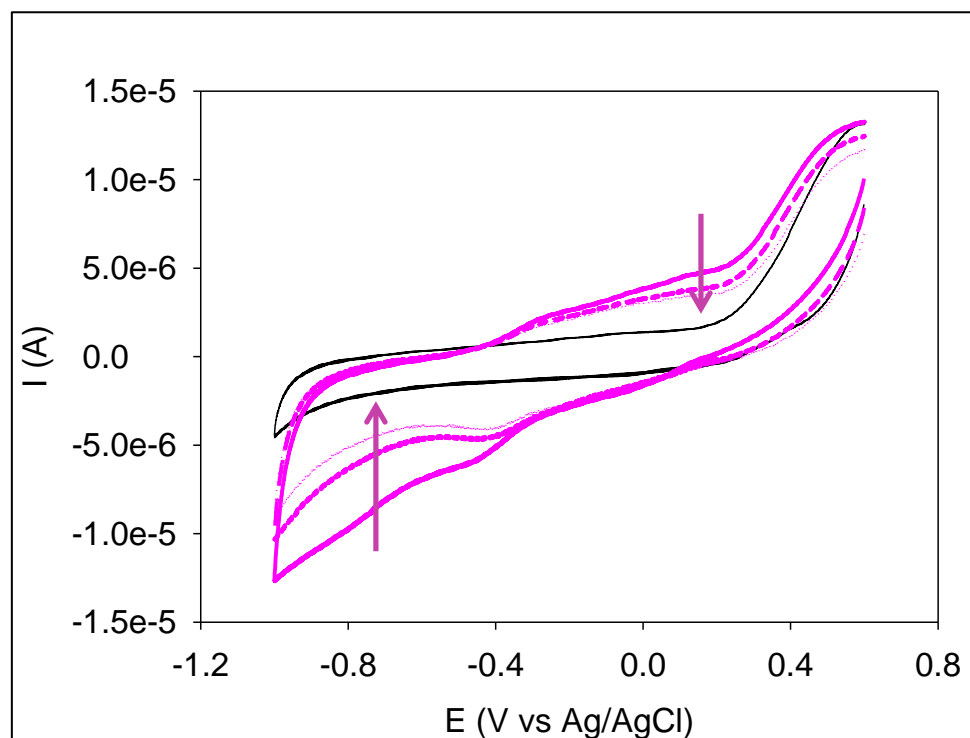


Fig. S6: Capacitive curves of the polished electrode (—) and of the PDA/(NH₄)₂S₂O₈-8h films deposited on the same electrode after the first (—), second (---) and third (···) CV cycle.

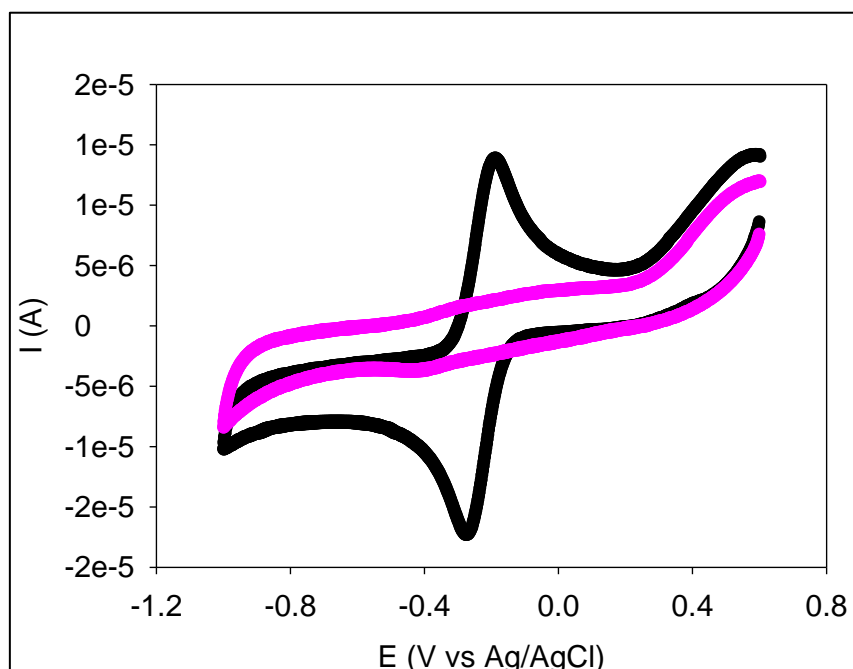


Fig. S7: Faradic CV curve (in the presence of 1 mM K₄Fe(CN)₆ dissolved in 50 mM sodium acetate buffer) of the polished electrode (black symbols) and of the electrode covered with a PDA/(NH₄)₂S₂O₈-8 h film (purple symbols).

Chapter 5

« Stay hungry, stay foolish. »

Steve Jobs

Chapter 5:

Gelatin@Polydopamine-based hydrogels

INTRODUCTION	113
1. BASIC FEATURES OF GELATIN AND PDA GEL	114
1.1. GELATIN HYDROGELS	114
1.2. GELATIN@POLYDOPAMINE-BASED HYDROGELS.....	114
1.3. OUR STRATEGY	116
2. FORMATION OF GELATIN@PDA HYDROGELS	117
2.1. INFLUENCE OF THE DOPAMINE CONCENTRATION.....	117
2.1.1. Influence on the elasticity	117
2.1.2. Influence on the adhesion energy.....	119
2.1.3. Microstructure analysis of gelatin@PDA hydrogels.....	120
2.2. INFLUENCE OF THE GELATION TIME AND PEELING SPEED.....	122
2.2.1. Influence of the gelation time and peeling speed on the maximal force	122
2.2.2. Influence of the gelation time and peeling speed on the adhesion energy	123
2.2.3. Type of rupture.....	124
CONCLUSION	125
REFERENCES	126
LIST OF THE FIGURES – CHAPTER 5:	128

Chapter 5 :

Gelatin@Polydopamine-based hydrogels

Introduction

In chapter 3 we studied the influence of a protein (Alkaline phosphatase) on the size and stability of PDA nanoparticles. Then in chapter 4 we analyzed the influence of different oxidants on the formation of PDA films. Finally, in this last chapter, we will explore the **influence of PDA nanoparticles on gelation of gelatin and on its rheological characteristics**.

The strong adhesive power of PDA makes it a material of interest in the development of hydrogels for **biomedical purposes**. Gelatin is a natural compound widely used to form hydrogels for various applications, and its primary amines can interact with quinones. However, gelatin hydrogels lack a lot of adhesion properties on solid substrates.

After studying PDA in the form of suspensions and films, we therefore wanted to broaden our study on PDA nanoparticles by analyzing their **impact within a hydrogel**. We will therefore analyze the **behavior of a hydrogel based on gelatin and PDA** (gelatin@PDA) at different **dopamine concentrations**, at different **gelation times**, and by varying the parameters of rheometer measurements.

This research effort was also led as part of a first draft towards the formulation of PDA-based hydrogel to develop surgical adhesives.

1. Basic features of gelatin and PDA gel

1.1. Gelatin hydrogels

Hydrogels have physicochemical properties useful for a wide range of applications. Gelatin, widely used as a hydrogel, is a soluble protein obtained from the hydrolysis of collagen (1), which is the main fibrous constituent in cartilages, skin, and bones. Collagen is a macromolecule made of three polypeptides chains coiled into a helix of around 300 kDa in molecular weight (2–4). Its denaturation and unfolding leads to gelatin. The properties of gelatin are intricately linked to the type of collagen and source of the animal. Two types of gelatin are obtainable depending on the pre-treatment method, acid or alkali method, of the collagen: gelatin type A with an isoelectric point at pH 8-9, and gelatin type B with an isoelectric point ranges from pH 4 to 6, respectively.

Gelatins are biocompatible, non-immunogenic (5) and display an amphoteric behavior (6). Gelatins are used in a wide range of applications due to their numerous properties. They are the most used proteins in the field of food such as gelling agent, or as capsules for cosmetic or pharmaceutical industries (7,8). The major interest in gelatin lies in its ability to undergo gelation from aqueous solution at a temperature below a critical temperature.

However, gelatins present poor mechanical properties. Some effort has been done to increase these properties by adding cross-linking agents. For instance, the effect of pH and the addition of milk proteins on the structure of gelatin have been demonstrated. It appears that high gelatin concentration and the addition of casein lead to strong and firm gels (9). To overcome the problem of mechanical stability and to obtain photocrosslinkable double bonds in gelatin derivatives, a modification consisting in reacting gelatin with methacrylic anhydride was achieved (10). Then the hydroxyl and carboxyl groups in gelatin were reacted with glycidyl methacrylate to obtain a double bond modified gelatin macromer. This double modification of gelatin results in a hydrogel that exhibits high storage modulus and low degradation. Another issue to enhance the mechanical properties implies the modification of gelatin by using tannic acid, a natural phenol compound, at pH 8 (11). Increasing the concentrations of alginate and gelatin in a blend results also in hydrogels with a higher compressive modulus (12).

1.2. Gelatin@polydopamine-based hydrogels

PDA-based gels can be formed through two approaches (13). One strategy involves amine- or thiol-terminated molecules as the cross-linker based on Schiff base-reaction and/or Michael addition reaction. Another strategy is based on the catechol-mediated coordination with metal ions (14).

Due to the adhesion ability of catechol, PDA-based gels should exhibit strong adhesion to various wet or dry surfaces. This adhesive property of PDA added to its biocompatibility, make

it an attractive material in the fields of biomedical research. For instance, to prevent bacterial infection, it is important to facilitate biointegration of medical implants. By combining microbial transglutaminase-crosslinked gelatin hydrogel and PDA coating (15), the adhesion between the surface of an aluminum or titanium implant or poly(methylmethacrylate) and pig cornea tissue was considerably increased. In addition, these hydrogels could promote the adhesion and the proliferation of human dermal fibroblasts. The combination of PDA and gelatin has risen to the rank of universal coatings for methacrylate-based medical materials (16).

Another simple approach consists in the crosslinking of gelatin hydrogels by oxidizing a mixture of gelatin and dopamine using sodium periodate under metal-free conditions oxidant (17) and thus opening a new route to prepare PDA-based injectable materials with fast self-healing ability and remoldability (fig.1).

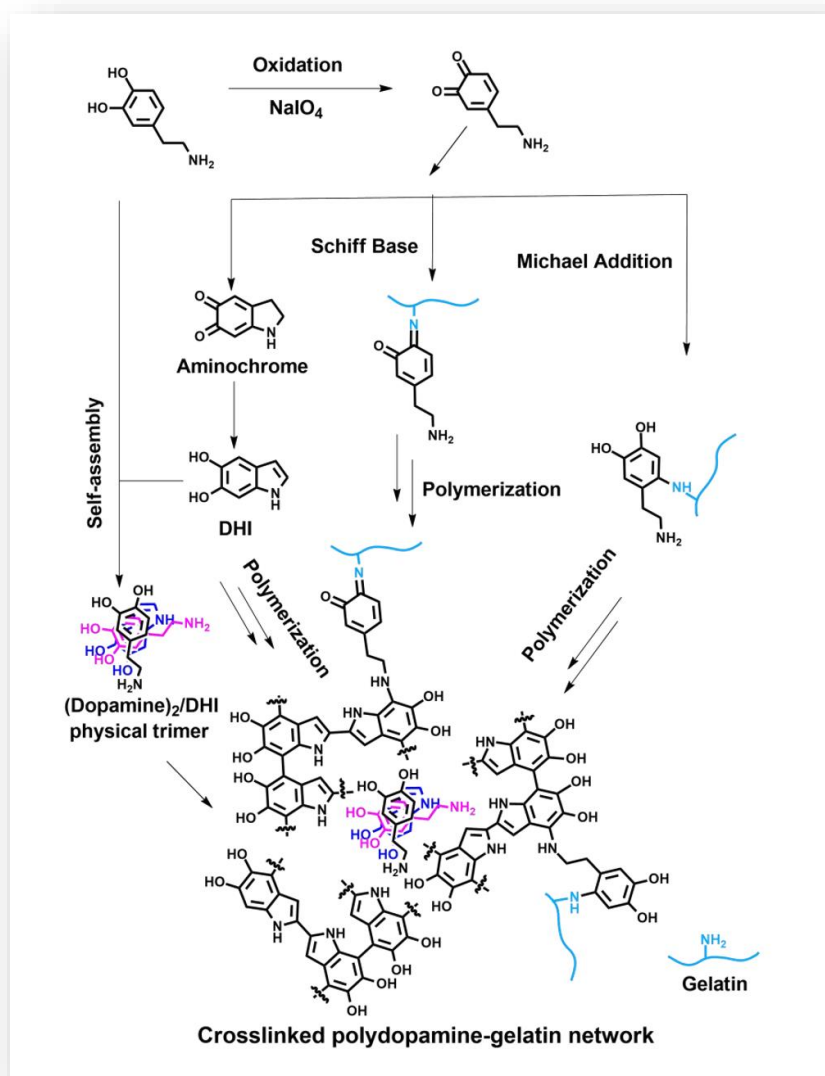


Figure 1: The proposed mechanism of the gelatin@PDA hydrogel formation (17).

PDMS-based microfluidic devices for myocardial differentiation of pluripotent stem cells are limited because of their hydrophobic surface. To improve cell interactive properties of PDMS, gelatin@dopamine was synthesized by grafting dopamine onto a gelatin backbone and resulted in higher protein adsorption on the PDMS surfaces (18).

1.3. Our strategy

After working with PDA nanoparticles and films, we were interested in the development of PDA-based gels for biomedical applications. We decided to focus on sodium periodate, the oxidant which allows PDA to be formed as quickly as possible. Copper sulphate mixed with hydrogen peroxide, the other oxidant mixture that allows for fast PDA formation has been ruled out for reasons of toxicity.

We worked with the hydrophilic polypeptide gelatin to provide primary amine groups and PDA as the crosslinker to crosslink gelatin by supramolecular and covalent bonds (17).

Gelatin was selected since it is quite simple to use, easily available and biocompatible. In this study only gelatin type B from bovine skin at high concentration (10% w/v) was studied at pH 5.0, the pH condition at which we oxidize dopamine by sodium periodate without significant auto-oxidation by dissolved oxygen. Gelatin behavior is constant in pH range from 4.6 to 8.0 in terms of rheology and texture (9). This material is positively charged in acidic systems and negatively charged in near-neutral systems.

Some studies have already been conducted to increase the gelatin adhesion by using PDA as described above. But according to our knowledge, there is no study on the relation between the hydrogel properties and the nanoparticles of PDA distribution. This project aims to better understand how the PDA can influence the gelation process of gelatin, and the consequences on the properties of this material.

Our strategy consists in analyzing the influence of the dopamine concentration on the adhesion of gelatin hydrogel, and the influence of the gelation time of these gelatin@PDA hydrogels on their adhesion energy and maximal force measured during a peeling test.

The results of this study were the first step towards a new surgical glue project that will not be detailed in this manuscript for confidential reasons.

2. Formation of gelatin@PDA hydrogels

2.1. Influence of the dopamine concentration

2.1.1. Influence on the elasticity

We studied the influence of the presence of dopamine on gelatin hydrogels and the influence of the concentration in gelation kinetics, elasticity, and adhesion of the composite hydrogels. We analyzed these characteristics by using a rheometer (more details on the technique are given in chapter 2 section 3.3).

We also investigated the impact of different formulations. We compared a gelatin@PDA hydrogels prepared by mixing gelatin solution and dopamine solution before adding the oxidant sodium periodate, with a gelatin@PDA hydrogel prepared by mixing gelatin powders and dopamine powders prior to putting them in solution. The two formulations led to identical results, there was no influence of the formulation on the elasticity of the hydrogels (fig.2-3). Therefore, the gelatin solution mixed with a dopamine solution was used in all the forthcoming performed experiments.

From the rheological results, we can see an important effect of PDA. The hydrogels became more elastic when the dopamine concentration was increased up to 4 mg/mL (fig.2), the storage modulus G' then reached a value close to 1000 Pa after 3h of gelation. Then the elasticity decreased suddenly when the dopamine concentration was further increased. Indeed, at 10 mg/ml the storage modulus drops even below the values of pure gelatin (at 10 % w/v) in the absence of PDA, used as a reference. At higher dopamine concentrations (above 10 mg/mL) gelation is no longer possible as we can see the loss modulus G'' value is higher than G' revealing the collapse of the hydrogel (fig.3). So there seems to be an optimal dopamine concentration allowing to get gels with the highest possible storage modulus.

Our hypothesis is that when the dopamine concentration is increased above a critical level, larger nanoparticles are formed which tend to clump together and to form large aggregates. These aggregates could then destabilize the network by reducing the junction zones, and as a result, the rigidity decreases (fig. 4). Subsequently we studied the relation between the elasticity and the adhesion behavior of the composite hydrogels.

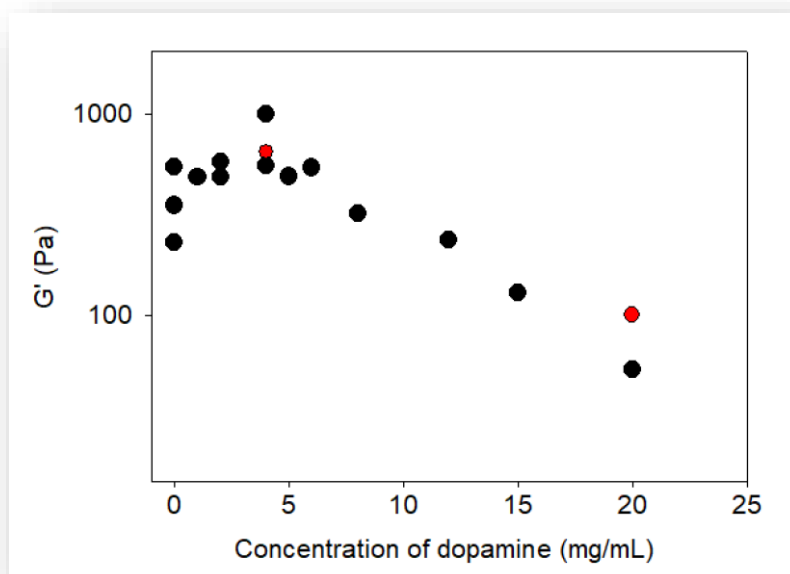


Figure 2: Storage modulus (G') of gelatin hydrogels with and without dopamine at different concentration after 3h of gelation.

Each dot represents an individual measurement. ● gelatin 10% (w/v) with dopamine at various concentration prepared by mixing solutions ● gelatin 10% (w/v) with dopamine at various concentration prepared by first mixing both powders before dissolution in sodium acetate buffer.

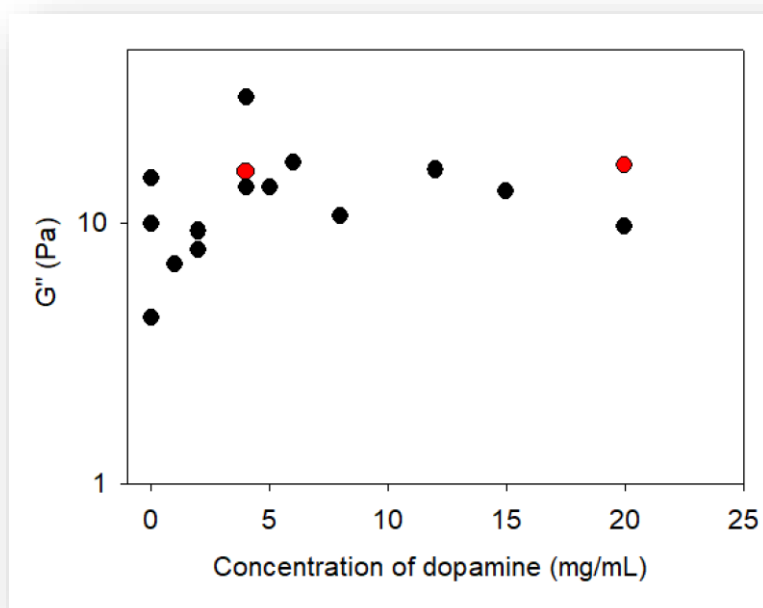


Figure 3: Loss modulus (G'') of gelatin hydrogels with and without dopamine at different concentration after 3h of gelation. Each dot represents an individual measurement

● gelatin 10% (w/v) with dopamine at various concentration prepared by mixing solutions ● gelatin 10% (w/v) with dopamine at various concentration prepared by first mixing both powders before dissolution in sodium acetate buffer.

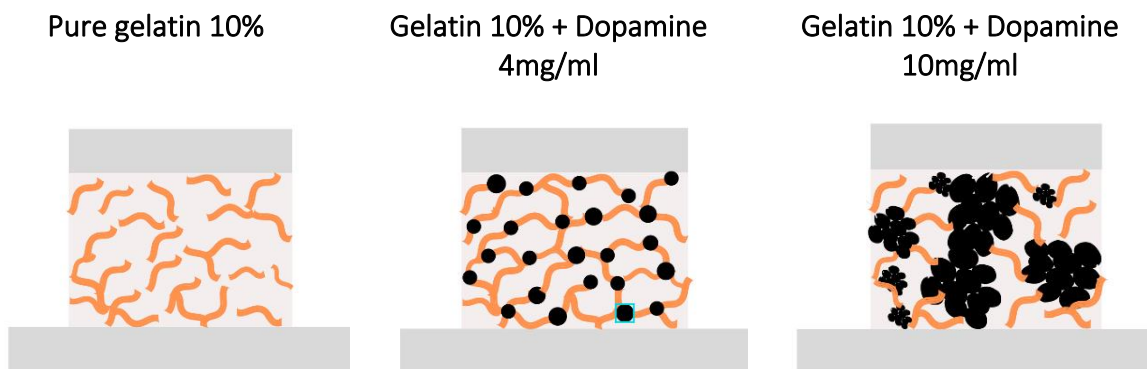


Figure 4: Schematic representation of the hypothetical PDA nanoparticles distribution within the hydrogel.
 ● represents the PDA nanoparticles ■ represents gelatin strands.

2.1.2. Influence on the adhesion energy

We investigated the impact of PDA nanoparticles on the specific adhesion energy (W/A where W and A stand for the work of adhesion and for the surface area of the gel respectively) of gelatin hydrogels. Our method to prepare gelatin@PDA hydrogels are different from those that are often described in literature since in our case, we prepared the gelling materials in only one step by forming the gelatin hydrogel in presence of dopamine. The PDA nanoparticles therefore form directly in the hydrogel. More details on the experimental part are listed in the chapter 2 section 2.4).

First, we compared 10% (w/v) pure gelatin with 10% (w/v) gelatin prepared in the presence of dopamine at different concentrations after 3h of gelation, hence in the same conditions as those corresponding to the experiments performed in figures 2 and 3. The appearance of hydrogels changed from yellow to dark brown with the presence of PDA, indicating the oxidation of dopamine during the hydrogel synthesis, whereas gelatin prepared without dopamine stayed yellow.

From our rheological results we have found that the specific adhesion energy (W/A) of gelatin increased when dopamine was present: at 4 mg/mL concentration the adhesion energy reached a value of almost 12 J/m^2 (fig. 5). Then, the adhesion energy decreased with the increase of the dopamine concentration, in correlation with figures 2 and 3. Indeed, at 10 mg/mL the value fell almost by half to 5 J/m^2 . It therefore confirms the presence of an optimal concentration around 4 mg/mL in dopamine for both the elastic and adhesive properties. Subsequently, pure 10% (w/v) gelatin or 10% (w/v) gelatin mixed with 4 mg/mL dopamine were used in the later experiments.

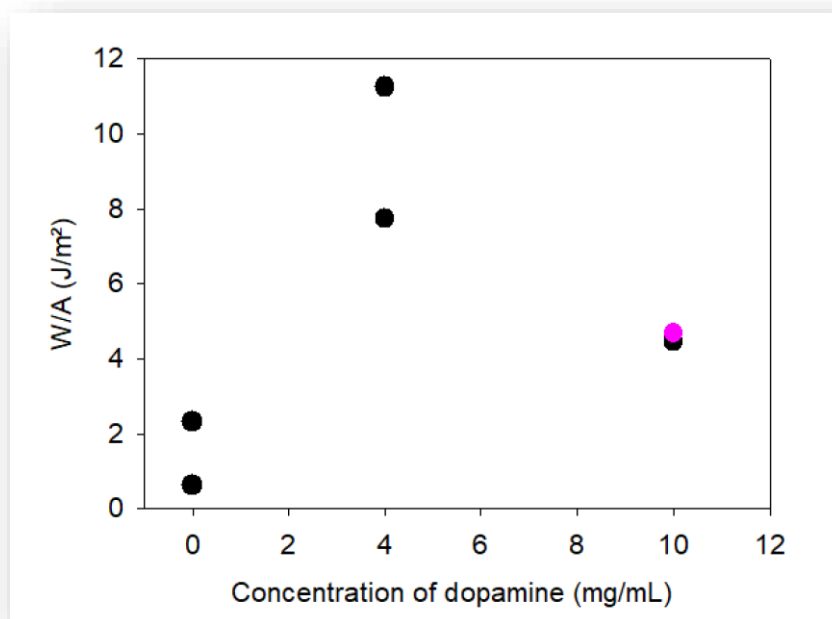


Figure 5: Adhesion energy of gelatin hydrogels prepared without and with dopamine at 4 mg/mL and 10 mg/mL after 3h of gelation.

Each point corresponds to an individual experiment. ● gelatin 10% (w/v) with dopamine at various concentration prepared by mixing solutions ● gelatin 10% (w/v) with dopamine at various concentration prepared by first mixing both powders before dissolution in sodium acetate buffer.

2.1.3. Microstructure analysis of gelatin@PDA hydrogels

To study the microstructure of the hydrogel, we analyzed these materials using a scanning electron microscope (SEM). Our results show that PDA had a marked influence on the hydrogel structure. Pure gelatin displays a compact and denser gel (fig.6a). In presence of 4 mg/mL dopamine, we could see that the hydrogel became much looser with some large pores (fig.6b). These pores are larger in case of gelatin with 10 mg/mL dopamine (fig. 6c). Individual strands are not observed, and the images do not clearly show the distribution of PDA nanoparticles.

Further analyzes with the transmission electron microscope (TEM) are necessary to better assess the size of the nanoparticles within these materials. The idea is to prepare gelatin in presence of dopamine at 4, 10 and 20 mg/mL to melt them and to dilute them below the critical gelation concentration before placing them on an TEM analysis grid. The experiments are still in progress but not yet detailed in this manuscript.

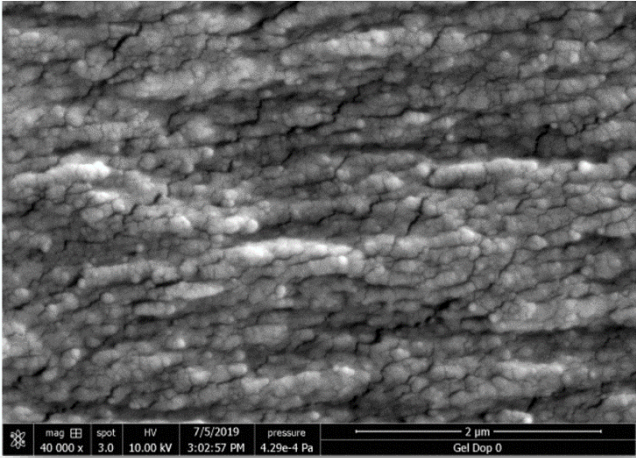
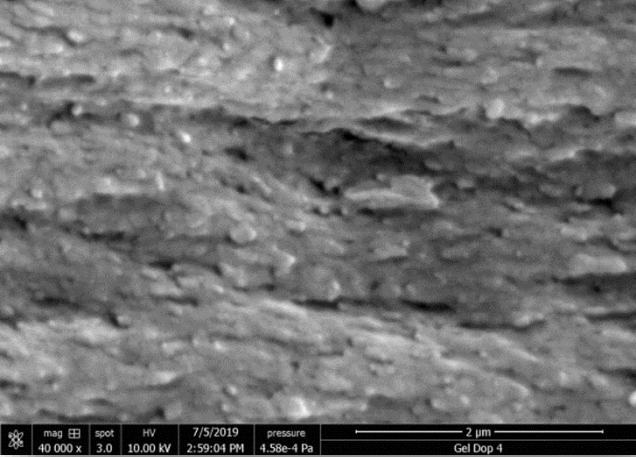
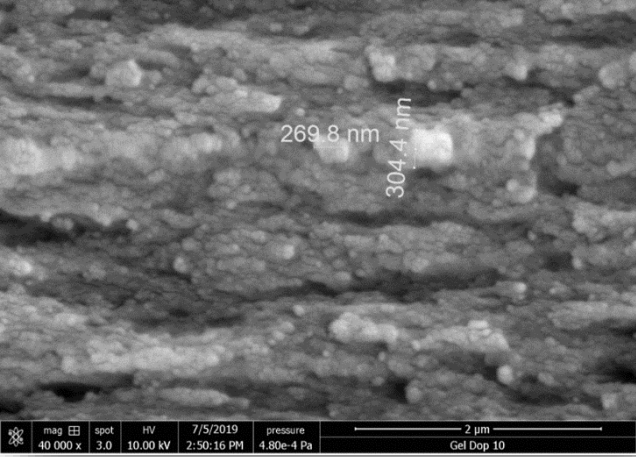
Gel	SEM pictures
<p>a) Gelatin 10% (w/v) without dopamine</p>	
<p>b) Gelatin 10% (w/v) with 4 mg/mL dopamine</p>	
<p>c) Gelatin 10% (w/v) with 10 mg/mL dopamine</p>	

Figure 6: SEM cross section pictures of the gelatin gels without and with dopamine at different concentrations as indicated on the left.

2.2. Influence of the gelation time and peeling speed

2.2.1. Influence of the gelation time and peeling speed on the maximal force

There is a clear increase in maximal force when gelatin hydrogels contains PDA nanoparticles (fig.7). We go from 1,52 N for a pure gelatin hydrogel without PDA to 23,67 N for a gelatin@PDA hydrogel at 2h. It is found that the force increases almost linearly over time, at least up to 4 h, while the peeling speed seems to have no specific influence. Indeed, whether the speed is 10, 100 or 1000 $\mu\text{m/s}$ there is an increase of the maximal force over time. Note that we did not perform adhesion experiments for gels aged for times longer than 4 h because this would have required special care to reduce the evaporation of water. We did not take such specific precautions, a chamber with controlled relative humidity, in our experiments. Anyway if such gels should be used as surgical glues, their setting time should be as short as possible, a few minutes typically.

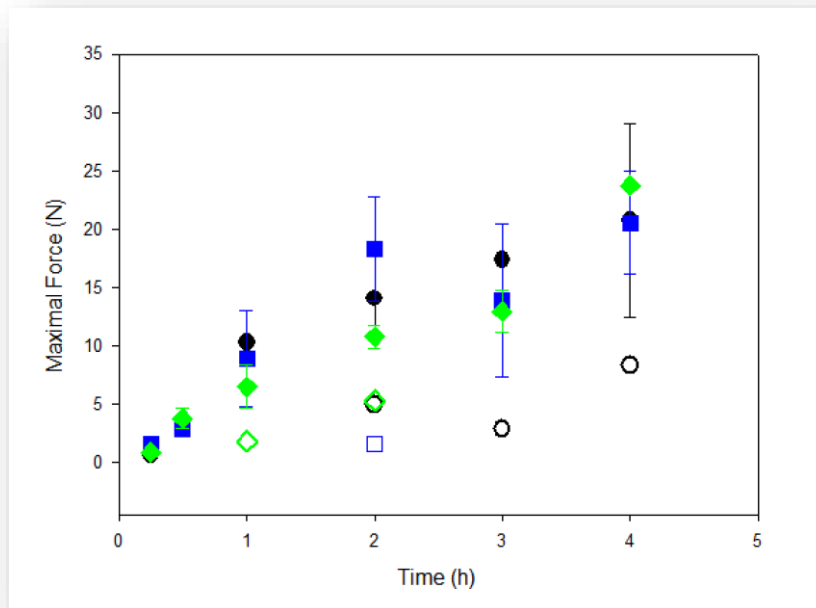


Figure 7: Maximal force of gelatin gels prepared without and with dopamine at 4 mg/mL after different gelation times and peeling speeds.

The individual points correspond to individual measurement.

Gelatin with dopamine at a peeling speed of: ● 10 $\mu\text{m/s}$, ■ 100 $\mu\text{m/s}$, ◆ 1000 $\mu\text{m/s}$

Gelatin without dopamine at a peeling speed of: ○ 10 $\mu\text{m/s}$, □ 100 $\mu\text{m/s}$, ◇ 1000 $\mu\text{m/s}$. The errors bars correspond to one standard deviation over $n = 3$ experiments.

2.2.2. Influence of the gelation time and peeling speed on the adhesion energy

The adhesion energy is obtained by the following calculations. First, we calculated the total work of adhesion which is defined as the product of the force and the displacement (equation 1). The displacement is the product of the gap time between each measurement (it is equal to 0.01s) and the peeling speed (10 $\mu\text{m/s}$ or 100 $\mu\text{m/s}$ or 1000 $\mu\text{m/s}$).

$$dW_i = F_i \times dx_i$$

(equation 1)

$$\text{with } dx_i = 0.01 \times (\text{peeling speed})$$

Finally, the adhesion energy is calculated by dividing the total work of adhesion (W) by the surface area (A) of the disc used, that is to say the product of π by the radius squared (equation 2).

$$W/A \text{ (J/m}^2\text{)} = \frac{W_{\text{total}}}{\pi \times r^2}$$

(equation 2)

$$\text{with } W_{\text{total}} = \sum dW_i$$

Here again, there is an increase in the adhesion energy when the PDA is present in the gel (fig. 8). We go from 0,41 J/m² for gelatin alone to 19,30 J/m² for gelatin with PDA after 2h gelation time. This value increased to 23,03 J/m² after 4h gelation time of gelatin with PDA. There is no major observable influence of the peeling speed whether the speed is 10, 100 or 1000 $\mu\text{m/s}$.

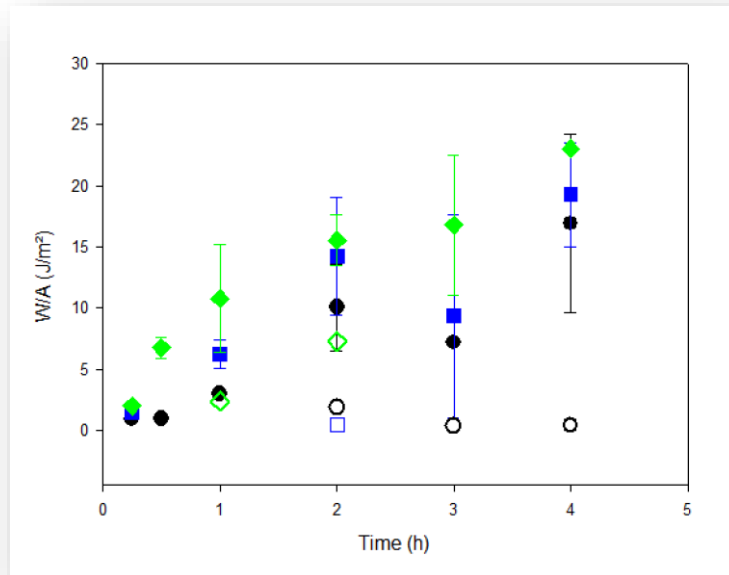


Figure 8: W/A values of gelatin gels prepared without and with dopamine at 4 mg/mL after different gelation times and peeling speeds.

Gelatin with dopamine at a peeling speed of: ● 10 $\mu\text{m/s}$, ■ 100 $\mu\text{m/s}$, ◆ 1000 $\mu\text{m/s}$
Gelatin without dopamine at a peeling speed of: ○ 10 $\mu\text{m/s}$, □ 100 $\mu\text{m/s}$, ◇ 1000 $\mu\text{m/s}$

2.2.3. Type of rupture

The type of rupture was also evaluated macroscopically (fig.9). After the adhesion test, it was observed that in absence of PDA, the gelatin hydrogel was found only on one side of the rheometer disc surface indicating weak adhesion. When PDA was present, the composite hydrogel was found on both sides, indicating stronger adhesion of the gelatin@PDA hydrogel, provided that the dopamine concentration during preparation does not exceed the critical threshold of 4 mg/mL. Thus, we can identify different types of ruptures during the gelation time. We go from an adhesive rupture (at the interface between the hydrogel and the measurement surface) to a cohesive rupture (within the body of the material). This hypothesis highlights the difference in chemical bonds inside the hydrogel and therefore its microstructure. The transformation from solution to hydrogel depends on the chemical network formation that is due to the cross-linking bridges of polymerized PDA among gelatin. The distribution and the size of the PDA nanoparticles play a huge role in this network and thus can allow or avoid the formation of the gelling material.


Gelatin 10% (w/v) without dopamine after 4h of gelation Speed = 100 $\mu\text{m/s}$	Gelatin 10% (w/v) with 4 mg/mL dopamine after 1h of gelation Speed = 100 $\mu\text{m/s}$	Gelatin 10% (w/v) with 4 mg/mL dopamine after 4h of gelation Speed = 100 $\mu\text{m/s}$
		

Figure 9: pictures of the gelatin hydrogels after the adhesion test without and with PDA after 1h and 4h of gelation at a peeling speed of 100 $\mu\text{m/s}$.

Conclusion

The addition of dopamine during the preparation of a gelatin hydrogel results in a marked increase in the **elasticity, the maximal force, and the adhesion energy**. These parameters are influenced by the **dopamine concentration** and the **gelation time**.

We could identify a **critical dopamine concentration** above which the hydrogel becomes more and more fragile until it no longer forms. This might be due to the **large PDA aggregates which prevent network connections** and therefore destabilize the structure. TEM analyzes are to be carried out to better correlate the size of the PDA nanoparticles with the formation mechanism of the hydrogel. It would also be interesting to study the antioxidant activity of such hydrogels as a function of the dopamine concentration.

This investigative effort was carried out with a view to formulating future PDA-based gels with a view to developing a **surgical adhesive**. This future project was selected during the *Mature Your PhD* competition from the technology transfer company Conectus. For obvious confidentiality reasons, this part has not been detailed in this manuscript.

Although the literature is full of examples of promising applications of PDA-based gels, the physicochemical mechanisms are not yet fully understood. **Deeper efforts should be pursued** to better understand this material, thus better controlling its properties for efficient uses.

References

1. Ward AG. The physical properties of gelatin solutions and gels. *Br J Appl Phys.* mars 1954; 5(3):85–90.
2. Pauling L, Corey RB. The Structure of Fibrous Proteins of the Collagen-Gelatin Group. *Proc Natl Acad Sci U S A.* mai 1951; 37(5):272-81.
3. Shoulders MD, Raines RT. Collagen structure and stability. *Annu Rev Biochem.* 2009; 78:929-58.
4. Cowan PM, McGAVIN S, North ACT. The Polypeptide Chain Configuration of Collagen. *Nature.* déc 1955; 176(4492):1062-4.
5. Pierce BF, Pittermann E, Ma N, Gebauer T, Neffe AT, Hölscher M, et al. Viability of human mesenchymal stem cells seeded on crosslinked entropy-elastic gelatin-based hydrogels. *Macromol Biosci.* mars 2012; 12(3):312-21.
6. Buhus G, Peptu C, Popa M, Desbrieres J. Controlled release of water soluble antibiotics by carboxymethylcellulose- And gelatin-based hydrogels crosslinked with epichlorohydrin. *Cellul Chem Technol.* 2009; 43(4-6):141-51.
7. Melnik J, Cheney MC, Vargas A. Odorless cosmetic compositions in gelatin capsules [Internet]. US5082661A, 1992 [cité 12 juill 2020]. Disponible sur: <https://patents.google.com/patent/US5082661A/en>
8. Story MJ. Gelatin pharmaceutical formulations [Internet]. US5532002A, 1996 [cité 12 juill 2020]. Disponible sur: <https://patents.google.com/patent/US5532002A/en>
9. Pang Z, Deeth H, Sopade P, Sharma R, Bansal N. Rheology, texture and microstructure of gelatin gels with and without milk proteins. *Food Hydrocoll.* 1 mars 2014;35:484-93.
10. Li X, Zhang J, Kawazoe N, Chen G. Fabrication of Highly Crosslinked Gelatin Hydrogel and Its Influence on Chondrocyte Proliferation and Phenotype. *Polymers.* août 2017;9(8):309.
11. Zhang X, Do MD, Casey P, Sulistio A, Qiao GG, Lundin L, et al. Chemical Modification of Gelatin by a Natural Phenolic Cross-linker, Tannic Acid. *J Agric Food Chem.* 9 juin 2010; 58(11):6809-15.
12. Giuseppe MD, Law N, Webb B, A. Macrae R, Liew LJ, Sercombe TB, et al. Mechanical behaviour of alginate-gelatin hydrogels for 3D bioprinting. *J Mech Behav Biomed Mater.* 1 mars 2018; 79:150-7.
13. Liu Y, Ai K, Lu L. Polydopamine and Its Derivative Materials: Synthesis and Promising Applications in Energy, Environmental, and Biomedical Fields. *Chem Rev.* 14 mai 2014; 114(9):5057-115.
14. Holten-Andersen N, Harrington MJ, Birkedal H, Lee BP, Messersmith PB, Lee KYC, et al. pH-induced metal-ligand cross-links inspired by mussel yield self-healing polymer networks with near-covalent elastic moduli. *Proc Natl Acad Sci U S A.* 15 févr 2011; 108(7):2651-5.

15. Dinh TN, Hou S, Park S, Shalek BA, Jeong KJ. Gelatin Hydrogel Combined with Polydopamine Coating to Enhance Tissue Integration of Medical Implants. *ACS Biomater Sci Eng*. 8 oct 2018; 4(10):3471-7.
16. Van De Walle E, Van Nieuwenhove I, Vanderleyden E, Declercq H, Gellynck K, Schaubroeck D, et al. Polydopamine–Gelatin as Universal Cell-Interactive Coating for Methacrylate-Based Medical Device Packaging Materials: When Surface Chemistry Overrides Substrate Bulk Properties. *Biomacromolecules*. 11 janv 2016; 17(1):56-68.
17. Zhao X, Zhang M, Guo B, Ma PX. Mussel-inspired injectable supramolecular and covalent bond crosslinked hydrogels with rapid self-healing and recovery properties via a facile approach under metal-free conditions. *J Mater Chem B*. 19 oct 2016; 4(41):6644-51.
18. Fu J, Quek KY, Chuah YJ, Lim CS, Fan C, Wang D. The effects of gelatin–dopamine coating on polydimethylsiloxane substrates on pluripotency maintenance and myocardial differentiation of cultured mouse embryonic stem cells. *J Mater Chem B*. 7 déc 2016 ; 4(48):7961-73.

List of the figures – Chapter 5:

Figure 1: The proposed mechanism of the gelatin@PDA hydrogel formation (17).	115
Figure 2: Storage modulus (G') of gelatin hydrogels with and without dopamine at different concentration after 3h of gelation.	118
Figure 3: Loss modulus (G'') of gelatin hydrogels with and without dopamine at different concentration after 3h of gelation. Each dot represents an individual measurement	118
Figure 4: Schematic representation of the hypothetical PDA nanoparticles distribution within the hydrogel.	119
Figure 5: Adhesion energy of gelatin hydrogels prepared without and with dopamine at 4 mg/mL and 10 mg/mL after 3h of gelation.	120
Figure 6: SEM cross section pictures of the gelatin gels without and with dopamine at different concentrations as indicated on the left.	121
Figure 7: Maximal force of gelatin gels prepared without and with dopamine at 4 mg/mL after different gelation times and peeling speeds.....	122
Figure 8: W/A values of gelatin gels prepared without and with dopamine at 4 mg/mL after different gelation times and peeling speeds.	123
Figure 9: pictures of the gelatin hydrogels after the adhesion test without and with PDA after 1h and 4h of gelation at a peeling speed of 100 $\mu\text{m/s}$	124

General conclusion and perspectives

PDA has risen to the rank of a material of great interest for surface modification and coating thanks to its strong adhesion and substrate-independence potential. In addition, PDA can be prepared and studied in different forms, as nanotubes, nanoparticles, films or in gels which opens the way to many applications.

During this thesis, we first started by studying the influence of alkaline phosphatase (ALP) on the control of the size and colloidal stability of the PDA nanoparticles. We demonstrated a significant reduction in the size of the nanoparticles when PDA is prepared with the presence of ALP during the oxidation of dopamine and that the dopamine/protein ratio also plays a huge role in controlling the size. A previous study has identified the crucial role of the presence of a specific sequence of two amino acids (KE)(1) in this mechanism.

In addition, those nanoparticles exhibit the enzymatic activity of the used enzyme. The TEM analysis and the study of the zeta potential let suppose that the structure of the composite PDA@ALP nanoparticles is enriched in enzyme on their corona with respect to their core. These nanoparticles formed from PDA and ALP display an interesting enzymatic activity. A first draft of application of these nanoparticles could be undertaken by immobilizing them in polyelectrolyte multilayer films with poly(allylamine) as a polycation. These films showed an enzymatic activity proportional to their thickness. It therefore appears interesting to continue this application research in order to develop reactors with various potentials, such as biosensors of molecules of interest.

Even if we demonstrated the possibility to produce enzymatically active PDA@ALP nanoparticles, some intensive research study is still required to improve the reproducibility of their synthesis. The biggest challenge of this research effort remains to determine the accurate distribution of the enzyme in the nanoparticle to better understand the mechanism by which the enzyme controls nanoparticle formation. Finally, the rate of oxidant addition to the dopamine and enzyme containing solution should be automatized specially since these materials can be used in 3D printing.

After the study of PDA in suspension, special interest was given to the study of PDA films. The objective was to carry out a comparative study between suspended PDA and films and between PDA films prepared from different oxidants in terms of structure and properties. And as we could see from the characterization of PDA films, the morphology, the electrochemical behaviour, and the composition of PDA films prepared by the oxidation of dopamine are distinctly dependent on the used oxidant. The films prepared by oxidation with sodium periodate or copper sulphate exhibit the greatest thicknesses and roughness in comparison with the standard method which consists of oxidizing dopamine in a Tris solution at pH 8.5 or ammonium peroxodisulfate. These morphological differences are due to the fact that sodium periodate and copper sulfate oxidize much faster than the other two methods and thus allow for the formation of thicker films.

Particular attention was paid to the analysis of the antioxidant activity of PDA films. All the films displayed some antioxidant properties, reflecting the presence of non-oxidized catechol groups.

The findings presented in this dissertation highlight the great diversity of PDA films and aim to help to facilitate future uses of PDA films according to specific expectations. It seems obvious that fundamental research efforts are welcome to try to shed more light on these results.

Finally, our endeavour focused on the analysis of the impact of PDA on gelatin hydrogels. Some studies have already been started in this area (2), but our approach was different since we were interested in the study of PDA nanoparticles synthesized directly in the hydrogel by simply mixing dopamine and gelatin simultaneously. The advantage of such a process, in addition to the ease of preparation, is to observe the influence of PDA on the elasticity, strength and adhesion energy of the gel. Our results have shown that PDA considerably increases the elasticity of the gel and its adhesion and strength in a dopamine concentration dependant manner. Indeed, we could identify a critical dopamine concentration above which the hydrogel becomes more and more fragile until it no longer forms. This could be explained because of the PDA aggregates formation tendency at high dopamine concentration which probably prevent network connections and therefore destabilize the hydrogel structure. Characterization of this material must be more in-depth to better understand the distribution of nanoparticles within the hydrogel, in particular by TEM image analyzes.

Given the properties of PDA, it would be interesting to explore the antioxidant activity of these gels, also to exploit the photothermal activity of PDA. Designing gels that can form in a controlled manner using near infrared illumination can be an asset in the medical field. Formulation efforts by adding crosslinking agents can improve the internal cohesion of future PDA-based gels and reduce gelation time. Although the literature is full of examples of promising applications of PDA-based gels, the physicochemical mechanisms are not yet fully understood. Deeper survey should be pursued to better understand this material, thus better controlling its properties for efficient uses.

This thesis was an opportunity to study PDA in different forms to better control its properties. Advances have been made to produce enzymatically active PDA nanoparticles of controlled size, then more light has been shed on the importance of the choice of oxidant in the preparation of PDA and at the end some progress has been made in the field of hydrogels based on PDA and gelatin. This work hopes to pave the way for more exciting and important studies concerning the PDA material, and to be a steppingstone towards a greater interest in bio-inspired materials since Nature is an infinite library of materials and methods.

References

1. Bergtold C, Hauser D, Chaumont A, El Yakhli S, Mateescu M, Meyer F, et al. Mimicking the Chemistry of Natural Eumelanin Synthesis: The KE Sequence in Polypeptides and in Proteins Allows for a Specific Control of Nanosized Functional Polydopamine Formation. *Biomacromolecules*. 10 2018;19(9):3693-704.
2. Dinh TN, Hou S, Park S, Shalek BA, Jeong KJ. Gelatin Hydrogel Combined with Polydopamine Coating To Enhance Tissue Integration of Medical Implants. *ACS Biomater Sci Eng*. 8 oct 2018;4(10):3471-7.

Conclusion Générale (french version)

La PDA s'est hissé au rang de matériau de grand intérêt pour la modification de surface et le revêtement grâce à son fort potentiel d'adhésion et d'indépendance vis-à-vis de la nature du substrat. De plus, la PDA peut être préparé et étudié sous différentes formes, sous forme de nanotubes, de nanoparticules, de films ou de gels ce qui ouvre la voie à de nombreuses applications.

Au cours de cette thèse, nous avons commencé par étudier l'influence de la phosphatase alcaline sur le contrôle de la taille des nanoparticules de PDA. Nous avons démontré une réduction significative de la taille des nanoparticules lorsque la PDA a été préparé en présence de phosphatase alcaline lors de l'oxydation de la dopamine. Nous avons également pu montrer le rôle important que joue le rapport dopamine/protéine dans le contrôle de la taille. Une étude précédente a identifié le rôle crucial de la présence d'une séquence spécifique de deux acides aminés (KE) (1) dans ce mécanisme de contrôle.

De plus, ces nanoparticules présentent l'activité enzymatique de l'enzyme utilisée. L'analyse TEM et l'étude du potentiel zêta laissent supposer que la structure des nanoparticules de PDA et de la phosphatase alcaline (PDA@ALP) est enrichie en enzyme sur la surface externe (couronne) par rapport à leur cœur. Ces nanoparticules présentent une activité enzymatique intéressante. Un premier projet d'application de ces nanoparticules a été entrepris en les immobilisant dans des films multicouches poly-électrolytiques avec la poly(allylamine) comme polycation. Ces films ont montré une activité enzymatique proportionnelle à leur épaisseur. Il apparaît donc intéressant de poursuivre cette recherche applicative afin de développer des réacteurs aux potentiels variés, tels que des biocapteurs de molécules d'intérêt.

Même si nous avons démontré la possibilité de produire des nanoparticules PDA@ALP enzymatiquement actives, des recherches intensives sont encore nécessaires pour améliorer la reproductibilité de leur synthèse. Le plus grand défi de cet effort de recherche reste de déterminer la distribution précise de l'enzyme dans la nanoparticule afin de mieux comprendre le mécanisme par lequel l'enzyme contrôle la formation des nanoparticules. Enfin, le taux d'ajout de l'oxydant à la solution contenant la dopamine et l'enzyme pourrait être automatisé, pour les exploiter dans le champ de l'impression 3D.

Après l'étude de la PDA en suspension, un intérêt particulier a été accordé à l'étude des films. L'objectif était de réaliser une analyse combinatoire des films préparés à partir de différents oxydants et d'étudier leur effet sur la structure et les propriétés. Comme on a pu l'observer à partir de la caractérisation des films de PDA, la morphologie, le comportement électrochimique et la composition chimique préparés sont clairement dépendants de l'oxydant utilisé. Les films préparés par oxydation au periodate de sodium ou au sulfate de cuivre présentent les plus grandes épaisseurs et rugosités par rapport à la méthode classique qui consiste à oxyder la dopamine dans une solution de Tris à pH 8,5 ou encore quand on compare à l'oxydant peroxydisulfate d'ammonium. Ces différences morphologiques sont dues au fait que le

periodate de sodium et le sulfate de cuivre s'oxydent beaucoup plus rapidement que les deux autres méthodes et permettent ainsi la formation de films plus épais.

Une attention particulière a été portée à l'analyse de l'activité antioxydante des films de PDA. Tous les films ont montré des propriétés antioxydantes, reflétant la présence de groupes catéchols non oxydés.

Les résultats présentés dans cette thèse mettent en évidence la grande diversité des films de PDA et visent à faciliter les futures utilisations de ces films en fonction des attentes spécifiques et application souhaitée. Il semble évident que des études fondamentales plus poussées soient les bienvenues pour tenter d'éclairer davantage ces résultats.

Enfin, notre effort s'est concentré sur l'analyse de l'impact du PDA sur les hydrogels de gélatine. Certaines études ont déjà commencé à voir le jour dans ce domaine (2), mais notre approche se différencie puisque nous nous sommes intéressés à l'étude des nanoparticules de PDA synthétisées directement dans l'hydrogel en mélangeant simplement la dopamine et la gélatine simultanément. L'avantage d'un tel procédé, en plus de la facilité de préparation, est d'observer l'influence de la PDA sur les propriétés élastique et adhésive de l'hydrogel. Nos résultats ont montré que la PDA augmente considérablement l'élasticité de l'hydrogel ainsi que son adhérence et sa force maximale. Cet effet est dépendant de la concentration en dopamine. En effet, nous avons pu constater une concentration critique en dopamine au-dessus de laquelle l'hydrogel devient de plus en plus fragile à tel point que la gélification soit perturbée. Ceci pourrait être expliqué en raison de la formation d'agrégats de PDA à une concentration élevée en dopamine ce qui a pour conséquence probable la restriction des connexions de réseau et donc la déstabilisation de la structure globale. La caractérisation de ce matériau doit être plus approfondie pour mieux comprendre la distribution des nanoparticules au sein de l'hydrogel, notamment par des analyses d'images TEM.

Compte tenu des propriétés de la PDA, il serait intéressant d'explorer l'activité antioxydante de ces gels, ainsi que d'exploiter l'activité photothermique de la PDA. La conception de gels pouvant se former de manière contrôlée à l'aide d'illumination peut être un atout dans le domaine médical en particulier. Les efforts de formulation comme par exemple par l'ajout d'agents de réticulation peuvent améliorer la cohésion interne des futurs gels à base de PDA et réduire le temps de gélification. Bien que la littérature regorge d'exemples d'applications prometteuses de gels à base de PDA, les mécanismes physico-chimiques ne sont pas encore entièrement compris. Une analyse plus approfondie doit être poursuivie pour mieux comprendre ce matériau, et ainsi mieux contrôler ses propriétés pour des utilisations plus efficaces.

Pour conclure, cette thèse a été l'occasion d'étudier la PDA sous différentes formes pour mieux maîtriser ses prometteuses propriétés. Des avancées ont été réalisées pour produire des nanoparticules de PDA actives d'un point de vue enzymatique, de taille contrôlée. Par la suite plus de lumière a été apporté sur l'importance du choix de l'oxydant dans la préparation de films de PDA. Enfin des progrès ont été réalisés dans le domaine des hydrogels à base de PDA et de gélatine. Ce travail espère ouvrir la voie à des études plus passionnantes et importantes

concernant la PDA, et constituer un tremplin vers un plus grand intérêt pour les matériaux bio-inspirés puisque la Nature est une bibliothèque infinie de « matériel et méthode ».

References

1. Bergtold C, Hauser D, Chaumont A, El Yakhli S, Mateescu M, Meyer F, et al. Mimicking the Chemistry of Natural Eumelanin Synthesis: The KE Sequence in Polypeptides and in Proteins Allows for a Specific Control of Nanosized Functional Polydopamine Formation. *Biomacromolecules*. 10 2018;19(9):3693-704.
2. Dinh TN, Hou S, Park S, Shalek BA, Jeong KJ. Gelatin Hydrogel Combined with Polydopamine Coating To Enhance Tissue Integration of Medical Implants. *ACS Biomater Sci Eng*. 8 oct 2018;4(10):3471-7.

ANNEXES

List of publications

El Yakhliifi, S.; Ihiawakrim, D.; Ersen, O.; Ball, V. "Enzymatically Active Polydopamine @ Alkaline Phosphatase Nanoparticles Produced by NaIO₄ Oxidation of Dopamine". *Biomimetics* 2018, 3, 3693.

El Yakhliifi S.; Ball V.; **Polydopamine as a stable and functional nanomaterial.** *Colloids Surf B Biointerfaces*. 1 févr 2020; 186:110719.

El Yakhliifi S. ; Alfieri M-L.; Arntz Y. ; Eredia M.; Ciesielski A. ; Samorì P.; d'Ischia M.; Ball V. **Oxidant-dependent antioxidant activity of polydopamine films: the chemistry-morphology interplay** (in submission).

Bergtold C.; Hauser D.; Chaumont A.; **El Yakhliifi S.**; Mateescu M.; Meyer F.; Metz-Boutigue M.-H.; Frisch B.; Schaaf P.; Ihiawakrim D.; Ersen O.; Monnier C.A.; Petri-Fink A., Rothen-Rutishauser B., and Ball V. **Mimicking the Chemistry of Natural Eumelanin Synthesis: The KE Sequence in Polypeptides and in Proteins Allows for a Specific Control of Nanosized Functional Polydopamine Formation.** *Biomacromolecules* 2018 19 (9), 3693-3704

Programme Valorisation des compétences,
Un nouveau Chapitre de la Thèse / NCT 2020

EL YAKHLIFI Salima

Ecole doctorale Physique – Chimie (ED182)

Institut de la santé et de la recherche médicale (INSERM UMRS 1121)

Un nouveau Chapitre de la Thèse / NCT 2020

Avec l'accompagnement de **Anna Dyngosz**

Sujet de thèse : *Contrôle de la structure et des propriétés de la polydopamine à l'état de suspension, de films et de gels pour des applications biomédicales*

Directeur de thèse : Prof. Vincent Ball (Université de Strasbourg)

Sommaire

INTRODUCTION	139
CADRE GENERAL ET ENJEUX DE MA THESE	140
MON TRAVAIL DE THESE	140
INTERET DE MON TRAVAIL.....	140
POURQUOI CETTE THESE.....	141
CONTEXTE PROFESSIONNEL.....	141
DEROULEMENT ET GESTION DU PROJET DE THESE	142
PRINCIPALES ETAPES DU PROJET.....	142
ANIMATION ET COORDINATION	143
I. LES REUNIONS DE PROJET	143
II. LES RELATIONS / PARTENAIRES EXTERIEURS	143
MISE EN VALEUR DES COMPETENCES TRANSVERSALES ET TRANSFERABLES	144
CONCLUSION / REMERCIEMENTS	145

Introduction

Le programme NCT s'adresse aux doctorant·e·s en **fin de doctorat** (3ème année et plus). L'objectif est de nous permettre de préparer notre mobilité professionnelle en **faisant le point sur nos compétences et notre projet professionnel**. Nous avons donc été accompagnés et encadrés dans ce travail de bilan par **un mentor**, en la personne d'Anna Dyncogcz.

Mes attentes étaient situées à plusieurs niveaux : je souhaitais apprendre à identifier et valoriser les compétences que j'ai acquise durant mon doctorat, apprendre aussi à penser ma thèse via une **approche « gestion de projet »** et développer des compétences dans ce domaine précisément. Enfin, je souhaitais apporter plus de lumière sur les possibilités professionnelles **après ma thèse**.

Dans ce chapitre, nous allons aborder dans un premier temps le **cadre général et les enjeux de ma thèse**, puis nous nous concentrerons sur le **déroulement et la gestion** de celle-ci. Enfin, nous identifierons un ensemble de **compétences transversales** que j'ai pu acquérir lors de mon aventure doctorale.

Cadre général et enjeux de ma thèse

Mon travail de thèse

“Va prendre tes leçons dans la nature, c’est là qu’est notre futur”. Je m’efforce d’appliquer ce sage conseil de Leonard de Vinci dans mes travaux de recherche : en m’inspirant des moules marines et de leur incroyable pouvoir d’adhésion, je tente de concevoir des biomatériaux capables d’améliorer notre santé.

En imitant les protéines présentes dans la substance adhésive des moules, on a réussi à créer en laboratoire une molécule qui s’appelle la Polydopamine (PDA). Celle-ci est comme un super-héros avec plusieurs capes : la PDA peut se mettre sous la forme d’une toute petite boule, ce qu’on appelle Nanoparticule, ou bien s’étaler comme un film, ou encore adopter la forme d’un gel.

Le cœur de ma thèse est d’étudier la PDA sous toutes ces formes et de réfléchir aux missions spéciales, donc aux applications que je peux lui donner.

Intérêt de mon travail

Plusieurs applications commencent à voir le jour à partir du matériau que j’étudie (polydopamine), mais encore aujourd’hui on ne le comprend pas vraiment d’un point de vue physico-chimique. Mes travaux permettent d’avancer nos connaissances sur le contrôle de ses propriétés et de sa structure et ainsi d’améliorer son utilisation pratique.

Il existe plusieurs recettes pour fabriquer la PDA, mais pendant sa préparation, le matériau forme de gros agrégats, précipite, et donc on doit faire face à un gaspillage non négligeable. Par ailleurs, les propriétés de la PDA sont fortement influencées par les techniques de préparation (plus précisément par l’oxydant).

L’intérêt de l’étude de la PDA sous forme de nanoparticules a permis de démontrer qu’en ajoutant des protéines, on arrive à synthétiser des nanoparticules stables et de taille contrôlée. De surcroît, par une méthode simple, on a réussi à montrer que ces nanoparticules présentent une activité enzymatique, ce qui ouvre alors le champ des applications possibles.

L’intérêt de l’étude de la PDA sous forme de films se situe à plusieurs niveaux : l’amélioration de connaissances fondamentales sur les mécanismes de formation de films de PDA ; l’identification des protocoles les plus adaptés selon les applications visées ; la production de films présentant des propriétés antioxydantes.

Enfin, l'intérêt de nos efforts sur la partie gel porte l'espoir du développement d'une colle chirurgicale. Bien qu'efficace, les fils de sutures sont des objets étrangers au corps humain et les risques d'infection existent toujours. L'utilisation d'une colle chirurgicale biocompatible permettra non seulement de limiter les infections, mais aussi de réduire les coûts hospitaliers. Les colles existantes sur le marché actuellement manquent encore d'efficacité (manque d'adhésion ou de biocompatibilité ou de simplicité).

Pourquoi cette thèse

Ce sujet consiste à travailler sur un matériau inspiré des moules marines. Passionnée de biomimétisme, j'y ai vu une opportunité de concrétiser cet intérêt et d'en faire mon métier. Je trouve fascinant qu'en s'inspirant de la forme, de la matière ou des fonctions du Vivant, nous arrivons à innover et dépasser nos limites scientifiques et technologiques.

Aussi une autre motivation est que ce projet est pluridisciplinaire : il me permet de travailler à l'interface de différents domaines, d'échanger avec des professionnels de santé. Je peux donc changer de casquette assez souvent, ce qui me convient totalement car j'aime le changement et la nouveauté.

En plus de ces moteurs, je souhaiterai plus tard créer un laboratoire de recherche sur les biotechnologies inspirées de la Nature. Pour toutes ces raisons, j'ai donc voulu me lancer dans cette aventure doctorale.

Contexte professionnel

J'effectue ma thèse au sein de l'institut national de la santé et de la recherche médicale (INSERM) dans l'unité 1121 « équipe biomatériaux et bio ingénierie », situé sur le site de l'hôpital civil et la faculté de médecine. Mon unité se compose d'une équipe pluridisciplinaire de physico-chimistes, biologistes, médecins, dentistes, et techniciens s'intéressant tous aux biomatériaux au sens large du terme : développement de nouveaux biomatériaux, compréhension de l'interaction des cellules avec les biomatériaux, mise au point de nouveaux types d'implants.

Ma thèse s'effectue sous la direction du Professeur Vincent Ball. Notre petite équipe se limite à nous deux. Toutefois, nous avons eu plusieurs collaborations.

Déroulement et gestion du projet de thèse

Principales étapes du projet

Ma thèse peut se diviser en trois grands axes :

- **Axe 1 : Recherche sur les nanoparticules**

La synthèse de PDA est lente (durée 24h) avec la méthode la plus largement utilisée, mais aussi elle aboutit à des agrégats (gaspillage de matériel). Une première étape de ma thèse a donc consisté à développer un protocole pour synthétiser des nanoparticules qui soient stables, et dont on peut contrôler la taille. L'intérêt d'un tel objectif est que nous voulions créer des nanoparticules avec un potentiel applicatif dans le relargage des médicaments par exemple.

Résultats de cette étape :

- Un article publié dans le journal *Biomimetics*
 - Une revue dans *Colloids and surface*
 - Un poster présenté lors d'un workshop à Barcelone, Espagne
 - Une présentation orale donnée à l'occasion du congrès EMRS à Nice
-

- **Axe 2 : Recherche sur les films de PDA**

Est-ce que les différents protocoles pour fabriquer la PDA aboutissent à des propriétés différentes et à des différences de morphologie et de composition chimique ? L'intérêt de cette recherche est que le contrôle des propriétés d'une molécule est très important pour les applications biomédicales.

A partir des résultats obtenus au cours du projet « nanoparticules », nous avons élaborés des films suivant différentes méthodes et analyser leurs caractéristiques physico-chimiques.

Résultat de cette étape : un article soumis pour publication

- **Recherche sur les gels**

La PDA est connu pour avoir un fort pouvoir adhésif. Une application de cette PDA peut donc être le développement d'une colle. Nous nous sommes donc concentrées sur l'élaboration d'une colle chirurgicale.

Résultat de cette étape :

- Ce projet d'application a été sélectionné au concours d'innovation « *Mature Your PhD* » de la SATT Conectus
 - Un article en cours de rédaction
-

Par ailleurs j'ai eu l'opportunité de présenter ma thèse lors la finale régionale du concours de vulgarisation scientifique « Ma thèse en 180 secondes ».

Animation et Coordination

i. Les réunions de projet

Les réunions avec mon directeur de thèse se font à la demande, très fréquemment, quasi quotidiennement pour des petits points de suivi, avec une réunion bilan à chaque fois qu'une longue série d'expériences se termine. Les décisions sont prises en concertation et en fonction des résultats. Avoir la chance de travailler avec un directeur de thèse aussi présent et disponible que le mien m'a grandement facilité ce travail de thèse.

ii. Les relations / partenaires extérieurs

Nous avons pu bénéficier de mesure et d'analyse d'images avec l'IPCMS Strasbourg avec la précieuse aide de l'équipe du Prof. Ovidiu, en la personne de Dris Ihiwakrim.

Nous avons eu l'opportunité de développer des liens à travers des collaborations avec des chercheurs de l'ISIS Strasbourg (Artur Cielsielski et Matilde Eredia): nous avons pu mener des expériences au sein de leur laboratoire de recherche, et utiliser des instruments de mesure que nous n'avons pas.

Nous avons aussi travaillé avec l'équipe du Professeur Marco d'Ischia de l'université de Naples en Italie. Il y a eu des échanges théoriques pour analyser mes résultats et des collaborations techniques avec sa doctorante.

Le concours « Mature Your PhD » de Conectus a également été une occasion d'enrichir mes relations externes au monde de la recherche. Les experts Conectus m'accompagnent sur le volet socio-économique de mon projet de recherche avec notamment des études de marché, ainsi qu'une formation en propriété intellectuelle.

Mise en valeur des compétences transversales et transférables

La communication

Conférences : les conférences données dans le cadre de ce doctorat m'ont aidé à me sentir beaucoup plus à l'aise pour communiquer sur mes travaux à la fois en français et en anglais.

Vulgarisation / Pitch : dans le cadre de ma participation à la finale régionale de Ma Thèse en 180 secondes, j'ai été formé à « vulgariser » mes travaux de recherche pour un public non familier avec mon domaine. Quant au concours de Conectus, celui-ci m'a poussé à aborder le côté socio-économique d'un projet de recherche et de le communiquer sous forme de pitch:

La pédagogie

Enseignement : j'ai eu l'opportunité de passer de l'autre côté du bureau pour me retrouver enseignante de TD à l'université. Cette expérience m'a permis de mieux découvrir l'art de transmettre, car j'ai dû réfléchir à comment élaborer mes cours, à gérer plusieurs groupes d'étudiants, à mettre en place un système d'évaluation des étudiants. J'ai donc plus facilement pu me projeter dans le rôle de l'enseignant-chercheur à l'université.

Formation : j'ai suivi plusieurs formations avec l'institut du développement et de l'innovation pédagogique de Strasbourg, pour apprendre à concevoir mes enseignements de manière innovante : l'élaboration de cartes conceptuelles, l'enseignement avec « l'approche par projet », le développement d'une offre de formation construite autour des compétences « approche par compétences ».

Expertise et méthode

La publication d'articles et la communication de nos résultats à nos pairs montrent que j'ai acquis une certaine expertise dans le domaine de la physique-chimie des matériaux. J'ai pu notamment apprendre à utiliser plusieurs techniques : la synthèse de nanoparticules et de gels, la préparation de films minces, l'utilisation de plusieurs techniques de caractérisation des matériaux : microscope à force atomique, microscope à balayage, rhéomètre, mesure de l'angle de contact, ellipsométrie, spin-coater... aussi le traitement de données de microscope avec le logiciel gwyddion. Mener une thèse m'a permis de mieux maîtriser les techniques expérimentales en laboratoire.

La gestion de projet

Le Programme NCT m'a permis de conscientiser le fait que ma thèse a été menée avec une approche « gestion de projet ».

Leadership

Durant mon doctorat, je me suis engagée en tant que bénévole au sein d'un centre de loisirs familial. J'y ai proposé un programme d'accompagnement scolaire, pour les jeunes de la 3^{ème} à la Terminale, alliant à la fois le soutien renforcé dans les matières principales et le coaching scolaire (gestion du stress, du temps...). Cette expérience m'a permis d'apprendre à gérer les moyens humains, à travers la recherche d'enseignants bénévoles, la répartition des groupes selon les niveaux et les matières à proposer. Aussi à mobiliser mon réseau pour le recrutement d'intervenants.

Motivée par ma volonté de partager l'amour des sciences, je me suis lancée dans une aventure associative qui au départ consistait à établir des ponts entre les chercheurs du CNRS et les habitants du quartier de Cronenbourg. Ce projet a néanmoins rencontré des freins qui ont rendu sa concrétisation difficile. Depuis, je me suis concentrée sur l'élaboration d'un programme de médiation scientifique à destination de jeunes filles habitantes des quartiers populaires.

Toutes ces compétences acquises durant le doctorat, qu'elles soient en lien direct ou développé en parallèle, me permettront de mieux faire face au marché du travail.

Conclusion / Remerciements

Conclusion

Ce programme a répondu à mes attentes et m'a apporté des pistes de réflexion quant à mon employabilité. Grâce à l'ensemble de la formation, j'appréhende moins l'après thèse et me sens plus apaisée quant à mon avenir professionnel : j'ai appris à identifier mes qualités et mes compétences, ainsi que mes points à améliorer.

L'alternance entre séances collectives et individuelles était assez rafraichissante et ludique. Ce programme devrait être étendu et pleinement intégrer dans les formations doctorales vu son utilité.

Remerciements

Le programme NCT a été une riche expérience humaine et intellectuelle. La rencontre de notre mentor Anna a été très enrichissante. J'ai pris énormément plaisir à assister à nos rdvs et à apprendre de son expertise. Sa bienveillance et son côté motivant telle une coach a été un élément déterminant dans ma volonté de poursuivre ce programme jusqu'au bout.

J'en profite donc pour la remercier chaleureusement ainsi que la responsable de ce programme Hafida Lrhezzioui et toutes les personnes qui ont contribué, pensé, travaillé sur

la mise en place de ce projet. Aussi, je remercie les intervenants qui ont pris de leur temps pour nous partager leur parcours et leurs expériences, le tout suivi de sages conseils.

Je remercie également mes collègues doctorant-e-s qui ont vécu cette aventure avec moi. Un grand merci à eux qui ont fait preuve de douceur et de bienveillance à chacune de nos séances.

Enfin, je remercie mon directeur de thèse pour son aide précieuse dans l'avancée de ma thèse et ma famille qui m'a toujours soutenu. Un merci infini à mon mari qui m'épaulé au quotidien, ainsi qu'à ma petite princesse qui me donne envie chaque jour de me surpasser.
